

# CHAPTER ONE

## INTRODUCTION AND SCOPE OF THESIS

### 1.1 Introduction

Modern power system can be characterized by wide spread system interconnections. The interconnected power system is comprised of multiple machines connected by the transmission network. The supply of reliable and economic electric energy is a major determinant of industrial progress and consequent rise in the standard of living. In practical terms this means that both voltage and frequency must be held within allowable tolerances so that the consumer's equipment can operate satisfactorily. Further, with deregulation of power supply utilities, the power network has become a highway for transmitting electric power from wherever it is available to places where required, depending on the pricing that varies with time of the day. In such scenario, the analysis of dynamic performance and stability of power system has great importance. The stability problem is concerned with the behavior of the synchronous machines under perturbed conditions. If the perturbation does not involve any net change in power, the machines should return to their original state and if an unbalance between the supply and demand is created by perturbation, a new operating state should be achieved. When the system changes its operating point from one stable point to the other, it is mandatory that all interconnected synchronous machines should remain in synchronism, they should all remain operating in parallel and at the same speed[1].The increasing magnitude and complexity of interconnected power systems due to competitive energy markets, economy and population development have created the need to operate the power systems close to their capacity limits. This leads sometimes to stability problems or poor dynamic behaviors like power oscillations. These oscillations can cause a reduction of the system components lifetime, expensive operations of the electrical grids and in the worst case, risks of partial system collapses. On the other hand, in the synchronous generator, the damping that the field and damper windings provide to the rotor oscillations is weakened due to excitation control system action. The reason for this is that in the rotor circuits appear additional currents induced by the voltage regulation and those currents oppose to the currents induced by the rotor speed deviations [2].

## **1.2 Motivation**

Power systems are usually large nonlinear systems, which are often subject to low frequency electro-mechanical oscillations. Power system operation is characterized by a wide range of operating conditions, random load changes and various unpredictable disturbances. Power system stabilizers (PSS) are often used as an effective and economic means of damping such oscillations. In the past fixed gain controllers were effectively used for damping out the low frequency oscillations. These stabilizers are designed based on linearized model of power systems for a particular operating and system condition. The application shows non optimal results, for that use an adaptive power system stabilizer to solve fixed gain controller problem, and the use of the adaptive control is possible because the loading variation and consequently variation of synchronous generator dynamic characteristic are in most essentially slower than the adaptation mechanism, and adaptive stabilizers able to perform well for all network and operating conditions.

## **1.3 Objectives**

This research deals with design adaptive power system stabilizer for damping low frequency oscillations in power system. The main objectives of this thesis are:

- To develop mathematical model of single machine infinite bus and multi machines power system in includes excitation system and power system stabilizer
- To evaluation performance of power system in case single machine and multi machine using Eigen values method
- To design power system stabilizer using model reference adaptive control.
- To estimate power system parameters by estimation method
- To achieve better performance with better accuracy, use MIT rules model reference adaptive control methods and compare the results.

- In addition to the theoretical, investigate how the Adaptive Power System Stabilizer behaves using Matlab/Simulink.

## **1.4 Contribution**

In this thesis, it will introduce the structure of the power system stabilizer and the mathematic model of the generator control system equipped with PSS. Based on the mathematic model, it will explain how the PSS increases the system damping. Due to the complexity of power system , and the lack of system parameters in most cases. The thesis introduces a new way to design PSS based on model reference adaptive control , which does not need to tuning parameters of the system off - line .

## **1.5 Organizations**

The remainder of this thesis consists of seven chapters.

**Chapter One** gives the introduction and general back round, objective and scope of thesis

**Chapter Two** gives surveys of design power system stabilizer based on conventional and intelligence methods.

**Chapter Three** describe dynamic model of Synchronous machine include excitation and Power System.

**Chapter Four** describe dynamic model of Multi Machine Power System. The detail description of eigenvalue analysis method used for evaluating small signal performance of power system and time domain simulations.

**Chapter Five** introduces adaptive control and design of power system stabilizer by MIT rule and model reference adaptive control.

**Chapter Six** results and discussions.

**Chapter Seven** gives the conclusion and future work.

# CHAPTER TWO

## GENERAL BACKGROUND AND LITRETURE REVIEW

### 2.1 Power System Stability

Today's power systems are large, complex and operated closer to security limit. Furthermore, environmental constraints restrict the expansion of transmission network and the need for long distance power transfers has increased. As a result, stability has become a major concern in power systems. Accidents of power system blackouts caused by rotor angle instability, voltage instability or frequency stability. Power system angle stability can be categorized in to small-signal and transient stabilities. Small-signal stability is the ability of the system to return to its normal operating state following a small disturbance. Investigation of this kind of stability usually involves the analysis of the linearized state space equations that define the power system dynamics. On the other hand, transient stability is the ability of the system to return to a normal operating state following a severe disturbance, such as a single-phase or multi-phase short-circuit or a generator lost. Under these conditions, the linearized power system model is not sufficient and the nonlinear equations must be used for the analysis [1]. For the convenience of analysis, power system stability is categorized shown as Figure (2.1).

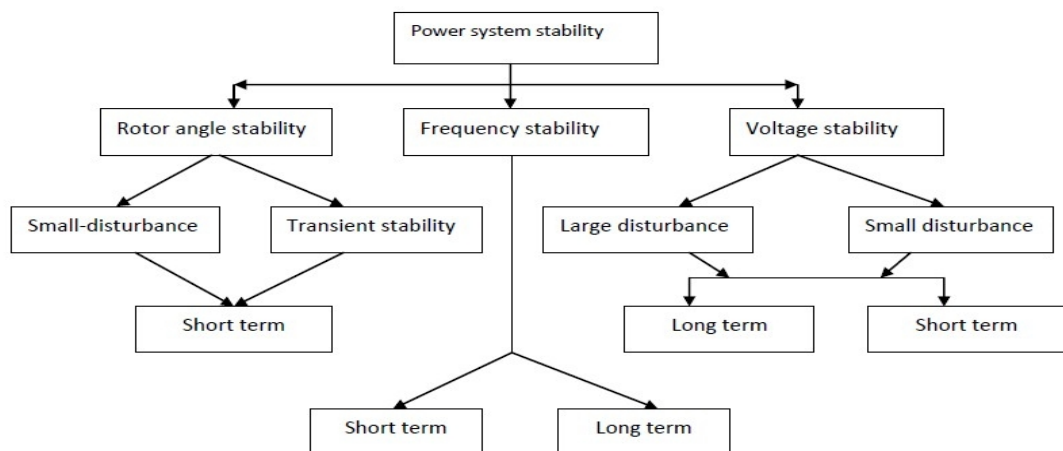


Figure (2.1): Categorized of power system stability.

### **2.2.1 Steady-State Stability**

Steady-state stability analysis is the study of power system and its generators in strictly steady state conditions and trying to answer the question of what is the maximum possible generator load that can be transmitted without loss of synchronism of any one generator. The maximum power is called the steady-state stability limit [3].

### **2.2.2 Transient Stability**

Transient stability is the ability of the power system to maintain synchronism when subjected to a sudden and large disturbance within a small time such as a fault on transmission facilities, loss of generation or loss of a large load. The system response to such disturbances involves large excursions of generator rotor angles, power flows, bus voltages [5].

### **2.2.3 Dynamic Stability**

A system is said to be dynamically stable if the oscillations do not acquire more than certain amplitude and die out quickly. Dynamic stability is a concept used in the study of transient conditions in power systems. Any electrical disturbances in a power system will cause electromechanical transient processes. Besides the electrical transient phenomena produced, the power balance of the generating units is always disturbed, and thereby mechanical oscillations of machine rotors follow the disturbance [4].

## **2.3 Nature of Oscillation**

Oscillations in the power system have the following properties:

1. Oscillations are due to natural modes of the system and therefore cannot be Completely eliminated.
2. With increase in complexity of the power system, the frequency and damping of oscillations may increase and new ones may be added.
3. Automatic Voltage Regulator (AVR) control is the primary source of introducing negative damping torque in the power system. With increase in the number of controls, negative damping may further increase.

4. Inter-area oscillations are associated with weak transmission lines and larger line loadings.
5. Inter-area oscillations may involve more than one utility.

## **2.4 Modes of Oscillations**

The disturbance is considered to be small, and therefore, the equations that describe the resulting response of the system can be linearized. The electromechanical oscillations are of two types [3].

### **2.4.1 Local Mode Oscillations**

Local mode Oscillations which are associated with the swing of units at a generating station with respect to the rest of the power systems. Typical range of frequency of oscillations is 1-3 Hz. The term local is used because the oscillations are localized at one station or a small part of the power system [3].

### **2.4.2 Inter-area Mode Oscillations**

Inter-area mode oscillations, which are associated with the swing of many machines in one part of the system against the machines in other parts of area. Typical range of frequency of these types of oscillations is less than 1 Hz. They are caused by two or more groups of closely coupled machines beings intercom.

### **2.4.3 Inter-unit Mode**

Inter-unit mode will act between different generators in the same power plant or between plants that are located near each other. This oscillation mode occurs in a frequency range from 1.5 to 3 Hz, and by implementing a power system stabilizer when having an inter-unit mode the oscillation may become unstable. This is because the PSS is often tuned at a lower frequency than the inter-unit mode, and the PSS settings are therefore critical. A complete eigenvalue analysis must be executed in order to ensure that the damping of a potential inter-unit mode not becomes troublesome [7].

## **2.5 Control Exciter Modes**

The control exciter mode is directly related to the control equipment of the generator and is a version of the local oscillation mode. These oscillations could be a result of poorly coordinated regulators in the system such as excitation systems, HVDC converters, and static VAR compensators. As a result of these oscillations the generator shaft may be affected and the torsional mode will then be more noticeable [6].

### **2.5.1 Local Machine Modes**

In this mode of oscillation typically one or more generators swing against the rest of the power system in a frequency range from 0.7 Hz to 2 Hz. This oscillation may occur and become a problem if the generator is highly loaded and connected to a weak grid. In an excitation system containing a high transient gain and no PSS, these local machine oscillations may increase. A correctly tuned PSS in such a system may decrease the local machine oscillations [7].

### **2.5.2 Inter-area Modes**

The inter-area oscillation mode can be seen in a large part of a network where one part of the system oscillates against other parts at a frequency below 0.5 Hz. Since there is a large amount of generating units involved in these oscillations, the network operators must cooperate, tune and implement applications that will damp this mode of oscillations. A PSS is often a good application to provide positive damping of the inter-area modes [7]. Also a higher frequency inter-area oscillation can appear (from 0.4 to 0.7 Hz) when side groups of generating units oscillate against each other [6].

### **2.5.3 Global Modes**

This mode of oscillations is caused by a large amount of generating units in one area that is oscillating against a large group in another area. The oscillating frequency is typically in the range from 0.1 to 0.3 Hz and the mode is closely related.

## **2.6 Power System Stabilizer**

Traditionally the excitation system regulates the generated voltage and there by helps control the system voltage. The automatic voltage regulators (AVR) are found extremely suitable (in comparison to, ammortisseur winding and „governor controls ) for the regulation of generated voltage through excitation control. But extensive use of AVR has detrimental effect on the dynamic stability or steady state stability of the power system as oscillations of low frequencies (typically in the range of 0.2 to 3 Hz) persist in the power system for a long period and sometimes affect the power transfer capabilities of the system [19]. The power system stabilizers (PSS) were developed to aid in damping these oscillations by modulation of excitation system and by this supplement stability to the system [9]. The basic operation of PSS is to apply a signal to the excitation system that creates damping torque which is in phase with the rotor oscillations.

## **2.7 PSS Input Signals**

Till date numerous PSS designs have been suggested. Using various input parameters such as speed, electrical power, rotor frequency several PSS models have been designed. Among those some are depicted below.

### **2.7.1 Speed Input Signal**

A power system stabilizer utilizing shaft speed as an input must compensate for the lags in the transfer function to produce a component of torque in phase with speed changes so as to increase damping of the rotor oscillations [23].

### **2.7. 2 Power Input**

The use of accelerating power as an input signal to the power system stabilizer has received considerable attention due to its low level torsional interaction. By utilizing heavily filtered speed signal the effects of mechanical power changes can be minimized. The power as input is mostly suitable for closed loop characteristic of electrical power feedback [23].

### 2.7.3 Frequency Input

The sensitivity of the frequency signal to the rotor input increases in comparison to speed as input as the external transmission system becomes weaker which tend to offset the reduction in gain from stabilizer output to electrical torque, that is apparent from the input signal sensitivity factor concept[23].

## 2.8 Excitation System

The performance of the excitation system can have a great influence on the stability of a power system. However, it depends mainly on parameter setting of the excitation system. Proper parameter setting of the excitation system can improve the stability and increase the damping of the power system. On the contrary, improper parameter setting of the excitation system can deteriorate the operation of the power system [11]. The IEEE Type-ST1 (1992) excitation system shown in Figure (2.2) is considered in this study.

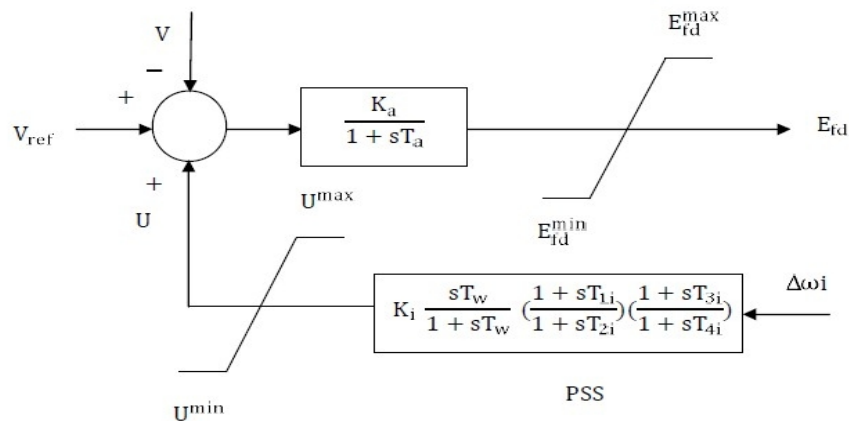


Figure (2.2) Block diagram of a typical Excitation System

## 2.9 Power System Stabilizer

For many years PSSs have been used to add damping to electromechanical oscillations. They were first introduced in the late 1960s to compensate for the AVR's adverse effect on the damping torque by means of positive feedback loop to provide additional damping in the system [12]. PSSs

essentially use the power amplification capability of the generators to generate a damping torque in phase with the speed change of the generator rotor. This is achieved by injecting a stabilizing signal into the excitation system voltage reference in such a way that a component of electrical torque proportional to the rotor speed deviation is produced [13-14]. This stabilizing signal is, in most cases, the deviations in generator rotor speed which fed through a compensation circuit to compensate for the phase lag between the exciter voltage reference and generator electrical torque [10].

### 2.9.1 Power System Stabilizer Structure

The basic objective of power system stabilizer is to modulate the generator's excitation in order to produce an electrical torque at the generator proportional to the rotor speed [10-13]. In order to achieve that, the PSS uses a simple lead-lag compensator circuit to adjust the input signal and correct the phase lag between the exciter input and the electrical torque. The PSS can use various inputs, such as the speed deviation of the generator shaft, the change in electrical power or accelerating power, or even the terminal bus frequency. However in many instances the preferred signal input to the PSS is the speed deviation. Figure (2.3) below illustrates the block diagram of a typical PSS. The PSS structure generally consists of a washout, lead-lag networks, a gain and a limiter stages. Each stage performs a specific function.

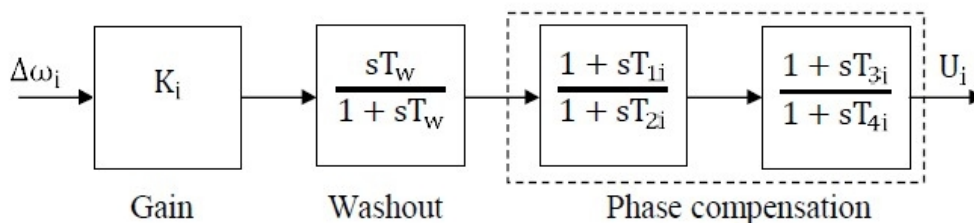


Figure (2.3) Block diagram of a typical PSS

### 2.9.2 Washout

Block serves as a high-pass filter. Without it steady changes in speed would modify the terminal voltage. It allows the PSS to respond only to changes in speed. From the view point of the washout function, the value of washout

time constant is not critical and may be in the range of 0.5 to 20 seconds. The main consideration is that it may be long enough to pass stabilizing signals at the frequencies of interest unchanged, but not so long that it leads to undesirable generator voltage excursions during system is landing conditions.

### **2.9.3 Input Signals**

That have been identified as valuable include deviations in the rotor speed  $\omega$ , the frequency  $f$ , the electrical power  $P_e$  and the accelerating power  $P_a$ . Since the main action of the PSS is to control the rotor oscillations, the input signal of rotor speed has been the most frequently advocated in the literature. However, it had been found that frequency is highly sensitive to the strength of the transmission system that is, more sensitive when the system is weaker - which may offset the controller action on the electrical torque of the machine. Other limitations include the presence of sudden phase shifts following rapid transients and large signal noise induced by industrial loads. On the other hand, the frequency signal is more sensitive to inter-area oscillations than the speed signal and may to better oscillation attenuation. In this thesis work a speed signal is used as input signal.

## **2.10 Conventional Power System Stabilizer Design Method**

For many years conventional control methods have been applied to design PSSs. These approaches consist of first linearizing the system at the nominal operating condition to be able to extract the dynamic characteristics of the power system and its frequency response. Once the phase lag is identified, the phase lead can be obtained by tuning the time constants of the lead-lag circuit. Ideally a phase lead, equal and opposite to the phase lag, is required to produce an electrical torque with a component proportional to the speed. However in practice this cannot be achieved but can be closely matched over the frequency range [12]. The gain on the other hand is obtained by applying the root locus method. The gain must be carefully selected to stabilize the electromechanical mode without adversely affecting the other modes such as the exciter mode [12-16]. It is important to choose an appropriate value for

the washout  $T_w$ . It would be adequate to choose the time constant between 1 and 2 seconds if the damping of the local mode is the only concern. However  $T_w$  of 10 seconds or higher when inter– area is considered [10-16-17]. Generally, determining the stabilizer’s parameters in systems with both local and inter –area modes has a more complex approach. For the most case this situation is encountered in a multi machine system. Therefore PSSs must be tuned one at a time through off-line analysis, and tuned further during commissioning. The validity of the model used in the off-line studies should be checked on commissioning. Setting power system stabilizers to typical values is particularly dangerous for systems in which inter – area modes are of concern. It is very easy for the stabilizer to have a destabilizing effect at low frequencies that cannot be observed during on-line commissioning test [15-18]. The performance of the CPSS often deteriorates over time due to nonlinearity and changes of operating conditions. Over the years, several approaches of controllers design have been investigated and implemented to overcome the shortcomings of the CPSSs. Some of these methods are reviewed in the next section.

## 2.11 Phase Compensation Design Technique

Consists of adjusting the stabilizer parameters to compensate for the phase lags through the generator excitation system, and power system such that the torque changes in phase with speed changes. This is the most straightforward approach, easily understood and implemented. The phase lag depends on the operating point and the system parameters. The algorithm for computing the PSS parameters is as follows:

**Step 1:** Obtain  $\omega_n$  from the mechanical loop

The characteristic equation of the mechanical loop can be written as:

$$MS^2 + DS + bK_1 = 0 \quad (2.1)$$

Where,  $\omega_b$  is the system frequency in rad/sec. and  $\omega_n$  is the undamped natural frequency of the mechanical mode and is given in (2.2)

$$\tilde{S}_n = \sqrt{\frac{bK_1}{M}} \quad (2.2)$$

**Step 2:** Compute phase lag  $G_e$  between  $U_m$  and  $T_m$  of the loop to be compensated by PSS.  $G_e$  is the transfer function.

**Step 3:** Design of phase lead lag compensator. The transfer function of phase lead compensator  $G_c$  is

$$G_c = \frac{(1 + sT_1)(1 + sT_3)}{(1 + sT_2)(1 + sT_4)} \quad (2.3)$$

$$\text{For full compensation } G_c + G_e = 180^\circ \quad (2.4)$$

The PSS parameters to be optimized are  $T_1$ - $T_4$  and  $K_i$ . Considering two identical cascade lead-lag networks for PSS.  $T_1 = T_3$  and  $T_2 = T_4$  and hence the problem reduces to that of optimization of  $K_i$ ,  $T_1$  and 3 only.  $T_w = 10$ s has been chosen. One lead lag block is used for compensating about 50o of phase lag and accordingly lead lag blocks are chosen. The PSS parameters  $T_1$  and  $T_2$  are chosen so as to fully compensate the phase lag as follows: Let, is the phase lag compensated by one block, then

$$T_2 = \frac{1}{\omega_n^2 \sqrt{a}} \quad (2.5)$$

$$a = \frac{1 - \sin \beta}{1 + \sin \beta} \quad (2.6)$$

$$T_1 = aT_2 \quad (2.7)$$

The adjustable PSS parameters are the gain of the PSS,  $K$  and the time constants,  $T_1$ - $T_3$ . The lead-lag block present in the system provides phase lead compensation for the phase lag that is introduced in the circuit between the exciter input and the electrical torque. The required phase lead can be derived from the lead-lag block even if the denominator portion consisting of  $T_2$  and  $T_4$  gives a fixed lag angle. Thus, to reduce the computational burden in this study, the values of  $T_1$  and  $T_3$  are kept constant at a reasonable value of 0.05 sec and tuning of  $T_2$  and  $T_4$  are undertaken to achieve the net phase lead required by the system.

**Step 4:** Gain setting the amount of damping introduced depends on the gain of PSS transfer function at that frequency. Ideally, the gain should be set at a value corresponding to maximum damping. The desired PSS gain  $K_i$  is computed from

$$K_i = 2\xi_n M / (|G_c| |G_e|) \quad (2.8)$$

Where,  $\xi_n$  is the desired damping ratio

## 2.12 Adaptive Control

Adaptive control can be described as the changing of controller parameters based on the changes in system operating conditions [19]. The idea is to constantly update the controller parameters according to recent measurement [3]. Power systems are inherently nonlinear with varying operating conditions, hence adaptive control technique is well suited to track the operating conditions and changes in the system. The resulting adaptive stabilizer uses an identification algorithm that tracks the actual system operating condition, which then adjusts its parameters on-line according to the environment in which it works. This method can provide good damping over a wide range of operating condition [20-21-22]. Despite the good performance of the stabilizer, adaptive controllers are difficult to design and susceptible to problems like non-convergence of parameters and numerical instability. The response time of the controller is the key factor to a good closed-loop performance. The adaptive power system stabilizer (APSS) employs complicated algorithms for parameter identification and optimization which require significant amount of computing time. The higher the order of the discrete model of the controlled system used in identification, the more computing time is needed.

## 2.9 Literature Review

Numerous works have been done and published on the damping of power system low frequency oscillations. This section will review some of the published work in this area. In 1969 [8], De Mello and Concordia discussed the phenomena of Stability of synchronous machines under small perturbations by examining the case of a SMIB through external reactance. The analysis developed insights into effects of thyristor-type excitation systems and established understanding of the stabilizing requirements for such systems. These stabilizing requirements included the voltage regulator gain parameters as well as the transfer function characteristics for a machine speed derived signal along with the voltage regulator reference for providing damping of machine oscillations. The study had explored a variety of machine loadings, machine inertias, and system external impedances with a determination of the oscillation and damping characteristics of voltage or speed following a small disturbance in mechanical torque. An attempt had been made to develop some unifying concepts that explain the stability phenomena of concern, and to predict desirable phase and magnitude characteristics of stabilizing functions. In 1989 Kundur et al. [24] provided the analytical work and systematic method to determine PSS parameters for large power generation in a practical power system. The basic PSS design idea based on the stabilizer proposed in. However, the phase characteristics were obtained using a multi-machine eigenvalue program instead of a single machine model. This work emphasized enhancement of overall system stability, and the authors considered simultaneous damping of inter-area and local modes and discussed the performance of the PSS under different system conditions. In addition to small signal stability performance, the authors also tested the transient stability performance of the PSS and the performance during system is landing. The authors also demonstrated the importance of appropriate choice of washout time constant, stabilizer output limits and other excitation system control parameters. The authors claimed that the frequency response method

used to compensate the lag between the excitation input and the electrical torque was fairly robust.

Chow and Sanchez-Gasc in [25], proposed four pole-placement techniques for the design of power system stabilizers, with the emphasis on frequency response characteristics of the controller. For controllers to exhibit desirable frequency response characteristics, a simple procedure was proposed to obtain controllers suitable for multiple operating conditions. The issue of robustness of state space designed controllers was investigated. to select all the parameters of the fuzzy controller. Abido [26] designed a hybrid rule based PSS by incorporating GA to search for optimal settings of his proposed PSS parameters. In [27], the simultaneous stabilization of a power system over a wide range of operating conditions via a single-setting conventional power system stabilizer using GA is investigated. The authors wanted to select a single set of power system stabilizer parameters which can make the PSS simultaneously stabilize the power system over a wide range of operating conditions. They treated the power system operating at various loadings as a finite set of plants. The problem was converted to a simple optimization problem which is solved by a genetic algorithm and an eigenvalue based objective function. Two objective functions were presented, allowing the selection of the stabilizer parameters to shift all or some of the system eigenvalues to the left-hand side of a vertical line and a wedge-shape sector in the complex s-plane. The authors proposed in [28] a similar idea to design a PSS. However, another optimization method, Tabu search was used to select PSS parameters. Lu, Nehrir and Pierre [29] proposed a power system stabilizer with a fuzzy logic based parameter tuner. Reduced order linear models for the synchronous generator at a large number of operating points were obtained and the optimal PSS at each operating point were designed by the traditional frequency domain method. Antal Soos in [14] discuss PSS design for damping of inter-area power oscillation by coherency-based equivalent model in Japan, low-frequency oscillations have been observed on trunk transmission systems,

and have been the subject for studies in fields of operation, control, and devices by many power system utilities. The method is based on the single-machine-infinite-bus models derived from the multi-machine power system by coherency-based reduction technique. Dynamic simulations using a 10-machine power system model are presented in order to show the effectiveness of the PSS.

P.L. Dandeno et al discuss installations of PSS were based on a variety of methods to derive an input signal that was proportional to the small speed deviations characteristic of electromechanical oscillations. After years of experimentation the first practical integral-of-accelerating-power based PSS units were placed in service. This design provided numerous advantages over earlier speed-based units and forms the basis for the PSS implementation that is used in most units installed in North America. This design is now a requirement in many Reliability Regions within North America and has been modeled in the IEEE standards as the PSS2A and PSS2B structures. For simplicity, the term PSS2A stabilizer will be used to refer to the integral-of-accelerating power based design in general throughout this paper. This paper briefly describes some of the earlier structures in order to explain the advantages of the accelerating-power design. This design is then described along with a detailed review of the role of the “ramp-tracking” mechanical filter and the basis for the present structure that is in wide use by many manufacturers [30]. Anta and Soos et al, in [30] discuss an optimal control algorithm with adaptive system parameters and state variables estimation. The optimal control algorithm is calculated by solving the algebraic Riccati equation of the linearized closed loop system model obtained by using an adaptive recursive least squares identification algorithm. The feedback control is achieved by recalculating the control sequence each sampling period. An application of the algorithm as a power system stabilizer is illustrated.

P.He Y.B. Wei C.X. Yang et al discuss Dynamic stability enhancement of electro-mechanical modes of multi-machine power systems by means of an

adaptive power system stabilizer. The proposed adaptive PSS is a variational configuration to self-adjusted tracking the system operation condition. The parameter optimization program is used to obtain him optimal parameter of every PSS under single operating conditions; the weighing coefficient is employed to adapt the actual operating condition. The study is carried out in details on a great of testing computation and analysis on a 8-machine testing system. Obtained result is compared with that of the previous PSS [31].

Chun Liu discusses an adaptive optimal controller, which will improve a power system's overall stability in the face of system non-linearity and external disturbances, is described in this thesis. The transfer function of the plant is estimated in real time by the Recursive Least-Squares (RLS) algorithm, and converted into its state equation. The plant states are estimated by Kalman filter. Control output is calculated by solving the Riccati algebraic equation. The applied structure enables improvement in performance from a linear controller [32].

Fariborz Parandin , el al .[33] discuss Power System Stabilizer Design based on Model Reference Adaptive System deals with a adaptive design method for the stability enhancement of a single machine infinite bus power system using Model Reference Adaptive System. To show effectiveness of the MRAS, this method is compared with the GA-PSS. Simulation results show that the proposed method guarantees robust performance under a wide range of operating conditions.

Fariborz Parandin, el al also discuss Adaptive Multi Machine PSS Design for Low Frequency Oscillations Damping, an adaptive method is presented to design a multi machine PSS. The proposed adaptive method changes itself structure according to power system operating conditions. This ability of adaptive controller Leads to an adaptive performance proportionate with different loading conditions. In order to show effectiveness of the proposed method, it is compared with a conventional PSS tuned by using PSO (PSO-

PSS). The nonlinear time domain Simulation results demonstrate the ability of the proposed Adaptive method to deal with uncertainties [39].

D P SEN Gupta et al, discuss low frequency oscillation in power system a physical account and adaptive stabilizer, briefly review some of adaptive or gain scheduling stabilizers proposed, elaborating on decomposition of damping torque and the PSS based on cancellation of negative damping the multi frequencies of oscillation at generated may experience in multi machine system are identified information is used in design of the PSS [40].

E.vlarsan and D.A swann discuss in their three part paper titled applying power system stabilizer –I,II,III,the history of power system stabilizer and its role in a power system they recommended that the objectives of most appropriate stabilizer tuning criterion is to provide an adequate amount of damping local mode oscillation and inter area mode oscillation .the studies and the field test conducting by authors indicate that a fast acting excitation system offers best opportunity for increased damping than the use of auxiliary signal in to voltage regulator[37].

Fariborz Parandin, et al . Discuss Power System Stabilizer Design based on Model Reference Adaptive System deals with adaptive design method for the stability enhancement of a single machine infinite bus power system using Model Reference Adaptive System. To show effectiveness of the MRAS, this method is compared with the GA-PSS. Simulation results show that the proposed method guarantees robust performance under a wide range of operating conditions [47].

Fariborz Parandin, et al also discuss Adaptive Multi Machine PSS Design for Low Frequency Oscillations Damping, an adaptive method is presented to design a multi machine PSS. The proposed adaptive method changes itself structure according to power system operating conditions. This ability of adaptive controller Leads to an adaptive performance proportionate with different loading conditions. In order to show effectiveness of the proposed method, it is compared with a conventional PSS tuned by using PSO (PSO-

PSS). The nonlinear time domain Simulation results demonstrate the ability of the proposed Adaptive method to deal with uncertainties [39].

Kothari et al (1995) designed a self-tuning PSS using the pole shifting technique. The controller used a state-feedback law, whose gains were evaluated from the pole-shifting factor. The proposed method was simple and computationally efficient. The dynamic performance of the proposed PSS was quite satisfactory and the PSS adapted quickly to varying operating conditions. The method used a model formulation which obviated the need for state observers and the output was directly used to derive the feedback control signal. It combined this with a simple pole-shifting control technique in this framework to achieve quite satisfactory dynamic performances. The control calculations are simple and require less computational effort [41].

Yuan-Yih Hsu et al discussed the identification and tuning of exciter constants for a generating unit at the Second Nuclear Power Plant of Taiwan Power Company. Field test was first performed on the excitation system with the generator open-circuited. Since the field test results differed from the computer simulation results using manufacturer's constants, he modified the manufacturer's constants based on previous experience to reach a preliminary set of parameters for the excitation system. Then a hybrid nonlinear simulation-sensitivity matrix method was developed to further refine the excitation system parameters. The exciter constants were tuned in order to give better dynamic response. Field tests were conducted in order to compare the dynamic response of the generator without and with PSS [42].

Simoes Costa et al proposed a method to design the power system controllers in order to damp electromechanical oscillations. It could be applied to the design of both PSS for synchronous generators and supplementary signals associated to other damping sources. Some attractive features of the method were: the parameters of all controllers were jointly determined, there was no restriction on the type of supplementary signals to be used, and controller structures were compatible with those nowadays employed in electric utilities.

The control problem solution exploits sparsity, combining a system description which preserves a sparse structure with an adequate mathematical formulation of the optimal design approach. The results were validated by using both eigenvalue analysis and nonlinear simulation. A method based on structurally constrained optimal controller design for the determination of controller settings in multimachine power systems was introduced. The settings for all controllers in a multimachine system could be simultaneously determined through an integrated procedure which takes into account all dynamic interactions. The results, were given both in terms of eigenvalues and nonlinear simulation curves illustrate the applicability of the method to realistic power systems [43].

Choi and Jia discussed the inherent dynamical relationship between the under-excitation limiter (UEL) and the PSS control loops in synchronous generators using the frequency response technique. It was shown that the limiters should be designed to affect much slower response characteristics as their main function was to prevent excessive stator end-core heating. The analysis also showed that a reduction in the values of the slope of the boundary curves, which prescribe the operating region of the limiters, was accompanied by a decrease in the damping level of the closed-loop excitation control systems. It was shown that the tuning of the UEL and the PSS could be carried out separately without considering the interaction between the two control loops. Analysis of the power system model showed that the damping level due to the UEL increased along with the slope of limiter boundary curve [44].

Soliman et al designed a simple robust PSS that could properly function over a wide range of operating conditions. The lead compensator design was achieved by drawing the root loci for a finite number of extreme characteristic polynomials. Such polynomials were obtained, using the Kharitonov theorem, to reflect wide loading conditions on characteristic equation coefficients. For this purpose the explicit analytical forms for the coefficients of the system transfer functions were derived. Simulation results illustrated the

effectiveness of the proposed stabilizer as it was applied to the original nonlinear differential equations describing system dynamics under wide loading conditions at lagging and leading power factors [45].

Milanovic investigated dynamic interactions among various Controllers used for stabilizing a synchronous generator .The effectiveness of a PSS connected to the exciter and/or governor in damping electromechanical oscillations of isolated synchronous generator was examined. The interactions among PSSs connected to the exciter and/or the governor loop, automatic voltage regulator, governor and multi-stage double-reheat turbine and dynamic load were considered. It was shown that depending on the type and number of controllers used and dynamics modeled, interactions could result in unstable operation of the system for a range of operating conditions. It was also shown that the PSS connected to the governor loop provides better damping of low-frequency oscillations and better robustness of the generator to a change in operating conditions than the PSS connected to the exciter loop. The paper further showed that a properly tuned PSS connected to governor loop could provide better overall damping of the system oscillations [46].

Shaoru Zhang and Fang Lin Luo discuss a new improved SAC based on quadratic performance index was proposed and adopted to the design of power system stabilizer. This control algorithm can simplify the controller structure and degrade the computing complexity. This approach can track the reference model and decrease the control increment. It also can improve the dynamic and static characteristic of the system because this law simultaneously takes in the increment of the control quantity and the sampling values of state error in  $k$  and  $k+1$ , and simulates the dynamic and transient stability of a synchronous generator active power. The results show that this stabilizer provides more effective damping than the conventional PSS, suppress the low frequency oscillation and improve the stability of the power system during its entire operating point[48].

M.A. Abido, proposed three novel approaches to improve a conventional PSS in a SMIB system. These improved stabilizers used the conventional PSS in the usual manner plus modification of the terminal voltage feedback signal to the excitation system as a function of the accelerating power on the unit. The nonlinear action increased the power system stability greatly. It was concluded that these three kinds of improved stabilizers can improve power system stability much more than the conventional PSS which has been used widely in power systems since the 1970's. Compared to the three kinds of improved stabilizers, the improved PSS is the best one since it is effective for both small and large disturbances, and is also effective to improve both overshoot and settling time of rotor speed deviations [60].

Chen et al discussed a new self-optimizing pole shifting control strategy for an adaptive PSS. Based on an identified model of the system, the control was computed by an algorithm which shifted the closed loop poles of the system to some optimal locations inside the unit circle in the z-domain to minimize a given performance criterion. With the self-optimization property, outside intervention in the controller design procedure was minimized and simplified the tuning procedure during commissioning. Also, a new method of calculating the variable forgetting factor in real-time parameter identification was discussed. For real-time control, a low order system model could be used to represent the controlled system. The proposed control strategy based on a pole-shifting approach combined the advantages of pole assignment control algorithm and minimum variance control algorithm. The closed loop pole locations were optimally calculated by the control algorithm in order to minimize the given performance index. The results for various conditions showed that the proposed adaptive stabilizer could provide good damping over a wide frequency range and increased the dynamic and transient stability margins [54].

Gupta et al designed PSS for a SMIB using periodic output feedback. The non-linear model of a machine was linearized at different operating points and

16 linear plant models were obtained. For each of these plants an output injection gain was obtained using the LQR technique. A robust periodic output feedback gain which realized these output gains was obtained using an LMI approach. This robust periodic output control was applied to a non-linear plant model of the machine at different operating points. This method did not require the complete set of states of the system for feedback and was easily implementable. The slip signal was taken as output and the periodic output feedback control was applied at an appropriate sampling rate. This method was more general in nature than the static output feedback method, and also required small magnitudes of the control inputs for these plants. It was found that the robust controller designed provided good damping enhancement for various operating points of a single-machine system connected to an infinite bus [59]. Chow et al discussed the practical experience in assigning PSS projects to provide the designer with a challenging design problem using three different techniques. The design of PSS projects using root-locus, frequency domain, and state-space methods were provided. The projects provided the designer with some realistic and challenging design experience and exposed them to a well-known power system design problem. A saturation block could be added to the output of the PSS to limit its contribution in the voltage regulator input. In [56] Hui Ni et al proposed a supervisory level PSS (SPSS) using wide area measurement. The robustness of the proposed controller was capable of compensating for the nonlinear dynamic operation of power systems and uncertain disturbances. The coordination of the robust SPSSs and local PSSs was implemented based on the principles of multi agent system theory. This theory was an active branch of applications in distributed artificial intelligence (DAI). The performance of the robust controller as a power system stability agent was studied using a 29-machine 179-bus power system. Using wide area measurements, the robust controller was a supervisory level controller that could track system inter-area dynamics online. An LMI-based method was applied to design controllers. Based on the

concept of multi agent systems, the robust controllers were embedded into a system-intelligent agent, which was coordinated with local agents to increase system damping. Based on limited testing, the simulation results showed that the proposed robust controller could effectively damp system oscillations under wide range of operating conditions [55]. Ellices et al discussed a physical interpretation of two state feedback controllers for damping power system electromechanical oscillations. They had been developed by Electricité de France (EDF). The first one was called the desensitized four loop regulator (DFLR) and it was designed to damp local electromechanical oscillations. It was a robust controller which offered good performance despite the variations of the generator operating conditions. The second controller was called the extended desensitized four loop regulator (EDFLR) and it was designed to address both local and inter-area oscillations. The physical interpretation was accomplished by converting the state feedback scheme to the standard structure formed with an AVR plus a PSS. Two widely used PSS design methods based on eigenvalue sensitivities and frequency response were reviewed to obtain the interpretation. The DFLR could be interpreted controller which provided the suitable phase compensation according to these two PSS design methods over a wider frequency range. The EDFLR could be interpreted as a controller which maximized its robustness under uncertainties at both PSS output and the input of the plant. The EDFLR achieved a better compromise between the damping ratio of the local and inter-area modes, and it was robust not only under uncertainties at the output of the PSS but also under uncertainties at the input of the plan [57].

# **CHAPTER THREE**

## **DESIGN OF POWER SYSTEM STABILIZER IN SIGLE MACHINE CONECTED INFINIT BUS**

### **3.1 Introduction**

Small-signal oscillations in a synchronous generator, particularly when it is connected to the power system through a long transmission line, are a matter of concern since before. As long transmission lines interconnect geographically vast areas, it is becoming difficult to maintain synchronism between different parts of the power system. Moreover, long lines reduce load ability of the power system and make the system weak, which is associated with inter-area oscillations during heavy loading. The phenomenon of small signal or small disturbance stability of a synchronous machine connected to an infinite bus through external reactance has been studied in by means of block diagrams and frequency response analysis. The objective of this analysis is to develop insights into the effects of excitation systems, voltage regulator gain, and stabilizing functions derived from generator speed and working through the voltage reference of the voltage regulator. The analysis based on linearization technique is ideally suitable for investigating problems associated with the small-signal oscillations. In this technique, the characteristics of a power system can be determined through a specific operating point and the stability of the system is clearly examined by the system eigenvalues. This chapter describes the linearized model of a single-machine infinite bus (SMIB) system given by Heffron and Philips that investigates the local mode of oscillations in the range of frequency 1-3 Hz. Voltage stability or dynamic voltage stability can be analyzed by monitoring the eigenvalues of the linearized power system with progressive loading. Instability occurs when a pair of complex conjugate eigenvalues crosses the right half of s-plane. This is referred to as dynamic voltage instability, and mathematically, this phenomenon is called Heffron bifurcation. The following

steps have been adopted sequentially to analyze the small-signal stability performance of an SMIB system [10].

1. The differential equations of the flux-decay model of the synchronous machine are linearized and a state-space model is constructed considering exciter output  $\Delta E_{fd}$  as input.

2. From the resulting linearized model, certain constants known as the K constants ( $K_1$ – $K_6$ ) are derived. They are evaluated by small-perturbation analysis on the fundamental synchronous machine equations and hence are functions of machine and system impedances and operating point.

3. The model so obtained is put in a block diagram form and a fast-acting exciter between terminal voltage  $\Delta V_t$  and exciter output  $\Delta E_{fd}$  is introduced in the block diagram.

4. The state-space model is then used to examine the eigenvalues and to design supplementary controllers to ensure adequate damping of the dominant modes. The real parts of the electromechanical modes are associated with the damping torque and the imaginary parts contribute to the synchronizing torque.

The following assumptions are generally made to analyze the small-signal stability problem in an SMIB power system:

- 1- The mechanical power input remains constant during the period of transient.
- 2- Stator resistance is equal to zero.
- 3- The synchronous machine can be represented by a constant voltage source (electrically) behind the transient reactance.
- 4- The mechanical angle of the synchronous machine rotor coincides with the electric phase angle of the voltage behind transient reactance.
- 5- No local load is assumed at the generator bus; if a local load is fed at the terminal of the machine, it is to be represented by constant impedance (or admittance)

### 3.2 Dynamic Model of Synchronous Machine

The differential algebraic equations of the synchronous machine of the flux-decay model with fast exciter .The Figure (3.1) configuration of Single Machine connected infinite bus.

$$\frac{dE'_q}{dt} = -\frac{1}{T'_{do}} (E'_q + (X_d - X'_d)I_d - E_{fd}) \quad (3.1)$$

$$\frac{d\delta}{dt} = \omega - \omega_o \quad (3.2)$$

$$\frac{d\omega}{dt} = \frac{\omega_s}{2H} [T_M - (E'_q I_q + ((X_q - X'_d)I_d I_q + D(\omega - \omega_o))] \quad (3.3)$$

$$\frac{dE_{fd}}{dt} = -\frac{E_{fd}}{T_A} + \frac{K_A}{T_A} (V_{ref} - V_t) \quad (3.4)$$

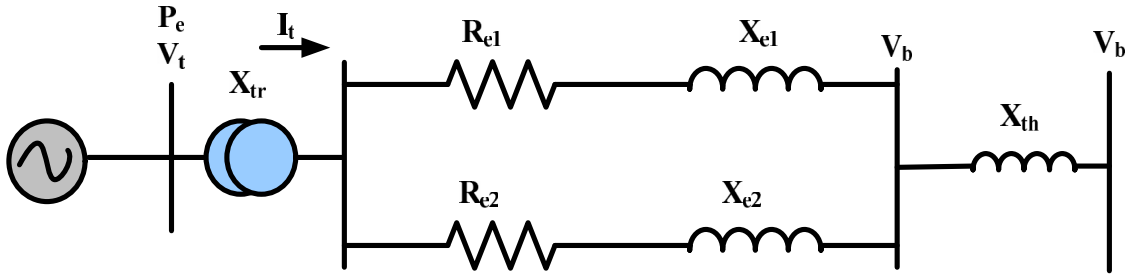


Figure (3.1) Configuration of single machine connected in finite bus

Where the state variables are

$E'_d \equiv$  direct axis component of voltage behind transient reactance

$E'_q \equiv$  quadrature axis component of voltage behind transient reactance

$\omega \equiv$  Angular velocity of rotor,  $\delta \equiv$  Rotor angle in radians, and

$$T_e = E'_d I_d + E'_q I_q - (X_q - X'_q) I_q I_d, \quad (3.5)$$

$$\tau_j = 4\pi f H \quad (3.6)$$

$x_d \equiv$  direct axis synchronous reactance,  $x_q \equiv$  quadrature axis synchronous reactance,  $x_d' \equiv$  direct axis transient reactance,  $x_q' \equiv$  quadrature axis transient reactance,  $\tau_{do}' \equiv$  quadrature axis open circuit time constant,  $\tau_{do} \equiv$  direct axis open circuit time constant,  $T_e \equiv$  electrical torque of synchronous machine,  $T_m \equiv$  mechanical torque of synchronous machine,  $D \equiv$  damping coefficient of synchronous machine,  $E_{FD} \equiv$  Equivalent stator emf corresponding to field voltage,  $I_q \equiv$  quadrature axis armature current,  $I_d \equiv$  direct axis armature current,  $H \equiv$  inertia constant of synchronous machine in sec,  $f \equiv$  frequency in Hz.

### 3.3 Stator Equation

The synchronous stator equations is written as below

$$V_t \sin(\delta - \theta) + R_s I_s - X_q I_q = 0 \quad (3.7)$$

$$E'_q - V_t \cos(\delta - \theta) - R_s I_s - X'_q I_q = 0 \quad (3.8)$$

As it is assumed stator resistance  $R_s=0$  and  $V_t$  denote the magnitude of the generator terminal voltage, the earlier-mentioned equations are reduced to

$$X_q I_q - V_t \sin(\delta - \theta) = 0 \quad (3.9)$$

$$E'_q - V_t \cos(\delta - \theta) - X'_q I_q = 0 \quad (3.10)$$

Now

$$(V_d + jV_q)e^{j(\delta - \frac{\pi}{2})} = V_t e^{j\theta}, V_d + jV_q = V_t e^{j\theta} \cdot e^{-j(\delta - \frac{\pi}{2})} \quad (3.11)$$

Expansion of the right-hand side results in

$$V_d + jV_q = V_t \sin(\delta - \theta) + jV_t \cos(\delta - \theta)$$

Therefore

$$V_d = V_t \sin(\delta - \theta) \& V_q = V_t \cos(\delta - \theta)$$

Substitution of  $V_d$  and  $V_q$  in Equations (3.6) and (3.7) gives

$$X_q I_q - V_d = 0 \quad (3.12)$$

$$E'_q - V_q - X'_d I_d = 0 \quad (3.13)$$

### 3.4 Network Equation

The equation of the Power System Network is gives

$$(I_d + I_q)e^{j(\delta - \frac{\pi}{2})} = \frac{V_t \angle \theta^\circ - V_\infty \angle \theta^\circ}{R_e + jX_e} \quad (3.14)$$

$$(I_d + I_q)e^{j(\delta - \frac{\pi}{2})} = \frac{(V_d + jV_q)e^{j(\delta - \frac{\pi}{2})} - V_\infty \angle \theta^\circ}{R_e + jX_e} \quad (3.15)$$

$$I_d R_e + jI_q R_e + jI_d X_e - I_q X_e = (V_d + jV_q) - V_\infty \quad (3.16)$$

$$(I_d R_e - I_q X_e) + j(I_q R_e + I_d X_e) = (V_d - V_\infty \sin \delta + j(V_q - V_\infty \cos \delta) \quad (3.17)$$

$$(I_d R_e - I_q X_e) = V_d - V_\infty \sin \delta \quad (3.18)$$

$$(I_q R_e + I_d X_e) = V_q - V_\infty \cos \delta \quad (3.19)$$

### 3.5 Linearization Process and State-Space Model

The linearization model of SMIB is obtained using the following steps:

**Step I:** The linearization of the stator algebraic equations (3.12)

and (3.13) gives

$$X_q \Delta I_q - \Delta V_d = 0 \quad (3.20)$$

$$\Delta E'_q - \Delta V_q - X'_d \Delta I_d = 0 \quad (3.21)$$

Rearranging Equations (2.18) and (2.19) gives

$$\Delta V_d = X_q \Delta I_q \quad (3.22)$$

$$\Delta V_q = -X'_d \Delta I_d + \Delta E'_q \quad (3.23)$$

Writing Equations (2.20) and (2.21) in matrix form gives

$$\begin{bmatrix} \Delta V_d \\ \Delta V_q \end{bmatrix} = \begin{bmatrix} 0 & X_q \\ -X'_d & 0 \end{bmatrix} \begin{bmatrix} \Delta I_d \\ \Delta I_q \end{bmatrix} + \begin{bmatrix} 0 \\ \Delta E'_q \end{bmatrix} \quad (2.24)$$

**Step II:** The linearization of the load-flow equations (3.18) and (3.19) results in

$$(\Delta I_d R_e - \Delta I_q X_e) = \Delta V_d - V_\infty \cos \delta \Delta \delta \quad (3.25)$$

$$(\Delta I_q R_e + \Delta I_d X_e) = \Delta V_q - V_\infty \sin \delta \Delta \delta \quad (3.26)$$

Rearranging Equations (2.23) and (2.24) gives

$$\Delta V_d = \Delta I_d R_e - \Delta I_q X_e + V_\infty \cos \delta \Delta \delta \quad (2.27)$$

$$\Delta V_q = \Delta I_d R_e + \Delta I_q X_e - V_\infty \sin \delta \Delta \delta \quad (3.28)$$

Writing Equations (3.25) and (3.26) in matrix form gives

$$\begin{bmatrix} \Delta V_d \\ \Delta V_q \end{bmatrix} = \begin{bmatrix} R_e & -X_e \\ X_e & R_e \end{bmatrix} \begin{bmatrix} \Delta I_d \\ \Delta I_q \end{bmatrix} + \begin{bmatrix} V_\infty \cos \delta \\ -V_\infty \sin \delta \end{bmatrix} \Delta \delta \quad (3.29)$$

**Step III:** Equating the right-hand side of Equations (3.24) and (3.29) gives

$$\begin{bmatrix} R_e & -X_e \\ X_e & R_e \end{bmatrix} \begin{bmatrix} \Delta I_d \\ \Delta I_q \end{bmatrix} + \begin{bmatrix} V_\infty \cos \delta \\ -V_\infty \sin \delta \end{bmatrix} \Delta \delta = \begin{bmatrix} 0 & X_q \\ -X'_d & 0 \end{bmatrix} \begin{bmatrix} \Delta I_d \\ \Delta I_q \end{bmatrix} + \begin{bmatrix} 0 \\ \Delta E'_q \end{bmatrix} \quad (3.30)$$

$$\left( \begin{bmatrix} R_e & -X_e \\ X_e & R_e \end{bmatrix} + \begin{bmatrix} 0 & X_q \\ -X'_d & 0 \end{bmatrix} \right) \begin{bmatrix} \Delta I_d \\ \Delta I_q \end{bmatrix} = \begin{bmatrix} 0 \\ \Delta E'_q \end{bmatrix} \begin{bmatrix} V_\infty \cos \delta \\ -V_\infty \sin \delta \end{bmatrix} \Delta \delta \quad (3.31)$$

$$\begin{bmatrix} R_e & -(X_e + X_q) \\ (X_e + X'_d) & R_e \end{bmatrix} \begin{bmatrix} \Delta I_d \\ \Delta I_q \end{bmatrix} = \begin{bmatrix} 0 \\ \Delta E'_q \end{bmatrix} + \begin{bmatrix} V_\infty \cos \delta \\ -V_\infty \sin \delta \end{bmatrix} \Delta \delta \quad (3.32)$$

$$\begin{bmatrix} R_e & -(X_e + X_q) \\ (X_e + X'_d) & R_e \end{bmatrix}^{-1} = \frac{1}{\Delta_e} \begin{bmatrix} R_e & (X_e + X_q) \\ -(X_e + X'_d) & R_e \end{bmatrix} \quad (3.33)$$

Where

$$\Delta_e = R_e^2 + (X_e + X_q)(X_e + X'_d)$$

Solving for  $\Delta I_d$  and  $\Delta I_q$  from Equation (3.32) results in

$$\begin{bmatrix} \Delta I_d \\ \Delta I_q \end{bmatrix} = \begin{bmatrix} 0 \\ \Delta E'_q \end{bmatrix} \begin{bmatrix} R_e & -(X_e + X_q) \\ (X_e + X'_d) & R_e \end{bmatrix}^{-1} + \begin{bmatrix} -V_\infty \cos \delta \\ V_\infty \sin \delta \end{bmatrix} \Delta \delta \cdot \begin{bmatrix} R_e & -(X_e + X_q) \\ (X_e + X'_d) & R_e \end{bmatrix}^{-1} \quad (3.34)$$

$$\begin{bmatrix} \Delta I_d \\ \Delta I_q \end{bmatrix} = \frac{1}{\Delta_e} \begin{bmatrix} 0 \\ \Delta E'_q \end{bmatrix} \begin{bmatrix} R_e & (X_e + X_q) \\ -(X_e + X'_d) & R_e \end{bmatrix} + \frac{1}{\Delta_e} \begin{bmatrix} -V_\infty \cos \delta \\ V_\infty \sin \delta \end{bmatrix} \Delta \delta \cdot \begin{bmatrix} R_e & (X_e + X_q) \\ -(X_e + X'_d) & R_e \end{bmatrix} \quad (3.35)$$

i.e.

$$\begin{bmatrix} \Delta I_d \\ \Delta I_q \end{bmatrix} = \frac{1}{\Delta_e} \begin{bmatrix} (X_e + X_q) \Delta E'_q \\ R_e \Delta E'_q \end{bmatrix} + \frac{1}{\Delta_e} \begin{bmatrix} -R_e V_\infty \cos \delta + V_\infty \sin \delta (X_e + X_q) \\ R_e V_\infty \sin \delta + V_\infty \cos \delta (X_e + X'_d) \end{bmatrix} \Delta \delta \quad (3.36)$$

Therefore:

$$\begin{bmatrix} \Delta I_d \\ \Delta I_q \end{bmatrix} = \frac{1}{\Delta_e} \begin{bmatrix} (X_e + X_q) & -R_e V_\infty \cos \delta + V_\infty \sin \delta (X_e + X_q) \\ R_e & R_e V_\infty \sin \delta + V_\infty \cos \delta (X_e + X'_d) \end{bmatrix} \begin{bmatrix} \Delta E'_q \\ \Delta \delta \end{bmatrix} \quad (3.37)$$

**Step IV:** The linearizations of the differential equations (3.1)–(3.4) are as

follows. Here, the frequency is normalized as  $\nu = \frac{\omega}{\omega_s}$  throughout our study:

$$\Delta \dot{E}'_q = -\frac{1}{T'_{do}} \Delta E'_q - \frac{1}{T'_{do}} (X_d + X'_d) \Delta I_d + \frac{1}{T'_{do}} \Delta E'_{fd} \quad (3.38)$$

$$\Delta \dot{\delta} = \omega \Delta V \quad (3.39)$$

$$\Delta\dot{V} = \frac{2}{H}\Delta T_M - \frac{2}{H}\Delta E'_q \cdot I_q - \frac{2}{H}E'_q \cdot I_q - \frac{(X_q - X'_d)}{2H}\Delta I_d I_q - \frac{(X_q - X'_d)}{2H}I_d \Delta I_q - \frac{D\omega_s}{2H}\Delta V \quad (3.40)$$

$$T_A \Delta \dot{E}'_q = -\Delta E'_{fd} + K_A(\Delta V_{ref} - \Delta V_t) \quad (3.41)$$

$$\begin{aligned} \begin{bmatrix} \Delta \dot{E}'_q \\ \Delta \dot{\delta} \\ \Delta \dot{V} \end{bmatrix} &= \begin{bmatrix} \frac{1}{T'_{do}} & 0 & 0 \\ 0 & 0 & \omega_s \\ I_q & 0 & \frac{D\omega_s}{2H} \end{bmatrix} \begin{bmatrix} \Delta E'_q \\ \Delta \delta \\ \Delta V \end{bmatrix} + \begin{bmatrix} -\frac{(X_d - X'_d)}{T'_{do}} & 0 \\ 0 & 0 \\ \frac{I_q(X'_d - X_q)}{2H} & \frac{(X'_d - X_q)}{2H} - \frac{E'_q}{2H} \end{bmatrix} \begin{bmatrix} \Delta I_d \\ \Delta I_q \end{bmatrix} \\ &+ \begin{bmatrix} \frac{1}{T'_{do}} & 0 \\ 0 & 0 \\ 0 & \frac{1}{2H} \end{bmatrix} \begin{bmatrix} \Delta E_{fd} \\ \Delta T_M \end{bmatrix} \end{aligned} \quad (3.42)$$

**Step V:** Obtain the linearized equations in terms of the K constants.

Expressions for  $\Delta I_d$  and  $\Delta I_q$  obtained from Equation (3.37) are

$$\Delta I_d = \frac{1}{\Delta_e} [(X_e - X_q)\Delta E'_q + \{-R_e V_\infty \cos\delta + (X_e - X'_d)V_\infty \sin\delta\}\Delta\delta] \quad (3.43)$$

$$\Delta I_q = \frac{1}{\Delta_e} [R_e \Delta E'_q + \{R_e V_\infty \sin\delta + (X_e - X'_d)V_\infty \cos\delta\}\Delta\delta] \quad (3.44)$$

On substitution of  $I_d$  and  $I_q$  in Equation (3.40), the resultant equations relating the constants  $K_1, K_2, K_3$ , and  $K_4$  can be expressed as

$$\Delta E'_q = -\frac{1}{K_3 T'_{do}} \Delta E'_q - \frac{K_4}{T'_{do}} \Delta\delta + \frac{1}{T'_{do}} \Delta E_{fd} \quad (3.45)$$

$$\Delta \dot{\delta} = \omega_s \Delta V \quad (3.46)$$

$$\Delta \dot{V} = -\frac{K_2}{2H} \Delta E'_q - \frac{D\omega_s}{2H} \Delta V + \frac{1}{2H} \Delta T_M \quad (3.47)$$

**Step VI:** The linearization of generator terminal voltage is as follows: The magnitude of the generator terminal voltage is

$$V_t = \sqrt{V_d^2 + V_q^2}, \quad V_t^2 = V_d^2 + V_q^2 \quad (3.48)$$

The linearization of Equation (3.46) gives

$$2V_t \Delta V_t = 2V_d \Delta V_d + 2V_q \Delta V_q \quad (3.49)$$

Therefore

$$\Delta V_t = \frac{V_d}{V_t} \Delta V_d + \frac{V_q}{V_t} \Delta V_q \quad (3.50)$$

Now, substituting Equation (3.37) into Equation (3.24),

$$\begin{bmatrix} \Delta V_d \\ \Delta V_q \end{bmatrix} = \frac{1}{\Delta_e} \begin{bmatrix} 0 & X_q \\ X_d & 0 \end{bmatrix} \begin{bmatrix} (X_e + X_q) & -R_e V_\infty \cos \delta + V_\infty \sin \delta (X_e + X_q) \\ R_e & R_e V_\infty \sin \delta + V_\infty \cos \delta (X_e + X_d) \end{bmatrix} \begin{bmatrix} \Delta E'_q \\ \Delta \delta \end{bmatrix} + \begin{bmatrix} 0 \\ \Delta E'_q \end{bmatrix} \quad (3.51)$$

Or

$$\begin{bmatrix} \Delta V_d \\ \Delta V_q \end{bmatrix} = \frac{1}{\Delta_e} \begin{bmatrix} R_e X_q & X_q (R_e V_\infty \sin \delta + V_\infty (X_e + X_d) \cos \delta) \\ -(X_e + X_q) & -X_d (-R_e V_\infty \cos \delta + V_\infty (X_e + X_q) \sin \delta) \end{bmatrix} \begin{bmatrix} \Delta E'_q \\ \Delta \delta \end{bmatrix} + \begin{bmatrix} 0 \\ \Delta E'_q \end{bmatrix}$$

Therefore

$$\Delta V_d = \frac{1}{\Delta_e} [R_e X_q \Delta E'_q + X_q R_e V_\infty \sin \delta + X_q V_\infty (X_e + X_d) \cos \delta \Delta \delta] \quad (3.50)$$

$$\begin{aligned} \Delta V_q = & [-X_d (X_e + X_q) \Delta E'_q + (X_d R_e V_\infty \cos \delta + X_d V_\infty (X_e + X_q) \sin \delta) \Delta \delta] \\ & + \Delta E'_q \end{aligned} \quad (3.52)$$

Replacing  $\Delta V_d$  and  $\Delta V_q$  from Equations (3.52) and (3.53) in Equation (3.50) results in

$$\Delta V_t = K_5 \Delta \delta + K_6 \Delta E'_q \quad (3.53)$$

### 3.6 Derivation of K Constants

From Equation (3.36), the expression of  $\Delta E'_q$  on substitution of  $\Delta I_d$  is [1]

$$\begin{aligned} \Delta \dot{E}'_q = & \left( -\frac{1}{T_{do}} \Delta E'_q - \frac{1}{T_{do}} (X_d + X'_d) \left( \frac{1}{\Delta_e} [(X_e - X_q) \Delta E'_q + \{-R_e V_\infty \cos \delta + (X_e \right. \right. \\ & \left. \left. - X'_d) V_\infty \sin \delta\} \Delta \delta] \right) + \frac{1}{T_{do}} \Delta E_{fd} \right) \end{aligned} \quad (3.54)$$

$$\begin{aligned} \Delta \dot{E}'_q = & \left( -\frac{1}{T_{do}} \left[ 1 + \frac{(X_d - X'_d)(X_e + X_q)}{\Delta_e} \right] \Delta E'_q - \frac{1}{T_{do}} \frac{V_\infty (X_d + X'_d)}{\Delta_e} \{ (X_e - X_q) \sin \delta \right. \\ & \left. - R_e \cos \delta \} \Delta \delta + \frac{1}{T_{do}} \Delta E_{fd} \right) \end{aligned} \quad (3.55)$$

$$\Delta \dot{E}'_q = -\frac{1}{K_3 T_{do}} \Delta E'_q - \frac{K_4}{T_{do}} \Delta \delta + \frac{1}{T_{do}} \Delta E_{fd} \quad (3.56)$$

$$\frac{1}{K_4} = 1 + \frac{(X_d - X'_d)(X_e + X_q)}{\Delta_e} \quad (3.57)$$

$$K_4 = \frac{V_\infty(X_d - X'_d)}{\Delta_e} [(X_e + X_q)\sin\delta - R_e\cos\delta] \quad (3.58)$$

Again from Equation (3.40), the expression of  $\Delta\dot{V}$  on substitution of  $\Delta I_d$  and  $\Delta I_q$  is

$$\begin{aligned} \Delta\dot{V} = & \left( -\frac{1}{2H}\Delta E'_q \cdot I_q - \frac{(X_q - X'_d)I_q}{2H} \frac{1}{\Delta_e} [(X_e + X_q)\Delta E'_q + \{-R_e V_\infty \cos\delta \right. \\ & + [(X_e + X_q)V_\infty \sin\delta]\Delta\delta] + \left( \frac{(X'_d - X_q)}{2H} I_d - \frac{1}{2H} E'_q \right) \frac{1}{\Delta_e} [R_e \Delta E'_q \\ & + \{R_e V_\infty \sin\delta + (X_e + X_q)V_\infty \cos\delta\}\Delta\delta - \frac{D\omega_s}{2H} \Delta V \\ & \left. + \frac{1}{2H} \Delta T_M \right) \end{aligned} \quad (3.59)$$

$$\begin{aligned} \Delta\dot{V} = & \left( -\frac{1}{2H} \frac{1}{\Delta_e} [I_q \Delta_e - I_q (X'_d - X_q)(X_e - X_q) - R_e I_d (X'_d - X_q) + R_e E'_q] \Delta E'_q \right. \\ & + \frac{V_\infty I_q}{2H \Delta_e} (X'_d - X_q) [(X_e + X_q)\sin\delta - R_e \cos\delta] \Delta\delta \\ & + \frac{V_\infty}{\Delta_e} [\{I_d (X'_d - X_q) - E'_q\} \{(X_e + X'_d)\cos\delta + R_e \sin\delta\}] - \frac{D\omega_s}{2H} \Delta V \\ & \left. + \frac{1}{2H} \Delta T_M \right) \end{aligned} \quad (3.60)$$

This can be written in terms of K constants as

$$\Delta\dot{V} = \frac{K_2}{2H} \Delta E'_q - \frac{K_1}{2H} \Delta\delta - \frac{D\omega_s}{2H} \Delta V + \frac{1}{2H} \Delta T_M \quad (3.61)$$

$$K_2 = \frac{1}{\Delta_e} [I_q \Delta_e - I_q (X'_d - X_q)(X_e - X_q) - R_e I_d (X'_d - X_q) + R_e E'_q] \quad (3.62)$$

$$\begin{aligned} K_1 = & \left( \frac{1}{\Delta_e} [V_\infty I_q (X'_d - X_q) [(X_e + X_q)\sin\delta - R_e \cos\delta] \right. \\ & \left. + V_\infty [(X'_d - X_q) I_d - E'_q] [(X_e + X'_d)\cos\delta + R_e \sin\delta] \right) \end{aligned} \quad (3.63)$$

On substitution of  $\Delta V_d$  and  $\Delta V_q$  in Equation (3.46), it reduces to

$$\begin{aligned} \Delta V_t = \frac{V_d}{V_q} \left[ \frac{1}{\Delta_e} \{ R_e X_q E'_q + R_e X_q V_\infty \sin \delta + X_q V_\infty (X'_d + X_q) \cos \delta \Delta \delta \} \right] \\ + \frac{V_q}{V_t} \left[ \frac{1}{\Delta_e} \{ -X'_d (X_e + X_q) \Delta E'_q + R_e X'_d V_\infty \cos \delta \right. \\ \left. + X'_d V_\infty (X_e + X_q) \sin \delta \Delta \delta \} + \Delta E'_q \right] \end{aligned} \quad (3.64)$$

Or

$$\begin{aligned} \Delta V_t = \left[ \frac{1}{\Delta_e} \left\{ \frac{V_d}{V_t} R_e X_q - \frac{V_d}{V_t} X'_d (X_e + X_q) \right\} + \frac{V_d}{V_t} \right] \Delta E'_q \\ + \left[ \frac{1}{\Delta_e} \left\{ \frac{V_d}{V_t} X_q (R_e V_\infty \sin \delta + V_\infty \cos \delta (X'_d + X_q)) \right. \right. \\ \left. \left. + \frac{V_q}{V_t} X'_d (R_e V_\infty \cos \delta - V_\infty (X'_d + X_q) \sin \delta) \right\} \right] \Delta \delta \end{aligned} \quad (3.65)$$

Therefore, Equation (3.65) can be written in terms of K constants as

$$\Delta V_t = K_5 \Delta \delta + K_6 \Delta E'_q \quad (3.66)$$

$$\begin{aligned} K_5 = \frac{1}{\Delta_e} \left\{ \frac{V_d}{V_t} X_q (R_e V_\infty \sin \delta + V_\infty \cos \delta (X'_d + X_q)) \right. \\ \left. + \frac{V_q}{V_t} X'_d (R_e V_\infty \cos \delta - V_\infty (X'_d + X_q) \sin \delta) \right\} \end{aligned} \quad (3.67)$$

$$K_6 = \frac{1}{\Delta_e} \left\{ \frac{V_d}{V_t} R_e X_q - \frac{V_d}{V_t} X'_d (X_e + X_q) \right\} + \frac{V_d}{V_t} \quad (3.68)$$

Now, the overall linearized machine differential equations (3.45)–(3.47) and the linearized exciter equation (3.43) together can be put in a block diagram shown in Figure (3.2) in this representation, the dynamic characteristics of the system can be expressed in terms of the K constants. These constants ( $K_1$ – $K_6$ ) and the block diagram representation were developed first by Heffron–Phillips and later by de Mello to study the synchronous machine stability as affected by local low-frequency oscillations and its control through excitation system [10].

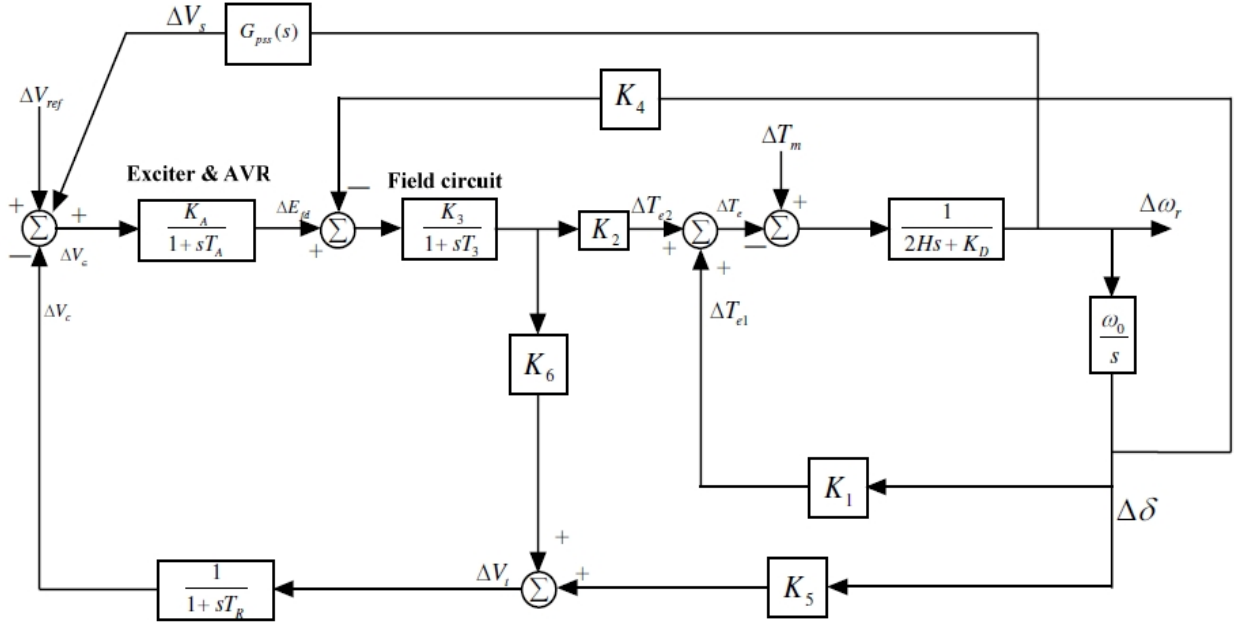


Figure (3.2) Block diagram of the synchronous Machine model

The K constants presented in the block diagram Figure 3.2 are defined as follows:

$K_1 = \frac{\Delta T_e}{\Delta \delta} \Big| E_q$  Change in electric torque for a change in rotor angle with constant flux linkages in the d-axis.

$K_2 = \frac{\Delta T_e}{\Delta E_q} \Big| \delta$  Change in electric torque for a change in d-axis flux linkages with constant rotor angle.

$K_3 = \frac{X_d + X_e}{X_d + X_e}$  The case where the external impedance is a pure reactance  $X_e$ .

$K_4 = \frac{1}{K_3} \frac{\Delta E_q}{\Delta \delta}$  Demagnetizing effect of change in rotor angle.

$K_5 = \frac{\Delta V_t}{\Delta \delta} \Big| E_q$  Change in terminal voltage with change in rotor angle for constant  $E_q$

$K_6 = \frac{\Delta V_t}{\Delta E_q} \Big| \delta$  Change in terminal voltage with change in  $E_q$  for constant rotor angle.

It is evident that the K constants are dependent on various system parameters such as system loading and the external network resistance (Re) and reactance (Xe). Generally, the value of the K constants is greater than zero 0, but under heavy loading condition (high generator output) and for high value of external

system reactance,  $K_5$  might be negative, contributing to negative damping and causing system instability. This phenomenon has been discussed in the following sections based on state space model [10].

The state-space representation of the synchronous machine can be obtained when Equations (3.43), (3.45) and (3.52) are written together in matrix form. Assuming  $T_M = 0$ , the state-space model of the SMIB system without exciter is therefore

$$\begin{bmatrix} \Delta E'_q \\ \Delta \delta \\ \Delta V \end{bmatrix} = \begin{bmatrix} -\frac{1}{K_3 T'_{do}} & -\frac{K_4}{T'_{do}} & 0 \\ 0 & 0 & \omega_s \\ -\frac{K_2}{2H} & -\frac{K_1}{2H} & \frac{D\omega_s}{2H} \end{bmatrix} \begin{bmatrix} \Delta E'_q \\ \Delta \delta \\ \Delta V \end{bmatrix} + \begin{bmatrix} \frac{1}{T'_{do}} \\ 0 \\ 0 \end{bmatrix} \Delta E'_{fd} \quad (3.69)$$

$$V_t = [K_6 \quad K_5 \quad 0] \begin{bmatrix} \Delta E'_q \\ \Delta \delta \\ \Delta V \end{bmatrix} \quad (3.70)$$

$$T_A \Delta E'_{fd} = -E_{fd} + K_A (\Delta V_{ref} + \Delta V_t) \quad (3.71)$$

$$E'_{fd} = \frac{1}{T_A} E_{fd} - \frac{K_A K_5}{T_A} \Delta \delta - \frac{K_A K_6}{T_A} \Delta V + \frac{K_A}{T_A} V_{ref} \quad (3.72)$$

$$\begin{bmatrix} E'_q \\ \delta \\ \dot{V} \\ E_{fd} \end{bmatrix} = \begin{bmatrix} -\frac{1}{K_3 T'_{do}} & -\frac{K_4}{T'_{do}} & 0 & \frac{1}{T'_{do}} \\ 0 & 0 & \omega_s & 0 \\ -\frac{K_2}{2H} & -\frac{K_1}{2H} & \frac{D}{2H} & 0 \\ -\frac{K_A K_6}{T_A} & -\frac{K_A K_5}{T_A} & 0 & -\frac{1}{T_A} \end{bmatrix} \begin{bmatrix} \Delta E'_q \\ \Delta \delta \\ \Delta V \\ \Delta E'_{fd} \end{bmatrix} + \begin{bmatrix} 0 \\ 0 \\ 0 \\ \frac{K_A}{T_A} \end{bmatrix} V_{ref} \quad (3.73)$$

### 3.7 Power System Stabilizer in State Matrix

Assume that the damping  $D$  in the torque loop is zero. The input to the stabilizer is  $V$ . An extra state equation will add. The washout filter stage is omitted since its objective is to offset only the DC steady state error, hence it does not play any role in the design. The added stage equation due to PSS is

$$\dot{V}_{PSS} = -\frac{1}{T_2} V_{PSS} + \frac{K_{PSS}}{T_2} \Delta V + K_{PSS} \frac{T_1}{T_2} \Delta V \quad (3.74)$$

$$V = -\frac{K_2}{2H} E_{fd} - \frac{K_2}{2H} \Delta V \quad (3.75)$$

By substitute eq. (3.75) in (3.76) it gives

$$\dot{V}_{PSS} = -\frac{1}{T_2} \Delta V_{PSS} + \frac{K_{PSS}}{T_2} \Delta V + K_{PSS} \frac{T_1}{T_2} \left( -\frac{K_2}{2H} \Delta E_{fd} - \frac{K_2}{2H} \Delta \delta \right) \quad (3.76)$$

Therefore

$$\dot{V}_{PSS} = -\frac{1}{T_2} \Delta V_{PSS} + \frac{K_{PSS}}{T_2} \Delta V - \frac{K_2 T_1}{T_2} \left( \frac{K_{PSS}}{2H} \right) \Delta E_{fd} - \frac{K_1 T_1}{T_2} \left( \frac{K_{PSS}}{2H} \right) \Delta \delta \quad (3.77)$$

The state matrix of the system model is

$$\begin{bmatrix} \dot{E}_q \\ \Delta \dot{\delta} \\ \Delta \dot{V} \\ \dot{E}_{fd} \\ \dot{V}_{PSS} \end{bmatrix} = \begin{bmatrix} -\frac{1}{K_3 T_{do}} & -\frac{K_4}{T_{do}} & 0 & \frac{1}{T_{do}} & 0 \\ 0 & 0 & \omega_s & 0 & 0 \\ \frac{K_2}{2H} & \frac{K_1}{2H} & \frac{D\omega_s}{2H} & 0 & 0 \\ -\frac{K_A K_6}{T_A} & -\frac{K_A K_5}{T_A} & 0 & -\frac{1}{T_A} & \frac{K_A}{T_A} \\ -\frac{K_2 T_1}{T_2} \left( \frac{K_{PSS}}{2H} \right) & -\frac{K_1 T_1}{T_2} \left( \frac{K_{PSS}}{2H} \right) & \frac{K_{PSS}}{T_2} & 0 & -\frac{1}{T_2} \end{bmatrix} \begin{bmatrix} E_q \\ \Delta \delta \\ \Delta V \\ \Delta E_{fd} \\ \Delta V_{PSS} \end{bmatrix} + \begin{bmatrix} 0 \\ 0 \\ 0 \\ \frac{K_A}{T_A} \\ \frac{K_{PSS}}{T_2} \end{bmatrix} \Delta V_{ref} \quad (3.78)$$

## 3.8 Analysis of Power oscillations in Single Machine

### Infinite Bus (SMIB)

The small-signal stability response of this system has been examined further by plotting the rotor speed deviation under different scenarios for a unit change in mechanical step power input with a reasonable simulation time of 10 s. The Simulink block diagram of Synchronous Machine showing in Figure (3.3)

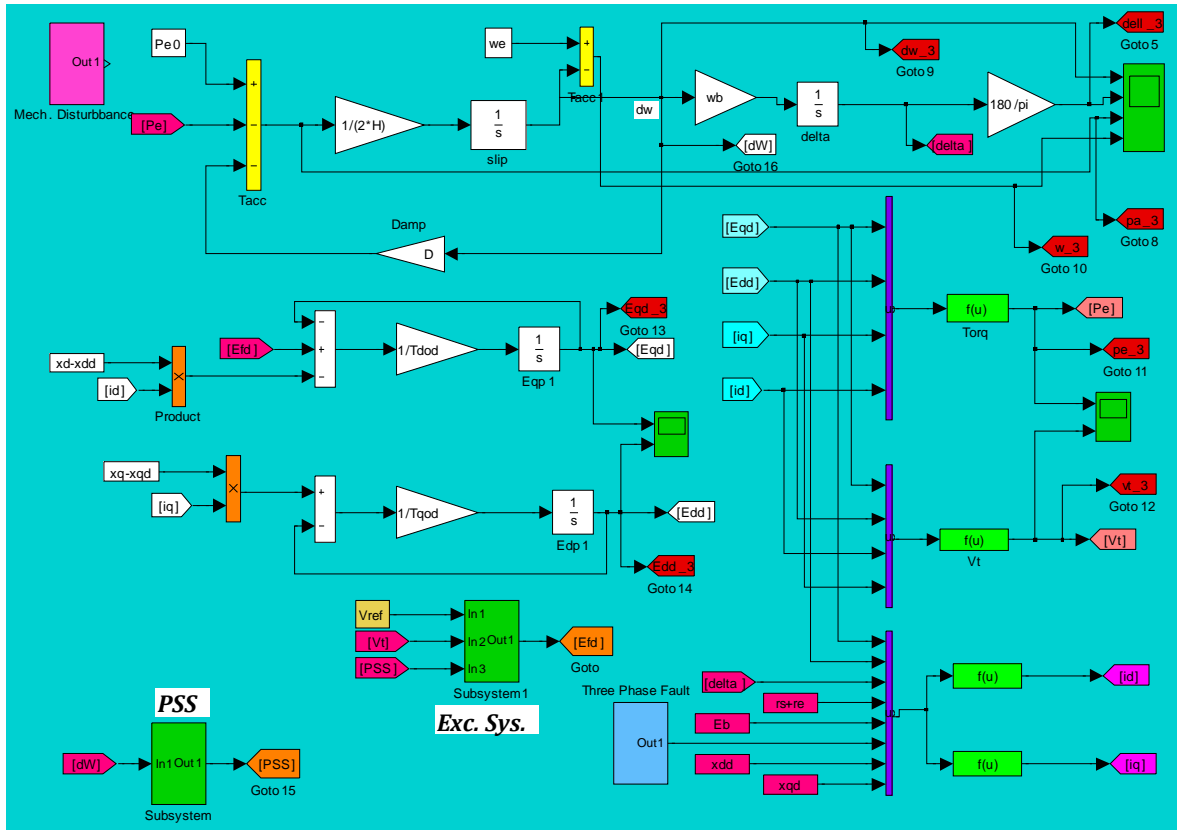


Figure (3.3) Simulink block diagram of single machine

### 3.8.1 Normal Load ( $P=1.0, Q=0.015 \text{ p.u.}$ ).

The Table (A.1) show the eigenvalue, nature frequency and damping ratio of single machine connected in finite bus system. The result shows the damping ratio increase after insert excitation system and power system stabilizer. The Figure (3.4) shows time response of speed deviation without controller and with controller, from the results the PSS having good settle time than the excitation system.

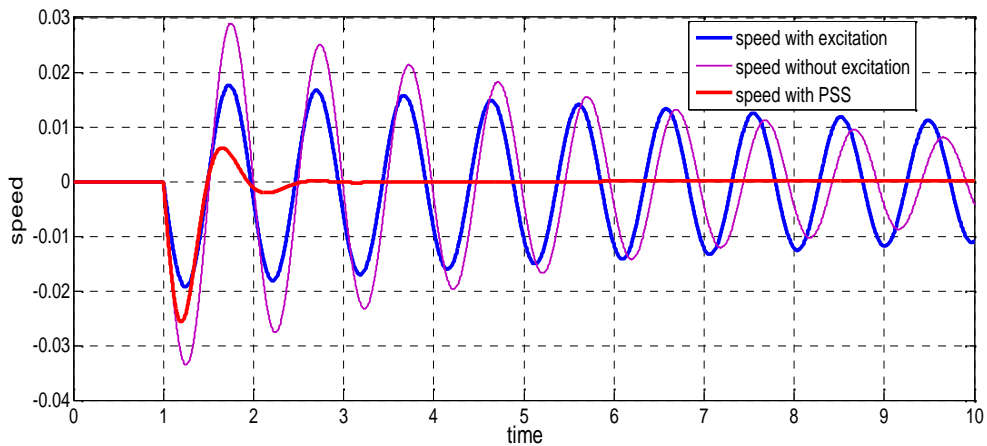


Figure (3.4) Speed deviation response in case of normal load

### 3.8.2 Heavy Load

The Table (A.2 ) show the eigenvalue, nature frequency and damping ratio of single machine connected in finite bus system. In case of heavy load ( $P=1.1$ ,  $Q=0.4$ ) p.u The results shows the damping ratio decrease after insert excitation system and power system stabilizer that cause system instability. The figure (3.5) shows time response of speed deviation without controller and with controller, from the results heavy load causes system to high amplitude of oscillations than normal load.

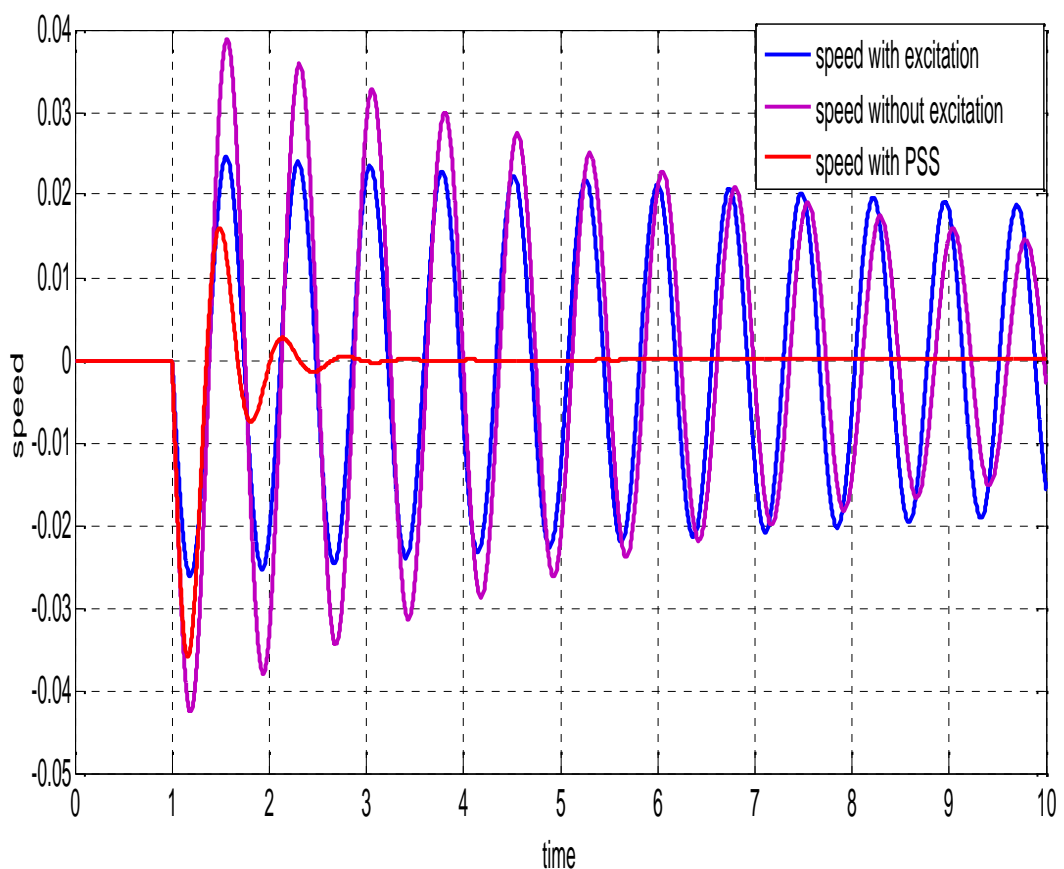


Figure (3.5) Speed deviation response in case of heavy load

### 3.8.3 Light load

In case of light load ( $p=0.3$ ,  $Q=0.015$ ) p.u the PSS settle the speed deviation during first cycle. The figure (3.6) shows time response of speed deviation with and without controller in case of light load and the table (A.3 ) show the eigenvalue, nature frequency and damping ratio of single machine connected in finite bus.

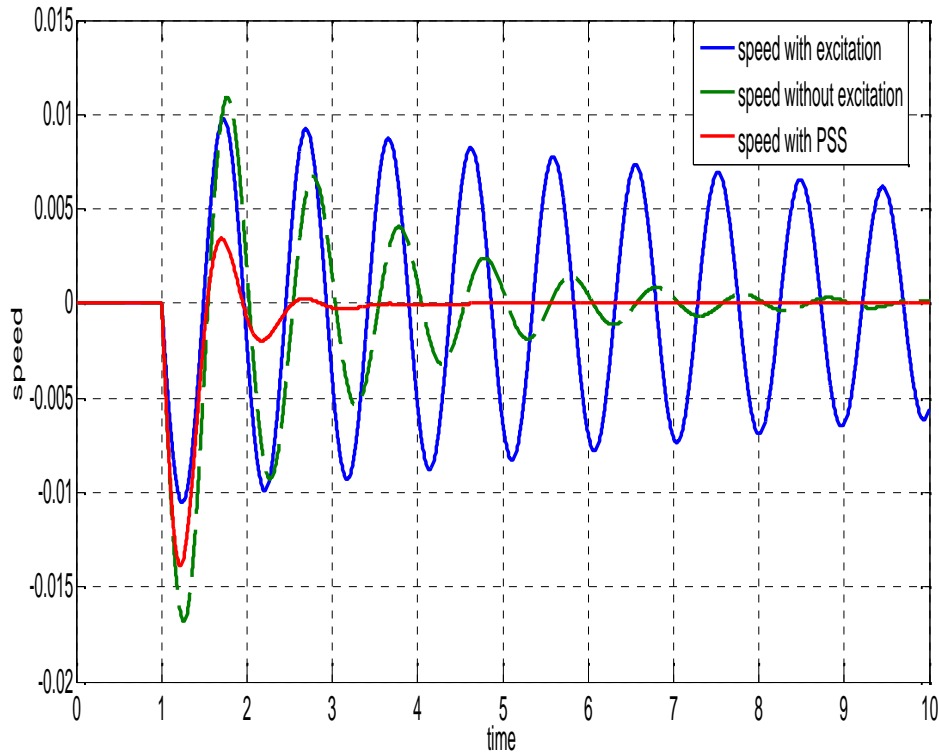


Figure (3.6) speed deviation response in case of light load

### 3.8.4 Leading Power Factor

In case of leading power factor the system growth instability during increasing time but after install the PSS settle the speed deviation during first cycle. The figure (3.7) shows time response of speed deviation with and without controller in case of leading power factor and the table ( A.4 ) show the eigenvalue, nature frequency and damping ratio of single machine connected in finite bus.

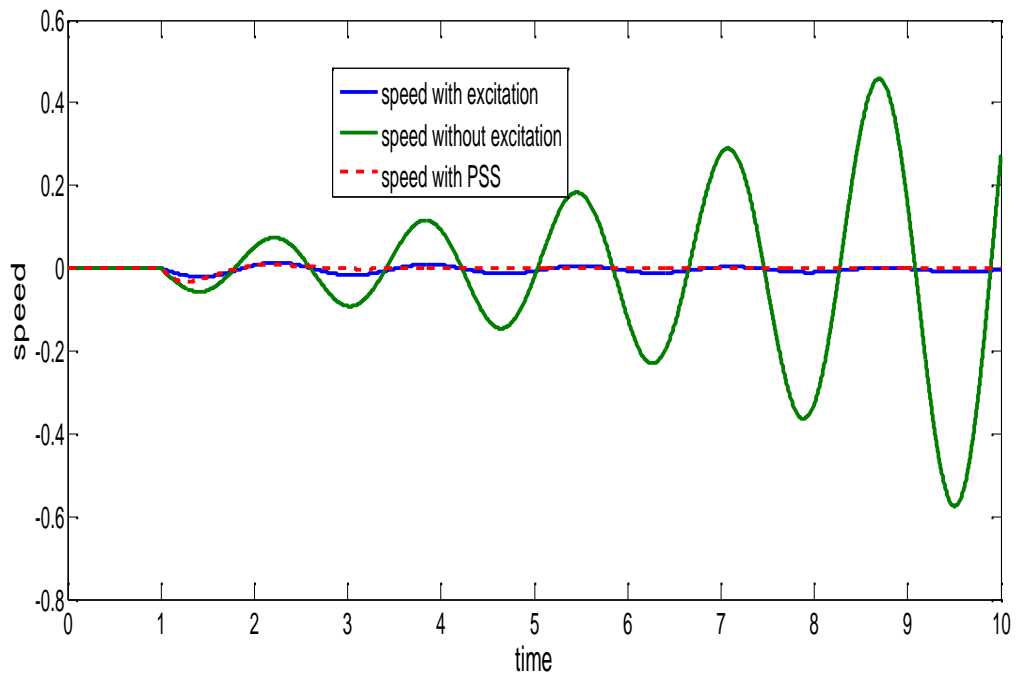


Figure (3.7) speed deviation response in case of leading power factor

### 3.9 Effect of Excitation Gain

The gain of excitation the system effect stability in case of heavy load the increasing of excitation gain effect the system stability during limit range The figure(3.8) shows effect of excitation system gain on speed deviation with and without controller in case of heavy load.

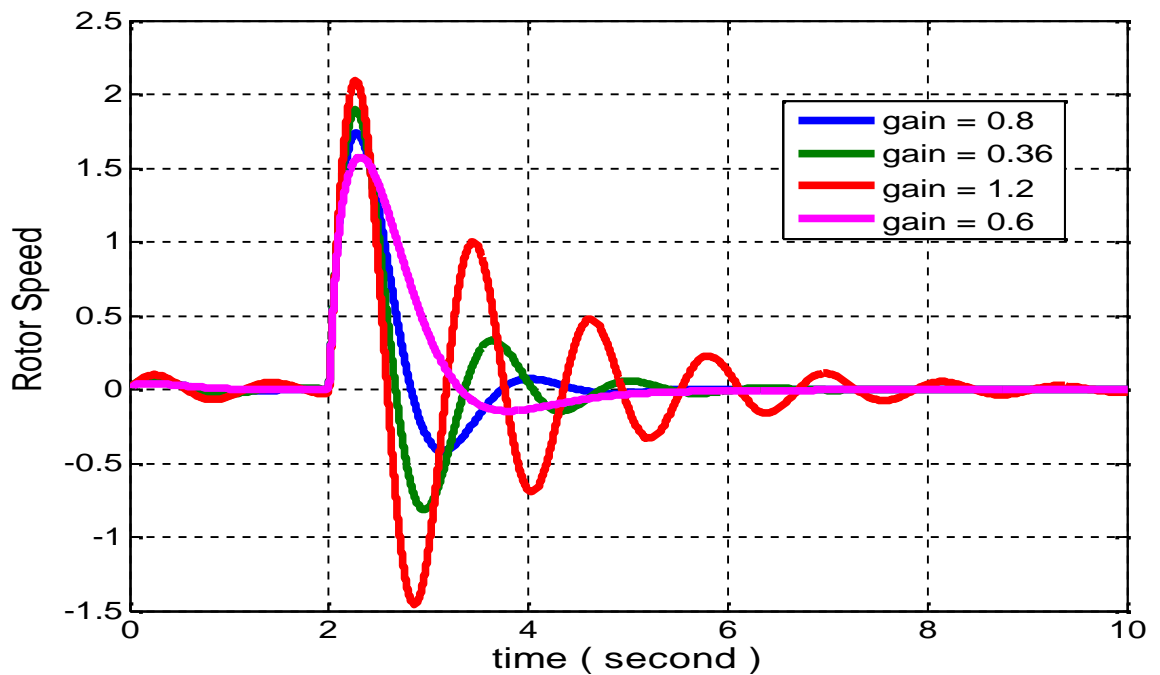


Figure (3.8) Effect of excitation system gain on speed deviation

## CHAPTER FOUR

### DYNAMIC STABILITY OF MULTIMACHINE POWER SYSTEM

#### 4.1 Model of Multi machine Power System

In stability analysis of a multi-machine system, modeling of all the machines in a more detailed manner is exceedingly complex in view of the large number of synchronous machines to be simulated. Therefore simplifying assumptions and approximations are usually made in modeling the system. In this thesis two axis models is used for all machines in the sample system taken for investigation. Models for power system components have to be selected according to the purpose of the system study, and hence, one must be aware of what models in terms of accuracy and complexity should be used for a certain type of system studies, while keeping the computational burden as low as possible. Selecting improper models for power system components may lead to erroneous conclusions [58]. Also one is required to have necessary background knowledge in order to understand the actual process that takes place in the power system in order to design a power system simulation as closely as possible. The mathematical models needed for small signal analysis of synchronous machine, excitation system and the lead-lag power system stabilizer are will need to model. To formulate multi machine small-signal model, the following assumptions are made without loss of generality

1. Mechanical power input is constant.
2. Constant-voltage behind transient- reactance model for the synchronous machines is valid.
3. The mechanical rotor angle of a machine coincides with the angle of the voltage behind transient- reactance.
4. Loads are represented by passive impedances.

#### 4.2 Two-axis Model of Multi machine System

The asynchronous generator can be mathematically described by a set of differential and algebraic equations [4].

$$X = (X, V, T_m, t) \quad (4.1)$$

Where  $X$  is a vector of state variables,  $V$  is a vector of voltages, and  $T_m$ , is the mechanical torque. The dimension of the vector  $x$  depends on the model used. For convenience we will use a complex notation defined as follows. For machine  $i$  we define the phases  $I_i$  and  $\bar{V}_i$

$$\bar{V}_i = V_{qi} + jV_{di} \quad \bar{I}_i = I_{qi} + jI_{di} \quad (4.2)$$

$$V_{qi} \triangleq v_{qi}/\sqrt{3}, \quad V_{di} \triangleq v_{di}/\sqrt{3}, \quad I_{qi} \triangleq i_{qi}/\sqrt{3}, \quad I_{di} \triangleq i_{di}/\sqrt{3} \quad (4.3)$$

$$\bar{V} \triangleq \begin{bmatrix} V_{q1} + V_{d1} \\ V_{q2} + V_{d2} \\ \dots \\ V_{qn} + V_{dn} \end{bmatrix} = \begin{bmatrix} \bar{V}_1 \\ \bar{V}_2 \\ \dots \\ \bar{V}_n \end{bmatrix} \quad \bar{I} \triangleq \begin{bmatrix} I_{q1} + I_{d1} \\ I_{q2} + I_{d2} \\ \dots \\ I_{qn} + I_{dn} \end{bmatrix} = \begin{bmatrix} I_1 \\ I_2 \\ \dots \\ I_n \end{bmatrix} \quad (4.4)$$

Using the block diagram reduction technique and with the simplifying assumptions the state equations for the two-axis model in p.u. form

$$E'_d = \frac{\{-E'_d - (X_q - X'_q)I_q\}}{\tau'_{qo}} \quad (4.5)$$

$$E'_q = \{E_{FD} - E'_q - (X_d - X'_d)I_q\}/\tau'_{do} \quad (4.6)$$

$$p = \frac{\{T_m - D\omega - T_e\}}{\tau_j} \quad (4.7)$$

$$p = -1 \quad (4.8)$$

### 4.3 Matrix Representation of a Passive Network

Consider the multi machine system shown in Figure (4:1). The network has  $n$  machines and  $r$  loads, and, the terminal voltages  $\bar{V}_i$ , for  $i = 1, 2, \dots, n$ , instead of the internal EMF'S. Since the loads are represented by constant impedances, the network has only  $n$  active sources. Note also that the impedance equivalents of the loads are obtained from the pre transient conditions in the system [4].

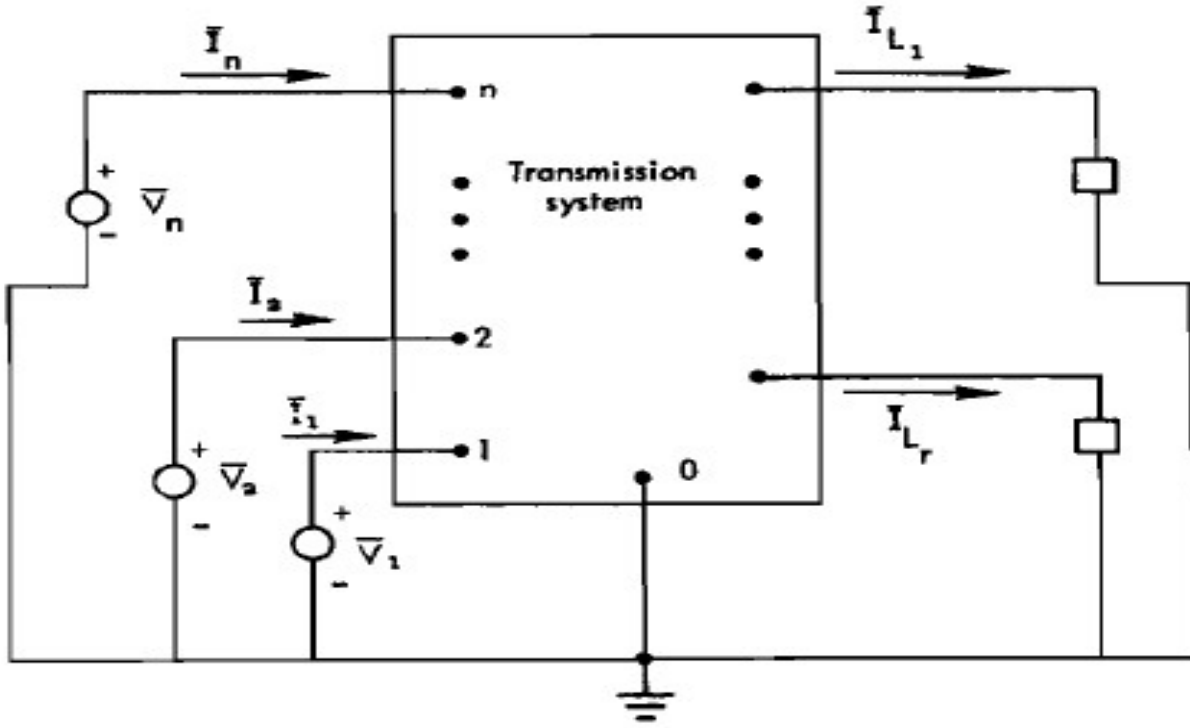


Figure (4.1) Configuration of multi-machine power system

$$I = \bar{Y}\bar{V} \quad (4.9)$$

$$I \triangleq \begin{bmatrix} I_1 \\ I_2 \\ \dots \\ I_n \end{bmatrix} \bar{V} \triangleq \begin{bmatrix} \bar{V}_1 \\ \bar{V}_2 \\ \dots \\ \bar{V}_n \end{bmatrix} \quad (4.10)$$

$$V_k = l_k i_k + r_k i_k \quad k = 1, 2, \dots, b \quad (4.11)$$

$$V_{abck} = l_k i_{abck} + r_k i_{abck} \quad k = 1, 2, \dots, b \quad (4.12)$$

$$PV_{abck} = l_k Pi_{abck} + r_k Pi_{abck} \quad (4.13)$$

$$Pi_{abck} = i_{odq} - w \begin{bmatrix} 0 \\ -i_q \\ i_d \end{bmatrix} \quad (4.14)$$

$$V_{odqk} = l_k \left( i_{odqk} - w \begin{bmatrix} 0 \\ -i_{qk} \\ i_{dk} \end{bmatrix} \right) + r_k i_{odqk} \quad (4.15)$$

$$V_{dqk} = l_k \left( i_{dqk} + w \begin{bmatrix} i_{qk} \\ -i_{dk} \end{bmatrix} \right) + r_k i_{dqk} \quad (4.16)$$

$$V_{dqk} = r_k i_{dqk} + x_k \begin{bmatrix} i_{qk} \\ -i_{dk} \end{bmatrix} \quad k = 1, 2, \dots, b \quad (4.17)$$

$$i = w_r t^+ / 2 + i \quad (4.18)$$

$$\bar{V}_{dk(i)} = r_k \dot{I}_{qk(i)} - x_k \dot{I}_{dk(i)}, \bar{V}_{qk(i)} = r_k \dot{I}_{dk(i)} + x_k \dot{I}_{qk(i)} \quad (4.19)$$

$$\bar{V}_{k(i)} = V_{qk(i)} + jV_{dk(i)} = (r_k \dot{I}_{qk(i)} - x_k \dot{I}_{dk(i)}) + j(r_k \dot{I}_{dk(i)} + x_k \dot{I}_{qk(i)}) = (r_k + jx_k)(\dot{I}_{qk} + j\dot{I}_{dk}) \quad \bar{V}_{k(i)} = \bar{Z}_k \bar{I}_{k(i)} \quad k = 1, 2, \dots, b_i] \quad (4.20)$$

#### 4.4 Converting to a common reference frame

To obtain general network relationships, it is desirable to express the various branch quantities to the same reference.

$$(V_{Qi} + jV_{Di} = (V_{qi} \cos \delta_i - V_{di} \sin \delta_i) + j(V_{qi} \sin \delta_i + V_{di} \cos \delta_i), \dot{V}_i = \bar{V}_i e^{j\delta_i}) \quad (4.21)$$

$$V_k e^{-j\delta_i} = \bar{Z}_k \dot{I}_k e^{-j\delta_i}, \dot{V}_k = \bar{Z}_k \dot{I}_k \quad k = 1, 2, \dots, b \quad (4.22)$$

#### 4.5 Converting Machine Coordinates to System Reference

Consider a voltage  $v_{abck}$  at node I. We can apply Park's transformation to this voltage to obtain  $V_{qdi}$ . From (4.2) this voltage can be expressed in phasor notation as  $\bar{V}$ , using the rotor of machine i as reference. It can also be expressed to the system reference as  $V_i$ , using the transformation (9.21)[4].

$$T = \begin{bmatrix} e^{j\delta_1} & 0 & \dots & 0 \\ 0 & e^{j\delta_2} & \dots & 0 \\ \dots & \dots & \dots & \dots \\ 0 & 0 & \dots & e^{j\delta_n} \end{bmatrix} \quad (4.23)$$

$$V = \begin{bmatrix} V_{Q1} + V_{D1} \\ V_{Q2} + V_{D2} \\ \dots \\ V_{Qn} + V_{Dn} \end{bmatrix} \bar{V} = \begin{bmatrix} V_{q1} + V_{d1} \\ V_{q2} + V_{d2} \\ \dots \\ V_{qn} + V_{dn} \end{bmatrix} \quad (4.24)$$

$$V = T \bar{V} \quad (4.25)$$

Thus T is a transformation that transforms the d and q quantities of all machines to the system frame, which a common frame is moving at synchronous speed. We can easily show that the transformation T is orthogonal.

$$T^{-1} = T \quad (4.26)$$

$$\bar{V} = T^* \dot{V} \quad (4.27)$$

$$\dot{I} = T \bar{I} = T^* \dot{I} \quad (4.28)$$

$$T I = \bar{Y} T \bar{V} \quad (4.29)$$

$$I = (T^{-1} \bar{Y} T) \bar{V} \triangleq \bar{M} \bar{V} \quad (4.30)$$

$$\bar{M} = (T^{-1}\bar{Y}T) \quad (4.31)$$

$$\bar{V} = (T^{-1}\bar{Y}T)^{-1}\bar{I} = (T^{-1}\bar{Z}T)\bar{I} \quad (4.32)$$

$$\bar{Y} = \begin{bmatrix} Y_{11}e^{j\theta_{11}} & Y_{12}e^{j\theta_{12}} & \dots & Y_{1n}e^{j\theta_{1n}} \\ Y_{21}e^{j\theta_{21}} & Y_{22}e^{j\theta_{22}} & \dots & Y_{2n}e^{j\theta_{2n}} \\ \dots & \dots & \dots & \dots \\ Y_{n1}e^{j\theta_{n1}} & Y_{n2}e^{j\theta_{n2}} & \dots & Y_{nn}e^{j\theta_{nn}} \end{bmatrix} \quad (4.33)$$

Derive the expression for the matrix for an n-machine system.

$$T = \begin{bmatrix} e^{j\delta_1} & & \\ & \ddots & \\ & & e^{j\delta_n} \end{bmatrix}, T^{-1} = \begin{bmatrix} e^{-j\delta_1} & & \\ & \ddots & \\ & & e^{-j\delta_n} \end{bmatrix} \quad (4.34)$$

$$\bar{Y}T = \begin{bmatrix} Y_{11}e^{j(\theta_{11}+\delta_1)} & Y_{12}e^{j(\theta_{12}+\delta_2)} & \dots & Y_{1n}e^{j(\theta_{1n}+\delta_n)} \\ Y_{21}e^{j(\theta_{21}+\delta_1)} & Y_{22}e^{j(\theta_{22}+\delta_2)} & \dots & Y_{2n}e^{j(\theta_{2n}+\delta_n)} \\ \dots & \dots & \dots & \dots \\ Y_{n1}e^{j(\theta_{n1}+\delta_1)} & Y_{n2}e^{j(\theta_{n2}+\delta_2)} & \dots & Y_{nn}e^{j(\theta_{nn}+\delta_n)} \end{bmatrix} \quad (4.35)$$

$$(T^{-1}\bar{Y}T) \triangleq \bar{M} = \begin{bmatrix} Y_{11}e^{j\theta_{11}} & Y_{12}e^{j(\theta_{12}-\delta_{12})} & \dots & Y_{1n}e^{j(\theta_{1n}-\delta_{1n})} \\ Y_{21}e^{j(\theta_{21}-\delta_{21})} & Y_{22}e^{j\theta_{22}} & \dots & Y_{2n}e^{j(\theta_{2n}-\delta_{2n})} \\ \dots & \dots & \dots & \dots \\ Y_{n1}e^{j(\theta_{n1}-\delta_{n1})} & Y_{n2}e^{j(\theta_{n2}-\delta_{n2})} & \dots & Y_{nn}e^{j\theta_{nn}} \end{bmatrix} \quad (4.36)$$

$$Y_{ik}e^{j(\theta_{ik}-\delta_{ik})} = (G_{ik}\cos \delta_{ik} + B_{ik}\sin \delta_{ik}) + j(B_{ik}\sin \delta_{ik} - G_{ik}\cos \delta_{ik})$$

$$F_{G+B}(\delta_{ik}) = F_{G+B} = G_{ik}\cos \delta_{ik} + B_{ik}\sin \delta_{ik}$$

$$F_{G-B}(\delta_{ik}) = F_{G-B} = B_{ik}\cos \delta_{ik} - G_{ik}\sin \delta_{ik} \quad (4.37)$$

$$\bar{M} = H + jS \quad (4.38)$$

$$h_{ii} = G_{ii}h_{ik} = F_{G+B}(\delta_{ik}), s_{ii} = B_{ii}s_{ik} = F_{G-B}(\delta_{ik}) \quad (4.39)$$

$$I = (H + jS) \begin{bmatrix} V_{q1} + jV_{d1} \\ \vdots \\ V_{qn} + jV_{dn} \end{bmatrix} (H + jS)(V_q + jV_d) = (HV_q - SV_d) + j(SV_q + HV_d) \quad (4.40)$$

## 4.6 linearized Model for the Network

$$I = \bar{M}_0\bar{V}_\Delta + \bar{M}_\Delta\bar{V}_0 \quad (4.41)$$

$$\bar{M} = \begin{bmatrix} Y_{11}e^{j\theta_{11}} & Y_{12}e^{j(\theta_{12}-\delta_{120}-\delta_{12\Delta})} & \dots & Y_{1n}e^{j(\theta_{1n}-\delta_{1n0}-\delta_{1n\Delta})} \\ \dots & \dots & \dots & \dots \\ Y_{1n}e^{j(\theta_{1n}-\delta_{n10}-\delta_{n1\Delta})} & Y_{n2}e^{j(\theta_{n2}-\delta_{n20}-\delta_{n2\Delta})} & Y_{nn}e^{j\theta_{nn}} & \dots \end{bmatrix} \quad (4.42)$$

$$\bar{m}_{ij} = Y_{ij}e^{j(\theta_{ij}-\delta_{ij0})}e^{-j\delta_{ij\Delta}}, \bar{m}_{ij} \cong Y_{ij}e^{j(\theta_{ij}+\delta_{ij0})}(1 - j\delta_{ij\Delta}) \quad (4.43)$$

$$\bar{m}_{ij\Delta} \cong -jY_{ij}e^{j(\theta_{ij}-\delta_{ij0})}\delta_{ij\Delta} \quad (4.44)$$

$$\begin{aligned} \bar{M}_{\Delta}\bar{V}_0 &= (-j \begin{bmatrix} 0 & \dots & Y_{1n}e^{j(\theta_{1n}-\delta_{1n0})}\delta_{1n\Delta} \\ Y_{21}e^{j(\theta_{21}-\delta_{210})}\delta_{21\Delta} & \dots & Y_{2n}e^{j(\theta_{2n}-\delta_{2n0})}\delta_{2n\Delta} \\ \dots & \dots & \dots \\ Y_{n1}e^{j(\theta_{n1}-\delta_{n10})}\delta_{n1\Delta} & \dots & 0 \end{bmatrix} \begin{bmatrix} \bar{V}_{10} \\ \bar{V}_{20} \\ \dots \\ \bar{V}_{n0} \end{bmatrix}) \\ &= -j \begin{bmatrix} \sum_{k=1}^n Y_{1k}e^{j(\theta_{1k}-\delta_{1k0})}\bar{V}_{k0}\delta_{1k\Delta} \\ \sum_{k=1}^n Y_{2k}e^{j(\theta_{2k}-\delta_{2k0})}\bar{V}_{k0}\delta_{2k\Delta} \\ \dots \\ \sum_{k=1}^n Y_{nk}e^{j(\theta_{nk}-\delta_{nk0})}\bar{V}_{k0}\delta_{nk\Delta} \end{bmatrix} \end{aligned} \quad (4.45)$$

$$\begin{aligned} &\begin{bmatrix} \bar{I}_{1\Delta} \\ \bar{I}_{2\Delta} \\ \dots \\ \bar{I}_{n\Delta} \end{bmatrix} \\ &= \begin{bmatrix} Y_{11}e^{j\theta_{11}} & \dots & Y_{1n}e^{j(\theta_{1n}-\delta_{1n0})} \\ Y_{21}e^{j(\theta_{21}-\delta_{210})} & \dots & Y_{2n}e^{j(\theta_{2n}-\delta_{2n0})} \\ \dots & \dots & \dots \\ Y_{n1}e^{j(\theta_{n1}-\delta_{n10})} & \dots & Y_{nn}e^{j\theta_{nn}} \end{bmatrix} \begin{bmatrix} \bar{V}_{1\Delta} \\ \bar{V}_{2\Delta} \\ \dots \\ \bar{V}_{n\Delta} \end{bmatrix} \\ &- j \begin{bmatrix} \sum_{k=1}^n \bar{V}_{k0} Y_{1k}e^{j(\theta_{1k}-\delta_{1k0})}\delta_{1k\Delta} \\ \sum_{k=1}^n \bar{V}_{k0} Y_{2k}e^{j(\theta_{2k}-\delta_{2k0})}\delta_{2k\Delta} \\ \dots \\ \sum_{k=1}^n \bar{V}_{k0} Y_{nk}e^{j(\theta_{nk}-\delta_{nk0})}\delta_{nk\Delta} \end{bmatrix} \end{aligned} \quad (4.46)$$

$$\begin{aligned} \mathbf{T} &= j\mathbf{T}_0\boldsymbol{\delta} \\ &\triangleq \text{diag}(\delta_{1\Delta} \dots \delta_{n\Delta}) \end{aligned} \quad (4.47)$$

$$\mathbf{N}_\Delta = (\mathbf{T}^{-1})_\Delta = -j\mathbf{N}_0\boldsymbol{\delta}_\Delta = -j\mathbf{T}_0^{-1}\boldsymbol{\delta}_\Delta \quad (4.48)$$

$$\bar{\mathbf{M}}_\Delta = -j(\mathbf{T}_0^{-1}\boldsymbol{\delta}_\Delta \bar{\mathbf{Y}}\mathbf{T}_0 - \mathbf{T}_0^{-1}\bar{\mathbf{Y}}\mathbf{T}_0\boldsymbol{\delta}_\Delta) \quad (4.49)$$

$$\mathbf{T}_0\boldsymbol{\delta} = \begin{bmatrix} e^{j\delta_{10}} & & \\ & \ddots & \\ & & e^{j\delta_{n0}} \end{bmatrix} \begin{bmatrix} \delta_{1\Delta} & & \\ & \ddots & \\ & & \delta_{n\Delta} \end{bmatrix} = \begin{bmatrix} e^{j\delta_{10}}\delta_{1\Delta} & & \\ & \ddots & \\ & & e^{j\delta_{n0}}\delta_{n\Delta} \end{bmatrix} \quad (4.50)$$

$$\begin{aligned} \mathbf{T}_0^{-1}\bar{\mathbf{Y}} &= \begin{bmatrix} e^{-j\delta_{10}} & & \\ & \ddots & \\ & & e^{-j\delta_{n0}} \end{bmatrix} \begin{bmatrix} Y_{11}e^{j\theta_{11}} & \dots & Y_{1n}e^{j\theta_{1n}} \\ \dots & \dots & \dots \\ Y_{n1}e^{j\theta_{n1}} & \dots & Y_{nn}e^{j\theta_{nn}} \end{bmatrix} \\ &= \begin{bmatrix} Y_{11}e^{j(\theta_{11}-\delta_{10})} & \dots & Y_{1n}e^{j(\theta_{1n}-\delta_{10})} \\ \dots & \dots & \dots \\ Y_{n1}e^{j(\theta_{n1}-\delta_{n0})} & \dots & Y_{nn}e^{j(\theta_{nn}-\delta_{n0})} \end{bmatrix} \end{aligned} \quad (4.51)$$

$$\begin{aligned} \mathbf{T}_0^{-1}\bar{\mathbf{Y}}\mathbf{T}_0\boldsymbol{\delta}_\Delta &= \\ &\left( \begin{bmatrix} Y_{11}e^{j\theta_{11}} & \dots & Y_{1n}e^{j(\theta_{1n}-\delta_{1n0})} \\ Y_{21}e^{j(\theta_{21}-\delta_{210})} & \dots & Y_{2n}e^{j(\theta_{2n}-\delta_{2n0})} \\ \dots & \dots & \dots \\ Y_{n1}e^{j(\theta_{n1}-\delta_{n10})} & \dots & Y_{nn}e^{j\theta_{nn}} \end{bmatrix} \begin{bmatrix} \delta_{1\Delta} & & \\ & \ddots & \\ & & \delta_{n\Delta} \end{bmatrix} \right) \\ &= \bar{\mathbf{M}}_0\boldsymbol{\delta}_\Delta \end{aligned} \quad (4.52)$$

$$\mathbf{T}_0^{-1}\boldsymbol{\delta} = \begin{bmatrix} e^{-j\delta_{10}}\delta_{1\Delta} & & \\ & \ddots & \\ & & e^{-j\delta_{n0}}\delta_{n\Delta} \end{bmatrix}$$

$$\bar{\mathbf{Y}}\mathbf{T}_0 = \begin{bmatrix} Y_{11}e^{j(\theta_{11}+\delta_{10})} & \dots & Y_{1n}e^{j(\theta_{1n}-\delta_{1n0})} \\ \dots & \dots & \dots \\ Y_{n1}e^{j(\theta_{n1}+\delta_{n0})} & \dots & Y_{nn}e^{j(\theta_{nn}+\delta_{n0})} \end{bmatrix}$$

$$\mathbf{T}_0^{-1}\boldsymbol{\delta} \bar{\mathbf{Y}}\mathbf{T}_0 = \begin{bmatrix} Y_{11}e^{j\theta_{11}}\delta_{1\Delta} & \dots & Y_{1n}e^{j(\theta_{1n}-\delta_{1n0})}\delta_{1\Delta} \\ \dots & \dots & \dots \\ Y_{n1}e^{j(\theta_{n1}-\delta_{n10})}\delta_{n\Delta} & \dots & Y_{nn}e^{j\theta_{nn}}\delta_{n\Delta} \end{bmatrix} = \bar{\mathbf{M}}_0 \quad (4.53)$$

$$\bar{\mathbf{M}}_0 = -j[\delta_\Delta \bar{\mathbf{M}}_{l_0} - \bar{\mathbf{M}}_0 \delta_\Delta] \quad (4.54)$$

$$\bar{\mathbf{I}}_\Delta = \bar{\mathbf{M}}_0 \bar{\mathbf{V}}_\Delta - j[\bar{\mathbf{M}}_0 - \bar{\mathbf{M}}_0 \delta_\Delta] \bar{\mathbf{V}}_\Delta \quad (4.55)$$

$$\bar{\mathbf{V}}_\Delta = \bar{\mathbf{M}}_0^{-1} \bar{\mathbf{I}}_\Delta - j[\delta_\Delta - \bar{\mathbf{M}}_0^{-1} \delta_\Delta \bar{\mathbf{M}}_0] \bar{\mathbf{V}}_\Delta \quad (4.56)$$

$$\bar{\mathbf{Q}} \triangleq \bar{\mathbf{I}}_\Delta^{-1} = \mathbf{T}^{-1} \bar{\mathbf{I}}_\Delta^{-1} \mathbf{T} \quad (4.57)$$

$$\bar{\mathbf{V}}_\Delta = \bar{\mathbf{Q}}_0 \bar{\mathbf{I}}_\Delta - j[\delta_\Delta \bar{\mathbf{Q}}_0 - \bar{\mathbf{Q}}_0 \delta_\Delta] \bar{\mathbf{I}}_0 \quad (4.58)$$

$$\bar{\mathbf{M}}_0 = \begin{bmatrix} Y_{11} e^{j\theta_{11}} & Y_{12} e^{j(\theta_{12} - \delta_{120})} \\ Y_{12} e^{j(\theta_{12} + \delta_{120})} & Y_{22} e^{j\theta_{22}} \end{bmatrix} \quad (4.59)$$

$$\delta_\Delta = \begin{bmatrix} \delta_{1\Delta} & 0 \\ 0 & \delta_{2\Delta} \end{bmatrix}, \quad \bar{\mathbf{V}}_\Delta = \begin{bmatrix} V_{q1\Delta} + jV_{d1\Delta} \\ V_{q2\Delta} + jV_{d2\Delta} \end{bmatrix} \quad (4.60)$$

$$\bar{\mathbf{M}}_0 \delta_\Delta = \begin{bmatrix} Y_{11} e^{j\theta_{11}} \delta_{1\Delta} & Y_{12} e^{j(\theta_{12} - \delta_{120})} \delta_{2\Delta} \\ Y_{12} e^{j(\theta_{12} + \delta_{120})} \delta_{1\Delta} & Y_{22} e^{j\theta_{22}} \delta_{2\Delta} \end{bmatrix} \quad (4.61)$$

$$\delta_\Delta \bar{\mathbf{M}}_0 = \begin{bmatrix} Y_{11} e^{j\theta_{11}} \delta_{1\Delta} & Y_{12} e^{j(\theta_{12} - \delta_{120})} \delta_{2\Delta} \\ Y_{12} e^{j(\theta_{12} + \delta_{120})} \delta_{1\Delta} & Y_{22} e^{j\theta_{22}} \delta_{2\Delta} \end{bmatrix}$$

$$j(\delta_\Delta \bar{\mathbf{M}}_0 - \bar{\mathbf{M}}_0 \delta_\Delta) \bar{\mathbf{V}}_0 = j \begin{bmatrix} 0 & Y_{12} e^{j(\theta_{12} - \delta_{120})} \delta_{12\Delta} \\ -Y_{12} e^{j(\theta_{12} + \delta_{120})} \delta_{12\Delta} & 0 \end{bmatrix} \quad (4.62)$$

$$\begin{bmatrix} V_{q10} + jV_{d10} \\ V_{q20} + jV_{d20} \end{bmatrix} = \begin{bmatrix} Y_{11} e^{j\theta_{11}} \delta_{1\Delta} & Y_{12} e^{j(\theta_{12} - \delta_{120})} \delta_{2\Delta} \\ Y_{12} e^{j(\theta_{12} + \delta_{120})} \delta_{1\Delta} & Y_{22} e^{j\theta_{22}} \delta_{2\Delta} \end{bmatrix} \delta_{12\Delta} \quad (4.63)$$

$$\begin{aligned} & \bar{\mathbf{M}}_0 \bar{\mathbf{V}}_\Delta \\ &= \begin{bmatrix} Y_{11} e^{j\theta_{11}} \delta_{1\Delta} (V_{q1\Delta} + jV_{d1\Delta}) & Y_{12} e^{j(\theta_{12} - \delta_{120})} \delta_{2\Delta} (V_{q2\Delta} + jV_{d2\Delta}) \\ Y_{12} e^{j(\theta_{12} + \delta_{120})} \delta_{1\Delta} (V_{q1\Delta} + jV_{d1\Delta}) & Y_{22} e^{j\theta_{22}} \delta_{2\Delta} (V_{q2\Delta} + jV_{d2\Delta}) \end{bmatrix} \end{aligned} \quad (4.64)$$

$$\begin{aligned} & \left( \begin{bmatrix} I_{q1\Delta} + jI_{d1\Delta} \\ I_{q2\Delta} + jI_{d2\Delta} \end{bmatrix} \right. \\ &= \begin{bmatrix} Y_{11} e^{j\theta_{11}} \delta_{1\Delta} V_{q1\Delta} + jY_{11} e^{j\theta_{11}} \delta_{1\Delta} V_{d1\Delta} & Y_{12} e^{j(\theta_{12} - \delta_{120})} \delta_{2\Delta} V_{q2\Delta} + jY_{12} e^{j(\theta_{12} - \delta_{120})} \delta_{2\Delta} V_{d2\Delta} \\ Y_{12} e^{j(\theta_{12} + \delta_{120})} \delta_{1\Delta} V_{q1\Delta} + jY_{12} e^{j(\theta_{12} + \delta_{120})} \delta_{1\Delta} V_{d1\Delta} & Y_{22} e^{j\theta_{22}} \delta_{2\Delta} V_{q2\Delta} + jY_{22} e^{j\theta_{22}} \delta_{2\Delta} V_{d2\Delta} \end{bmatrix} \\ & \left. - \begin{bmatrix} jY_{12} e^{j(\theta_{12} - \delta_{120})} (V_{q20} + jV_{d2\Delta}) \\ -jY_{12} e^{j(\theta_{12} + \delta_{120})} (V_{q10} + jV_{d10}) \end{bmatrix} \right) \quad (4.65) \end{aligned}$$

$$I_{qi} = (C$$

$$\begin{aligned}
I_{di} &= (B_{ii}\Delta V_{qi} - G_{ii}\Delta V_{di} + \sum_{\substack{j=1 \\ \neq i}}^n [Y_{ij}\cos(\theta_{ij} - \xi_{qi0})\Delta V_{di}] \\
&+ \sum_{\substack{j=1 \\ \neq i}}^n [Y_{ij}\sin(\theta_{ij} - \xi_{qi0})\Delta V_{qi}] \\
&+ \sum_{\substack{j=1 \\ \neq i}}^n [(Y_{ij}\sin(\theta_{ij} - \xi_{qi0})\Delta V_{di0} - \cos(\theta_{ij} - \xi_{qi0})\Delta V_{qi0}]\Delta\delta_{ij} \Big), i \\
&= 1, \dots, n
\end{aligned} \tag{4.67}$$

The state space model for linearized system is obtained by linearizing the differential and algebraic equations at an operating point. While doing this linearization process, additional terms involving terminal voltage components (which are not state variables) remain in the differential equations. To express the voltage components in terms of state variables, the machine currents are also linearized and expressed in terms of state variables and voltage components. Finally the current components are eliminated using the interconnecting network algebraic equations. From the initial conditions,  $E_d' i_0$ ,  $E_q' i_0$ ,  $I_{qi0}$ ,  $I_{di0}$ ,  $E_{FDi0}$  and  $i_0$  are determined. Linearizing equation (4.5) we get [4].

$$P E'_{di} = \frac{\{-\Delta E'_{di} - (X_{qi} - X'_{qi})\Delta I_{iq}\}}{\tau'_{qoi}} ; i = 1, \dots, n \quad (4.68)$$

$$P \quad i = \frac{\{\Delta T_{FDi} - (I_{dio}\Delta E'_{qi} + I_{qio}\Delta E'_{qi} + E'_{dio}\Delta I_{di} + E'_{qio}\Delta I_{qi}) - D_i\omega_i\}}{\tau_j} ; i = 1, \dots, n \quad (4.70)$$

$$P \quad i = \omega_i ; i = 1, \dots, n \quad (4.71)$$

$$\begin{aligned} & P \Delta E'_{qi} \\ &= \frac{1}{\tau'_{qoi}} \left\{ [(X_{qi} - X'_{qi})B_{ii} - 1]\Delta E'_{di} \right. \\ &+ (X_{qi} - X'_{qi}) \sum_{\substack{k=1 \\ \neq i}}^n [Y_{ik} \{\sin(\theta_{ik} - \theta_{ik0}) \angle E'_{dk}\} - (X_{qi} - X'_{qi})G_{ii}\Delta E'_{qi} \\ &- (X_{qi} - X'_{qi}) \sum_{\substack{k=1 \\ \neq i}}^n [Y_{ik}\cos(\theta_{ik} - \theta_{ik0})\Delta E'_{qk}] \\ &- (X_{qi} - X'_{qi}) \sum_{\substack{k=1 \\ \neq i}}^n [Y_{ik}\cos(\theta_{ik} - \theta_{ik0})] \cdot E'_{dk0}] \\ &\left. + \sin(\theta_{ik} - \theta_{ik0}) \angle E'_{dk0} \angle \theta_{ik} \right\} ; i \\ &= 1, 2, \dots, n \quad (4.72) \end{aligned}$$

$$\begin{aligned}
 P_i = \frac{1}{j_i} & \left\{ [\Delta T_{mi} - D_i \Delta \theta_i - [I_{dio} + G_{ii} \Delta E'_{dio} - B_{ii} \Delta E'_{qio}] \Delta E'_{di} \right. \\
 & - [I_{qio} + B_{ii} \Delta E'_{dio} - G_{ii} \Delta E'_{qio}] \\
 & - \sum_{\substack{k=1 \\ \neq i}}^n [Y_{ik} \cos(\theta_{ik} - \theta_{ik0})] E'_{dio} - Y_{ik} \sin(\theta_{ik} - \theta_{ik0}) \Delta E'_{qio} \Delta E'_{dk} \\
 & - \sum_{\substack{k=1 \\ \neq i}}^n [Y_{ik} \sin(\theta_{ik} - \theta_{ik0})] E'_{dio} - Y_{ik} \cos(\theta_{ik} - \theta_{ik0}) \Delta E'_{qio} \Delta E'_{dk} \\
 & - \sum_{\substack{k=1 \\ \neq i}}^n [Y_{ik} \cos(\theta_{ik} - \theta_{ik0})] \Delta E'_{dio} \\
 & - Y_{ik} \cos(\theta_{ik} - \theta_{ik0}) (-E'_{qk0} E'_{dio} + E'_{dk0} E'_{qio}) \\
 & + Y_{ik} \sin(\theta_{ik} - \theta_{ik0}) (-E'_{dk0} E'_{dio} \\
 & \left. + E'_{qk0} E'_{qio}) \Delta \theta_{ik} \right\} ; i \\
 & = 1, 2 \dots n
 \end{aligned} \tag{4.74}$$

The above set of equations (4.72 to 4.75) gives the state space model of n-machine system.

## 4.7 Exciter Representation

The state space equation of the exciter can be derived from the block

Diagram of the exciter shown in the Figure (2.2)

$$E_{FD} = \frac{-K_{Ai}}{1+sT_A} \Delta V_t \dots \dots \quad (4.76)$$

For n, number of exciters, the state equations is as follows:

$$P \ E_{fdi} = \frac{-K_{Ai}}{T_{Ai}} (-V_{ref1} + \angle V_i) - \frac{1}{T_{Ai}} \Delta E_{fdi}; i = 1, \dots, n \quad (4.77)$$

Now the state vector of the n machine state model including exciter

Equation is as follows

$$X_i^T = [\Delta E'_{di} \ \Delta E'_{qi} \ \Delta \alpha_i \ \Delta \omega_i \ \Delta E_{DFi}]; i = 1, \dots, n \quad (4.78)$$

## 4.8 Conventional Power System Stabilizer representation

The Conventional Power System Stabilizer (PSS) adds damping to the generator rotor oscillations by controlling its excitation using auxiliary stabilizing signals. To provide damping, the stabilizer must produce a component of electrical torque in phase with the rotor speed deviations.

From the wash out block, we get

$$V_2 = \frac{sT_w}{1+sT_w} (K_{PSS} \Delta \omega) \quad (4.79)$$

$$P \ V_{2i} = K_{PSSi} P \Delta \omega_i - (1/T_{wi}) \Delta V_{2i}; i = 1, \dots, n \quad (4.80)$$

$$V_s = V_2 \left[ \frac{1+sT_1}{1+sT_2} \right] \quad (4.81)$$

$$P V_{Si} = \left(\frac{T_{1i}}{T_{2i}}\right) P \Delta V_{2i} + \left(\frac{1}{T_{2i}}\right) \Delta V_{Si} - \left(\frac{1}{T_{2i}}\right) \Delta V_{Si}; i = 1, \dots, n \quad (4.82)$$

The state vector of the complete system after the inclusion of power

System stabilizer is as follows

$$X_i^T = [\Delta E'_{di} \Delta E'_{qi} \Delta \alpha_i \Delta \delta_i \Delta E_{DFi} \Delta V_{2i} \Delta V_{Si}]; i = 1, \dots, n \quad (4.83)$$

## 4.9 Dynamic Stability Evaluation

### 4.9.1 Techniques of Stability Evaluation

Stability can be evaluated by different methods, such as using Eigenvalues, Damping Torques and Time-Domain Simulations. These methods are techniques that are used to determine if the system is stable or unstable. The following sections describes these techniques in details by taking different operating points [1].

### 4.9.2 Stability Evaluation Using Eigen values Technique

Consider the following state-space equations:

$$\dot{x} = A x + B u \quad (4.84)$$

$$y = C x + D u \quad (4.85)$$

Note that all the partial derivatives above are evaluated at which small perturbation is being analyzed. Now we need to get the state Equations (4.84)-(4.85) in the frequency domain. This is done by taking the Laplace transform as follow

$$s X(s) - X(0) = A X(s) + B U(s) \quad (4.86)$$

$$Y(s) = C X(s) \quad (4.87)$$

$$(sI - A) X(s) = \Delta X(0) + B U(s) \quad (4.88)$$

$$X(s) = (sI - A)^{-1}(\Delta X(0) + B U(s)) \quad (4.89)$$

$$Y(s) = C[(sI - A)^{-1}(\Delta X(0) + B U(s))] \quad (4.90)$$

Note that both Equations (4.86)-(4.87) have two components, one dependent on the initial conditions and the other one dependent on the input [1]. The poles of  $X(s)$  and  $Y(s)$  are obtained from the roots of the characteristic equation of matrix A, which is

$$\det(sI - A) = \text{zero} \quad (4.91)$$

Where  $s$  is the eigenvalue of matrix A.

The stability of any system is determined by its eigenvalues as follows:

1. The real eigenvalue corresponds to a non-oscillatory mode. If it is negative, this represents the decaying mode, and it decays fast as long as the magnitude of the eigenvalue is high. However if it is positive, this would represent an aperiodic instability. Note that if there is at least one positive real eigenvalue in the system, this would lead the system to instability mode [1].
2. The complex eigenvalues appear in conjugate pairs, and each pair corresponds to an oscillatory mode. The real component of the complex pair represents the damping, while the imaginary component represents the frequency of oscillations [1]. For a complex pair of eigenvalue

$$\lambda = \sigma \pm j\omega \quad (4.92)$$

The damping ratio can be expressed as:

$$\zeta = \frac{\sigma}{\sqrt{\sigma^2 + \omega^2}} \quad (4.93)$$

$$f = \frac{\omega}{2\pi} \quad (4.94)$$

Where  $f$  the frequency of oscillations in Hz is:

Equation (4.93) determines the rate of decay of the amplitude of the oscillation. The stability of power system is related to position of the power system eigenvalues in real-imaginary plane. The real component of the eigenvalue presents the damping, where the imaginary component presents the frequency of oscillations. If the real part of the eigenvalue is negative, the response is represented as damped oscillations which tends the system to be

stable, whereas if it is positive, the response is represented as increasing amplitude oscillations, thus the system is instable.

## **4:10 Power System Representation for Dynamic Study**

In the performance of a transient stability study, the following data are needed:

1. A load-flow study of the pre-transient network to determine the mechanical power  $P_m$  of the generators and to calculate the values of  $E$ , for all generators. The equivalent impedances of the loads are obtained from the load bus data.
2. System data as follows, the inertia constant  $H$  and direct axis transient reactance  $x_d$  for all generators.
  - b. Transmission network impedances for the initial network conditions.
3. The type of location of disturbance, time of switching, and the maximum time for which a solution is to be obtained.

## **4.11 Preliminary Calculations**

To prepare the system data for a stability study, the following preliminary calculations are made:

1. All system data are converted to a common base; a system base of 100MVA.
2. The loads are converted to equivalent impedances or admittances. The necessary data for this step are obtained from the load-flow study. Thus if a certain load bus has a voltage, power, reactive power, and current flowing into a load admittance.
3. The internal voltages of the generators are calculated from the load-flow data. These internal angles may be computed from the pre-transient terminal voltages as follows.
4. The  $Y$  matrix for each network condition is calculated. The following steps are usually needed:
  - (a) The equivalent load impedances (or admittances) are connected between the load buses and the reference node; additional nodes are provided for the internal generator voltages (nodes 1,2,...,n in Figure( 4.1 )and the appropriate

values of  $X_d$  are connected between these nodes and the generator terminal nodes

(b) All impedance elements are converted to admittances.

(c) Elements of the Y matrix are identified .

5. Finally, all the nodes except for the generator nodes are eliminated and the Ymatrix for the reduced network is obtained. The reduction can be achieved by matrix operation considering zero injection currents at all the nodes except for the internal generator nodes.

## 4.12 Simulation and Analysis

The method mention above for stability evaluation use in case of three machine nine bus system the system data obtained in appendix(B). The case study of three machine nine bus system uses different scenarios. For analysis use Power System Toolbox (PSAT).The Figure (4.2) represent three machine nine bus PSAT configuration.

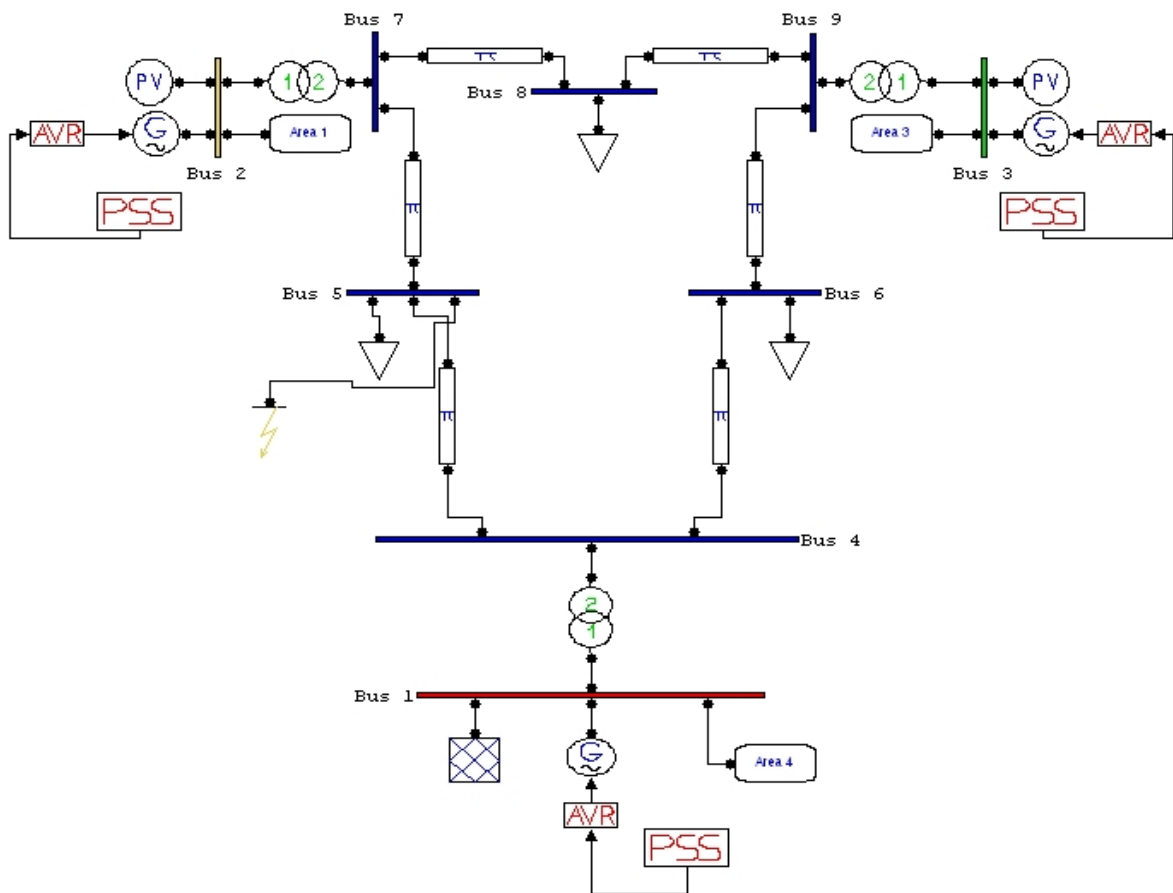
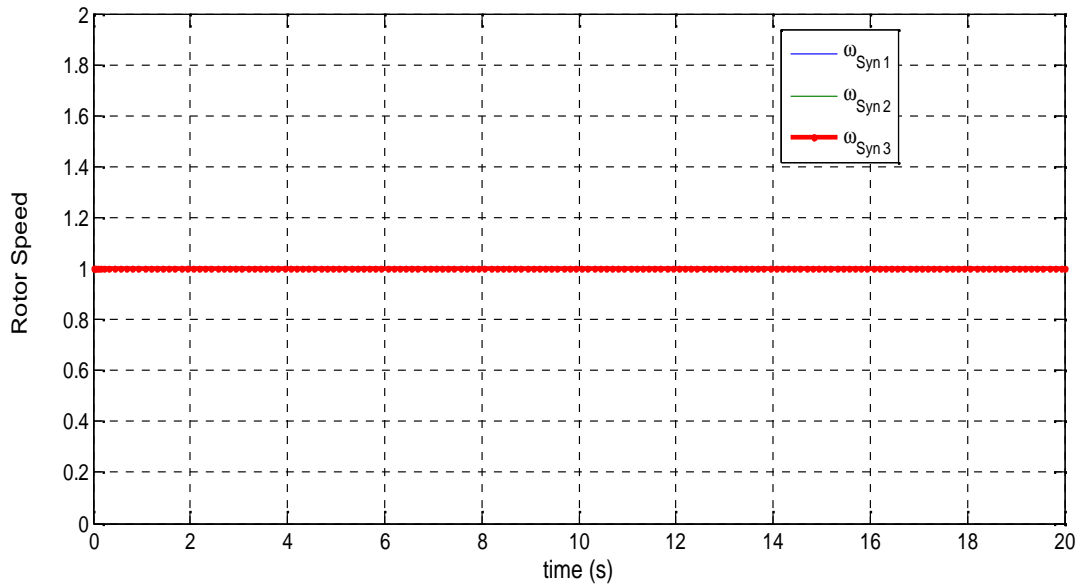


Figure (4.2) Simulink diagram of three machine nine bus system

### 4.12.1 Normal Case

The Simulation results shows in Table (A.5), Table (A.6) and Table (A.7) power flow in buses, voltages, Eigen values report and participation factor for all state . The Figure (4.3) show time domain of speed for three machines.



The Figure (4.3) Time response of speed in three machine

### 4.12.2 Increasing load at Buses 8,6 and 5

The Simulation results shows in Table (A.8), Table (A.9) and Table (A.10) power flow in buses, voltages , Eigen values and participation factor for all state . The Figure (4.4) show time domain of speed deviation for three machine in case of increasing load at buses 5,8 and 6.

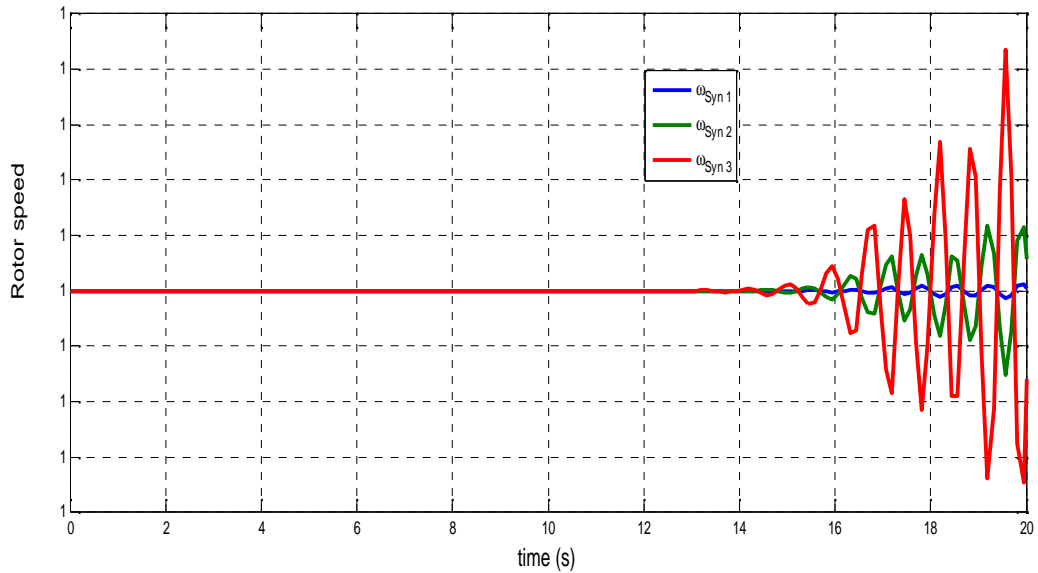


Figure (4.4) Speed in three machines in case of increasing load at buses

#### 4.12.3 Short Circuit in Bus 5 but without Power System Stabilizer

The Simulation results shows in Table (A.11) ,Table (A.12) and Table (A.12) power flow in buses , voltages , Eigen values and participation factor for all state .The figure (4.5) shows the time domain of speed deviation for three machine in case of short circuit at bus 5.

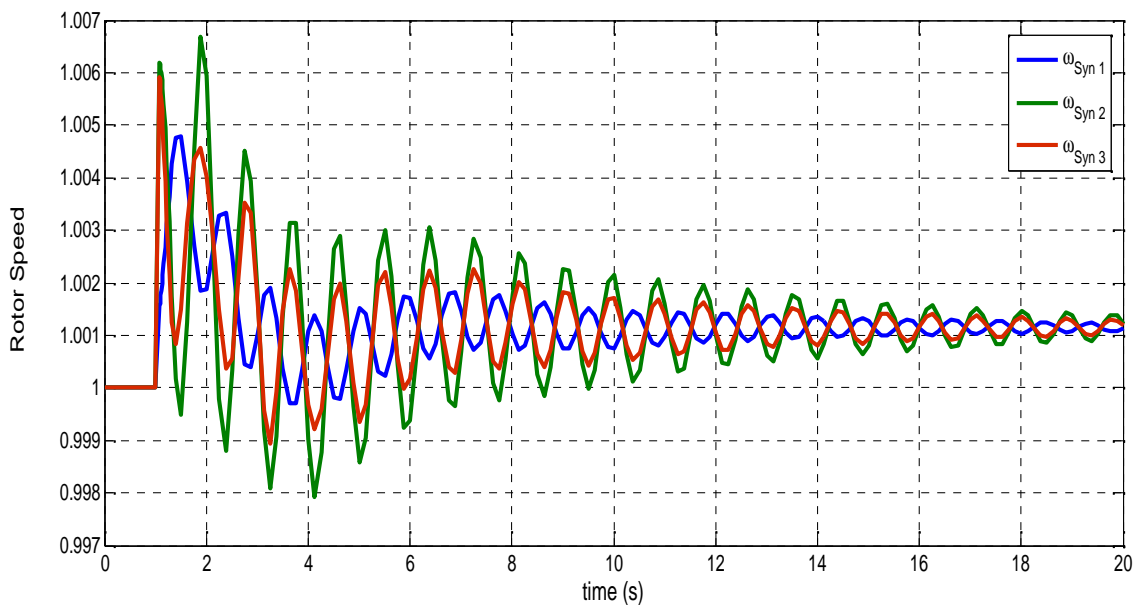


Figure (4.5) Rotor speed in three machine in case of short circuit at bus 5

#### 4.12.4 Short Circuit in Bus 5 with PSS

The Simulation results shows in Table (A.13) ,Table (A.14) and Table( A.15) power flow in buses,voltages,Eigenvalues report for all state and participation factor. The Figure (4.6) shows the time domain of speed deviation for three machine in case of short circuit but with PSS.

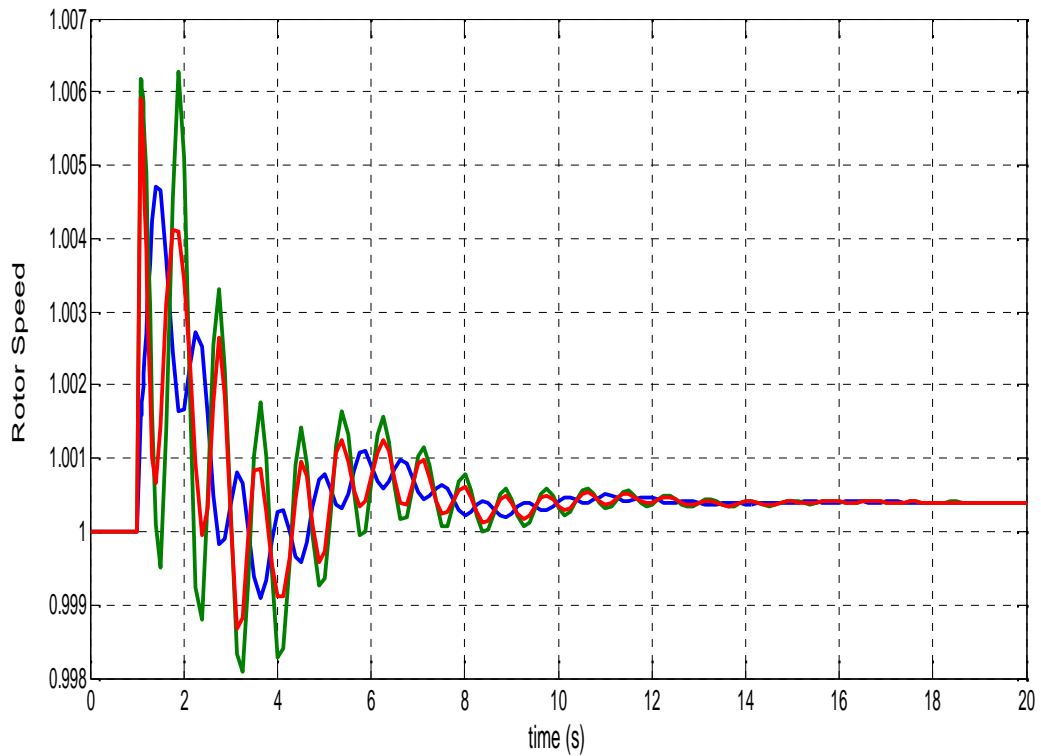


Figure (4.6) Rotor speed in three machines in case of short circuit at bus 5 with PSS

## CHAPTER FIVE

### DESIGN OF POWER SYSTEM BASED ON ADAPTIVE CONTROL

#### 5.1 Introduction

The majority of processes met in industrial practice have stochastic character. Traditional controllers with fixed parameters are often unsuited to such processes because their parameters change. Parameter changes are caused by changes in the manufacturing process, in the nature of the input materials, fuel, machinery use (wear), power system *etc.* Fixed controllers cannot deal with this. One possible alternative for improving the quality of control for such processes is the use of adaptive control systems, which has been made possible by the development of modern digital automation based on microprocessor technology. Naturally this must be taken together with the development and improvement of adaptive control algorithms, and the exploration of their potential, advantages and limitations[49]. Adaptive control is an area of feedback control theory that has recently received a great deal of attention. Although there is no clear-cut definition of adaptive control, an adaptive controller may be viewed as a regulator that can modify its behavior according to changes in the dynamics of the process it is controlling.[50] According to Webster's dictionary, to adapt means to "change (oneself) so that one's behavior will conform to new or changed circumstances." The words adaptive systems and adaptive control have been used as early as 1950,[52]. This generic definition of adaptive systems has been used to label approaches and techniques in a variety of areas despite the fact that the problems considered and approaches followed often have very little in common. The specific definition of adaptive control, Adaptive control is the combination of a parameter estimator, which generates parameter estimates online, with a control law in order to control classes of plants whose parameters are completely unknown and/or could change with time in an

unpredictable manner. The choice of the parameter estimator, the choice of the control law, and the way they are combined leads to different classes of adaptive control schemes.

## **5.2 Adaptive Control**

Adaptive Control covers a set of techniques which provide a systematic approach for automatic adjustment of controllers in real time, in order to achieve or to maintain a desired level of control system performance when the parameters of the plant dynamic model are unknown and or change in time. Consider the case when the parameters of the dynamic model of the plant to be controlled are unknown but constant (at least in a certain region of operation). In such cases, although the structure of the controller will not depend in general upon the particular values of the plant model parameters, the correct tuning of the controller parameters cannot be done without knowledge of their values. Adaptive control techniques can provide an automatic tuning procedure in closed loop for the controller parameters. In such cases, the effect of the adaptation vanishes as time increases.

## **5.3 Development of Adaptive Control**

The history of adaptive control goes back nearly 50 years [51]. The development of adaptive control started in the 1950's with the aim of developing adaptive flight control systems, although that problem was eventually solved by gain scheduling. Among the various solutions that were proposed for the flight control problem, the one that would have the most impact on the field was the so-called model-reference adaptive system (MRAS). Adaptive controllers are generally broken into two different types direct and indirect with the direct adaptive controller, regulator parameters are directly changed as the dynamics of the system change. This is demonstrated in Figure(5:1). The closed-loop plant is forced to act like a model system; the regulator parameters are adjusted until the error  $e$  in Figure (5.1) is driven to zero. Direct adaptive control is often termed model-reference adaptive control

(MRAC). With an indirect adaptive controller the regulator parameters are indirectly updated; an indirect controller is shown in Figure(5.2). The controller's operation occurs in two distinct steps. First, the dynamics of the system are identified at a particular instant in time; then the regulator is adjusted according to the identified dynamics. The plant's input and output are passed to a recursive identifier which identifies a linear model of the plant. The linear model parameters are passed to a regulator design block. Here the regulator parameters are calculated and passed to the regulator. With a discrete-time adaptive controller, the whole process may be updated with each time sample. Indirect adaptive controllers are also termed self-tuning adaptive controllers [53].

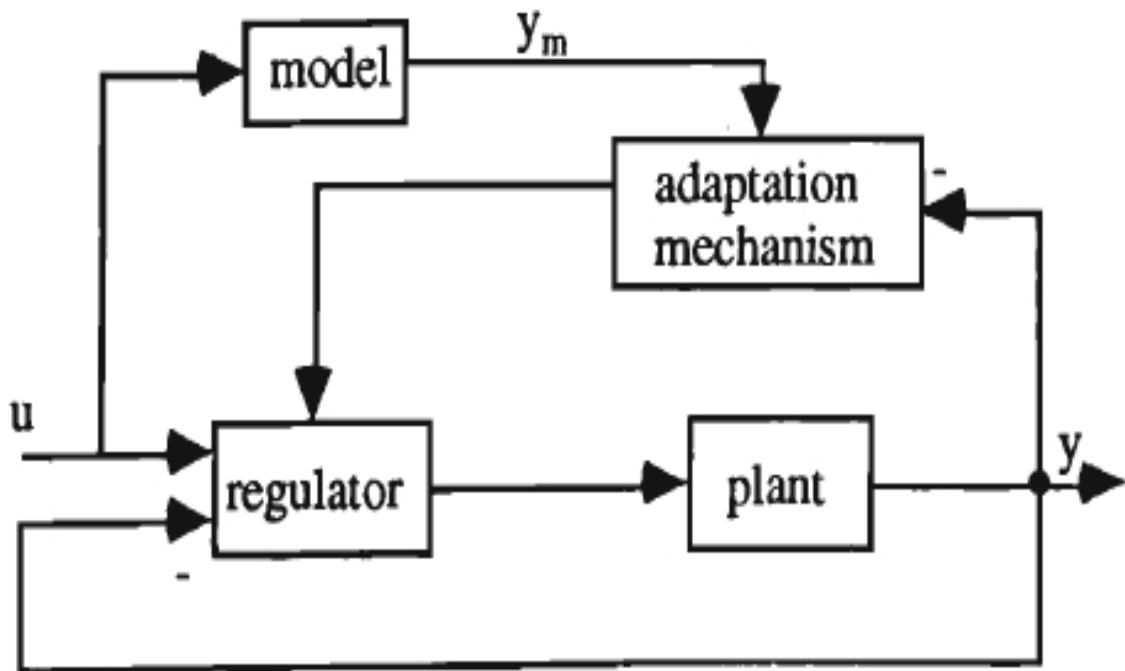


Figure (5.1) Configuration of direct model reference adaptive control

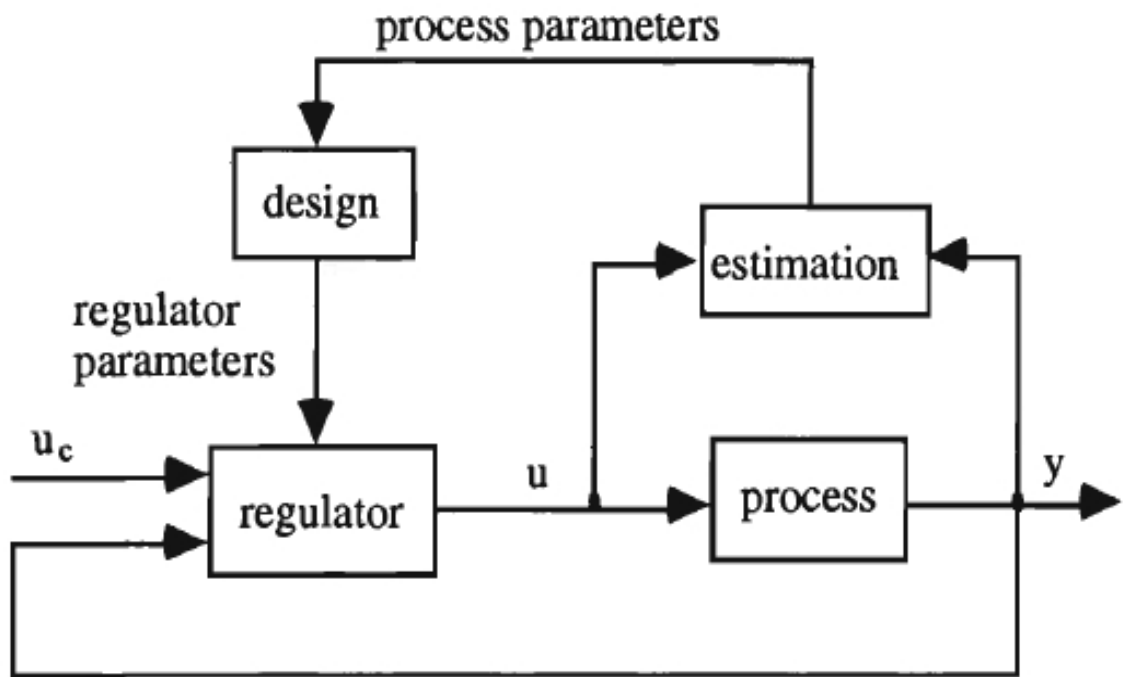


Figure (5.2) Configuration of indirect model reference adaptive control

## 5.4 model reference adaptive control

The basic MRAC system consists of four main components:

- i) Plant to be controlled
- ii) Reference model to generate desired closed loop output response
- iii) Controller that is time-varying and whose coefficients are adjusted by adaptive mechanism
- iv) Adaptive mechanism that uses ‘error’ (the difference between the plant and the desired model output) to produce controller coefficient. Regardless of the actual process parameters, adaptation in MRAC takes the form of adjustment of some or all of the controller coefficients so as to force the response of the resulting closed-loop control system to that of the reference model. Therefore, the actual parameter values of the controlled system do not really matter. Two types of MRAC design methods will be discussed in this thesis. They are ( i) Gradient Method/ MIT Rule.

ii) Lyapunov Method.

## 5.5 MRAC Design Using Gradient Method/MIT Rule

The Gradient Method of designing an MRAC controller is also known as the MIT Rule as it was first developed at the Massachusetts Institute of Technology (MIT), USA. This is the original method developed for adaptive control design before other methods were introduced to overcome some of its weaknesses. However, the Gradient method is relatively simple and easy to use. In designing the MRAC controller, we would like the output of the closed-loop system  $y(t)$  to follow the output of the reference model  $y_m(t)$ . Therefore, we aim to

minimize the error ( $e = y - y_m$ ) by designing a controller that has one or more adjustable parameters such that a certain cost function is minimized.

### Controller Design Method

Consider a closed-loop system with a controller that has only one adjustable parameter, Let

$r(t)$  = Reference input signal

$u(t)$  = Control signal

$y(t)$  = Plant output,  $y_m(t)$  = Reference model output

$e(t) = y(t) - y_m(t)$

The control objective is to adjust the controller parameter  $\theta$ , so that  $e(t)$  is minimized. To do this, a cost function,  $J(\theta)$  is chosen and minimized.

### Possibility 1:

Adjust  $\theta$  such that the cost function

$$J(\theta) = \frac{1}{2} e^2 \quad (5.2)$$

is minimized. To do this, we need,

$$\frac{d_{\theta}}{dt} = \chi \frac{\partial J}{\partial \theta} \quad (5.3)$$

i.e.  $\theta$  is changed in the direction of negative gradient of  $J$ , where the negative sign implies that  $\theta$  is changed such that  $J$  becomes small. From (5.1),

$$\frac{d_{\theta}}{dt} = \chi \frac{\partial J}{\partial e} \frac{\partial e}{\partial \theta} = -\chi e \frac{\partial e}{\partial \theta} \quad (5.4)$$

$\frac{\partial e}{\partial \theta}$  is called the ‘sensitivity derivative’, which indicates how the error is influenced

### Possibility 2:

Adjust  $\theta$  such that the cost function  $d(\theta) = |e|$  is minimized. We then have,

$$\frac{d_{\theta}}{dt} = -\chi \frac{\partial j}{\partial \theta} = -\chi \frac{\partial J}{\partial e} \frac{\partial e}{\partial \theta} = -\chi \frac{\partial e}{\partial \theta} \sin(e) \quad (5.5)$$

Where  $\sin(e) = \begin{cases} +1 & \text{if } e > 0 \\ -1 & \text{if } e < 0 \end{cases}$

< 0

## 5.6 Design of model reference adaptive control based on MIT

Consider first order differential equation transfer function

$$G(s) = \frac{y(s)}{u(s)} = \frac{dy}{dt} = -ay(t) + bu(t) \quad (5.6)$$

And Plant model:

$$G_m(s) = \frac{y_m(s)}{r(s)} = \frac{dy_m}{dt} = -ay(t) + b_m r(t) \quad (5.7)$$

Where  $y$  is the system output,  $u$  is the control input and parameter  $a$  is unknown and time-varying. The system is controlled by a proportional controller

Controller:

$$u(t) = \theta_1 r(t) - \theta_2 y(t) \quad (5.8)$$

$$G_m(s) = \frac{y_m(s)}{r(s)} = \frac{dy_m}{dt} = -ax(t) + b_m r(t) = \frac{b_m}{s+a_m} \quad (5.9)$$

$$G(s) = \frac{y(s)}{u(s)} = \frac{dy}{dt} = -ax(t) + bu(t) = \frac{b}{s+a} \quad (5.10)$$

But a ,b unknown and To do this, a cost function, J( ) is chosen and minimized which is given by equation Cost function:

$$J(\theta) = \frac{1}{2} e^2 \Rightarrow \frac{\partial J}{\partial \theta} = e \quad (5.11)$$

We aim to find the adjustable parameter  $\theta_1$  and  $\theta_2$  which can be found from Equation (5.2)

$$\frac{d\theta}{dt} = -\lambda \frac{\partial J}{\partial \theta} = -\lambda \frac{\partial J}{\partial e} \frac{\partial e}{\partial \theta} = -\lambda \frac{\partial e}{\partial \theta} \sin(e) \quad (5.12)$$

To find  $\frac{d\theta}{dt}$  we need to find  $\frac{\partial e}{\partial \theta}$  the expression of e in terms of  $\theta$

$$e = y - y_m = \frac{b}{s+a} u - \frac{b_m}{s+a_m} r \quad (5.13)$$

$$\text{Note that } y = \frac{b}{s+a} u = \frac{b}{s+a} (\theta_1 r(t) - \theta_2 y(t))$$

$$y = \frac{b}{s+a+\theta_2} \theta_1 r \quad (5.14)$$

$$e = \frac{b}{s+a+\theta_2} \theta_1 r - \frac{b_m}{s+a_m} r \quad (5.15)$$

$$\frac{\partial e}{\partial \theta_1} = \frac{b}{s+a+\theta_2} r \quad (5.16)$$

$$\frac{\partial e}{\partial \theta_2} = -\frac{b^2 \theta_1}{(s+a+\theta_2)^2} r \quad (5.17)$$

$$\frac{\partial e}{\partial \theta_2} = -\frac{by}{(s+a+\theta_2)} \quad (5.18)$$

$$\frac{d_{n_1}}{dt} = -\chi e \frac{\partial e}{\partial_{n_1}} = -\chi e \left[ \frac{b}{(s+a+b_{n_2})} r \right] \quad (5.19)$$

$$\frac{d_{n_2}}{dt} = -\chi e \frac{\partial e}{\partial_{n_2}} = \chi e \left[ \frac{b}{(s+a+b_{n_2})} y \right] \quad (5.20)$$

However, a and b are unknown. Also, both  $\frac{d_{n_1}}{dt}$  and  $\frac{d_{n_2}}{dt}$  are a function of  $(n)$ , which we need for adaptation. In this case we need to do some approximation: Assume that the input and output relation of the system and the model are the same i.e. perfect model following,

$$y = y_m$$

And so  $e$  in (5.15) tends to zero at steady state. We then have,

$$\frac{b}{s+a+b_{n_2}} r = \frac{b_m}{s+a_m} r \quad (5.21)$$

If we approximate  $s+a+b_{n_2} = s+a_m$  and  $b_{n_1} r = b_m r$

$$\frac{d_{n_1}}{dt} = -\chi e \left[ \frac{b}{(s+a_m)} r \right] = -\chi e \frac{b}{b_m} y_m = \chi' y_m e \quad (5.22)$$

$$\frac{d_{n_2}}{dt} = \chi e \left[ \frac{b}{(s+a_m)} y \right] = \chi e \left[ \frac{b}{b_m r} y_m \right] y = \chi e \frac{b}{b_m} \cdot \frac{y_m}{r} y = \chi \frac{b}{b_m} \cdot \frac{b_m}{s+a_m} y e = \chi' \frac{b_m}{s+a_m} y e \quad (5.23)$$

## 5.7 MRAC Design using Lyapunov Method

The model reference adaptive controller designed using the Gradient method/MIT rule has been described. It has also been shown that the method does not guarantee stability to the resulting closed-loop system. However, MRAC can also be designed such that the globally asymptotic stability of the equilibrium point of the error difference equation is guaranteed. To do this, we use the Lyapunov method (Popov, 1973). The first requires an appropriate Lyapunov function to be chosen, which could be difficult, whereas the second method is more systematic. This section looks at the MRAC system designed using the Lyapunov Method.

## Controller Design Method

It has been seen in Section (5.5) that there is no guarantee that an adaptive controller designed based on MIT Rule will give a stable adaptive system. On the other hand, designing an MRAC using Lyapunov Method will ensure a stable closed loop system. In designing an MRAC using Lyapunov Method, the following steps should be Followed

- i) Derive a differential equation for error,  $e = y - y_m$  (i.e.  $e, \dot{e}, \ddot{e}$ ) that contains the adjustable parameter,  $\theta$ .
- ii) Find a suitable Lyapunov function,  $v(\theta, e)$  usually in a quadratic form (to ensure positive definiteness).
- iii) Derive an adaptation mechanism based on  $v(\theta, e)$  such that  $e$  goes to zero.

### 5.7.1 Lyapunov Method

Consider an adaptive control system with the following plant, reference model and controller:

Plant model:

$$\frac{dy}{dt} = -ay(t) + bu(t) \quad (5.24)$$

Reference model:

$$\frac{dy_m}{dt} = -a_m y_m(t) + b_m r(t) \quad (5.25)$$

Controller:

$$u(t) = \theta_1 r(t) - \theta_2 y(t) \quad (5.26)$$

It follows from equation (5.1) and (5.3), that

$$y = \frac{b}{s + a + b\theta_2} \theta_1 r \quad (5.27)$$

$$y_m = \frac{b_m}{s + a_m} r \quad (5.28)$$

Step 1: Derive differential equation for  $e$  that contains

$$\dot{e} = \dot{y} - \dot{y}_m \quad (5.29)$$

$$\dot{y} + (a + b_{r2})y = b_{r1}r \quad (5.30)$$

$$\dot{y} = -(a + b_{r2})y + b_{r1}r \quad (5.31)$$

$$\dot{y}_m + a_m y_m = b_1 r \quad (5.32)$$

$$\dot{y}_m = -a_m y_m + b_1 r \quad (5.33)$$

$$\begin{aligned} \dot{e} &= \dot{y} - \dot{y}_m \\ &= -(a + b_{r2})y + b_{r1}r + a_m y_m - b_1 r \end{aligned} \quad (5.34)$$

$$= -ay - b_{r2}y + b_{r1}r + a_m y_m - b_1 r \quad (5.35)$$

$$= -ay - b_{r2}y + b_{r1}r + a_m (y - e) - b_1 r \quad (5.36)$$

$$= -a_m e - (a + b_{r2} - a_m)y + (b_{r1} - b_1)r \quad (5.37)$$

$$= -a_m e - \left[ \frac{a - a_m}{b} + b_{r2} \right] by + \left[ b_{r1} - \frac{b_1}{b} \right] br \quad (5.38)$$

$$= -a_m e - [X_1]by + [X_2]br \quad (5.39)$$

Step 2: Find the suitable Lyapunov function (usually in quadratic form), The Lyapunov function,  $V(e, X_1, X_2)$  is chosen based on (5.39). Let

$$V(e, X_1, X_2) = [e \quad X_1 \quad X_2] \begin{bmatrix} a_m & 0 & 0 \\ 0 & \lambda_1 & 0 \\ 0 & 0 & \lambda_2 \end{bmatrix} \begin{bmatrix} e \\ X_1 \\ X_2 \end{bmatrix} \quad (5.40)$$

$$V(e, X_1, X_2) = a_m e^2 + \lambda_1 X_1^2 + \lambda_2 X_2^2 \quad (5.41)$$

Where  $\lambda_1, \lambda_2 > 0$  so that V is positive definite

$$V \cdot = \frac{\partial V}{\partial e} \frac{\partial e}{\partial t} + \frac{\partial V}{\partial X_1} \frac{\partial X_1}{\partial t} + \frac{\partial V}{\partial X_2} \frac{\partial X_2}{\partial t} \quad (5.42)$$

$$V \cdot = a_m 2e \dot{e} + 2\} X_1 X_1 \dot{X}_1 + 2\} X_2 X_2 \dot{X}_2 \quad (5.43)$$

$$V \cdot = a_m 2e [-a_m e - X_1 b y + X_2 b r] + 2\} X_1 X_1 \dot{X}_1 + 2\} X_2 X_2 \dot{X}_2 \quad (5.44)$$

$$V \cdot = 2e^2 a_m^2 - 2a_m X_1 b y e + 2a_m X_2 b r e + 2\} X_1 X_1 \dot{X}_1 + 2\} X_2 X_2 \dot{X}_2 \quad (5.45)$$

For stability  $V \cdot < 0$

$$-Y + Z < 0 \Rightarrow Z < Y$$

Therefore, we can take  $Z=0$

$$-2a_m X_1 b y e + 2a_m X_2 b r e + 2\} X_1 X_1 \dot{X}_1 + 2\} X_2 X_2 \dot{X}_2 = 0 \quad (5.46)$$

For expression

$$X_1 = \left[ \frac{a - a_m}{b} + n_2 \right] \Rightarrow X_1 \dot{X}_1 = n_1 \dot{X}_1, X_2 = \left[ n_1 - \frac{b_m}{b} \right] \Rightarrow X_2 \dot{X}_2 = n_2 \dot{X}_2$$

$$-2a_m X_1 b y e + 2a_m X_2 b r e + 2\} X_1 n_1 \dot{X}_1 + 2\} X_2 n_2 \dot{X}_2 = 0 \quad (5.47)$$

Derive an adaptation mechanism (for  $n_1$  and  $n_2$ )

$$-2X_1 [-a_m b y e + \} X_1 n_2 \dot{X}_1] + 2X_2 [a_m b r e + \} X_2 n_1 \dot{X}_2] = 0 \quad (5.48)$$

This is possible if

$$-a_m b y e + \} X_1 n_2 \dot{X}_1 = 0 \quad (5.49)$$

$$a_m b r e + \} X_2 n_1 \dot{X}_2 = 0 \quad (5.50)$$

$$n_2 \dot{X}_1 = \frac{-a_m b y e}{\} X_1} = X_2 y e \Rightarrow \text{where } X_2 = \frac{a_m b}{\} X_1} \quad (5.52)$$

$$\dot{x}_1 = \frac{-a_m b r e}{\} _2} = x_1 y e \Rightarrow \text{where } x_1 = \frac{a_m b}{\} _2} \quad (5.53)$$

## 6.8 Full-State Measurement

Let us now consider the nth order plant

$$\dot{x} = Ax + Bu, x \in R^n \quad (5.54)$$

where  $A \in R^{n \times n}$ ,  $B \in R^{n \times q}$  are unknown constant matrices and (A,B) is controllable. The control objective is to choose the input vector  $u_m \in R^q$  such that all signals in the closed-loop plant are bounded and the plant state  $x$  follows the state  $x_m \in R^n$  of a reference model specified by the LTI system

$$\dot{x}_m = A_m x_m + B_m u, x \in R^n \quad (5.55)$$

where  $A_m \in R^{n \times n}$  is a stable matrix,  $B_m \in R^{n \times q}$ ,  $r \in R^q$  is a bounded reference input vector. The reference model and input  $r$  are chosen so that  $x_m(t)$  represents a desired trajectory that  $x$  has to follow. Control Law If the matrices A;B were known, we could apply the control Law

$$u = -K^* x + L^* r \quad (5.56)$$

and obtain the closed-loop plant

$$\dot{x} = (A - BK^*)x + BL^* r \quad (5.57)$$

Hence, if  $K^* \in R^{q \times n}$  and  $L^* \in R^{n \times q}$  are chosen to satisfy the algebraic equations

$$A - BK^* = A_m, BL^* = B_m \quad (5.58)$$

then the transfer matrix of the closed-loop plant is the same as that of the reference model and  $x(t) \rightarrow x_m(t)$ , exponentially fast for any bounded reference input signal  $r(t)$ . We should note that given the matrices  $A, B, A_m, B_m, no K^*, L^*$  may exist to satisfy the matching condition (5.57) indicating that the control law (5.56) may not have enough structural flexibility to meet the control

objective. In some cases, if the structure of A,B is known,  $A_m, B_m$  may be designed so that (5.57) has a solution for  $K^*, L^*$ . Let us assume that  $K^*, L^*$  in (5.57) exist, i.e., that there is sufficient structural flexibility to meet the control objective, and propose the control law

$$u = -K(t)x + L(t)r$$

where  $K(t); L(t)$  are the estimates of  $K^*, L^*$  respectively, to be generated by an appropriate adaptive law. Adaptive Law By adding and subtracting the desired input term, namely,  $-B(K^*x - L^*r)$ , in the plant equation and using (5.57), we obtain

$$\dot{x}_m = A_m x_m + B_m r + B(K^*x - L^*r + u) \quad (5.59)$$

$$\dot{e} = A_m e + B_m r + B(-\tilde{K}x + \tilde{L}r^*) \quad (5.60)$$

This also depends on the unknown matrix B. In the scalar case we manage to get away with the unknown B by assuming that its sign is known. Let us assume that  $L^*$  is either positive definite or negative definite and  $\Gamma^{-1} = L^* \sin(l)$  where  $l = 1$  if  $L^*$  is positive definite and  $l = -1$  if  $L^*$  is negative definite. Then

$$B = B_m, L^{*-1} \text{ and (5:60) becomes}$$

$$\dot{e} = A_m e + B_m r + B_m L^{*-1}(-\tilde{K}x + \tilde{L}r^*) \quad (5.61)$$

We propose the following Lyapunov function candidate

$$V(e, \tilde{K}, \tilde{L}) = e^T P e + B_m r + t \eta [\tilde{K}^T \Gamma \tilde{K} + \tilde{L}^T \Gamma \tilde{L}] \quad (5.62)$$

Where  $P = P^T \succ 0$  satisfies the lyapunov equation

$$P A_m + A_m^T P = -Q \quad (5.63)$$

For some  $Q = Q^T \succ 0$  then

$$\dot{V} = -e^T Q e + 2e^T P B_m L^{*-1} [-\tilde{K}x + \tilde{L}r] + 2t \eta [\tilde{K}^T \Gamma \dot{\tilde{K}} + \tilde{L}^T \Gamma \dot{\tilde{L}}] \quad (5.64)$$

Now

$$2e^T P B_m L^{*-1} \tilde{K}x = \text{tr}[x^T \tilde{K}^T \Gamma B_m P e] \sin(l) = \text{tr}[\tilde{K}^T \Gamma B_m^T P e] \sin(l) \quad (5.65)$$

$$e^T P B_m L^{\bullet-1} \tilde{L} r = \text{tr}[\tilde{L}^T \Gamma B_m^T P e r^T] \sin(l)$$

There for

$$K^{\bullet} = K^{\bullet} = B_m^T P e x^T \sin(l), \tilde{L}^{\bullet} = L^{\bullet} = B_m^T P e r^T \sin(l) \quad (5.66)$$

We have

$$V^{\bullet} = -e^T Q e \quad (5.67)$$

# CHAPTER SIX

## RESULTS AND DISCUSSION

### 6.1 Introduction

This chapter presents the simulation results for the single machine connected to the infinite bus system. The PSS design based on model reference adaptive control using lyapunov and gradient method. The performance of the PSSs is accessed via the modal analysis stated in chapter three and validated using time domain simulations. The effectiveness of the resulting PSSs to damp the low frequency oscillations is tested under various operating conditions. The results are validated through simulations of the system's response for three different operating conditions. The comparison is carried out between the system equipped with CPSS and adaptive PSS.

### 6.2 Adaptive Power System Stabilizer

Following the application of adaptive control to tune the PSS, the Simulink diagram shown in Figure (6.1) obtain implementation of adaptive power system stabilizer in single machine finite bus and Figure (6.2) show time response of speed deviation of generator in case of normal load with conventional and adaptive PSS. The adaptive PSS that would give the best damping for the most dominant poles of the system.

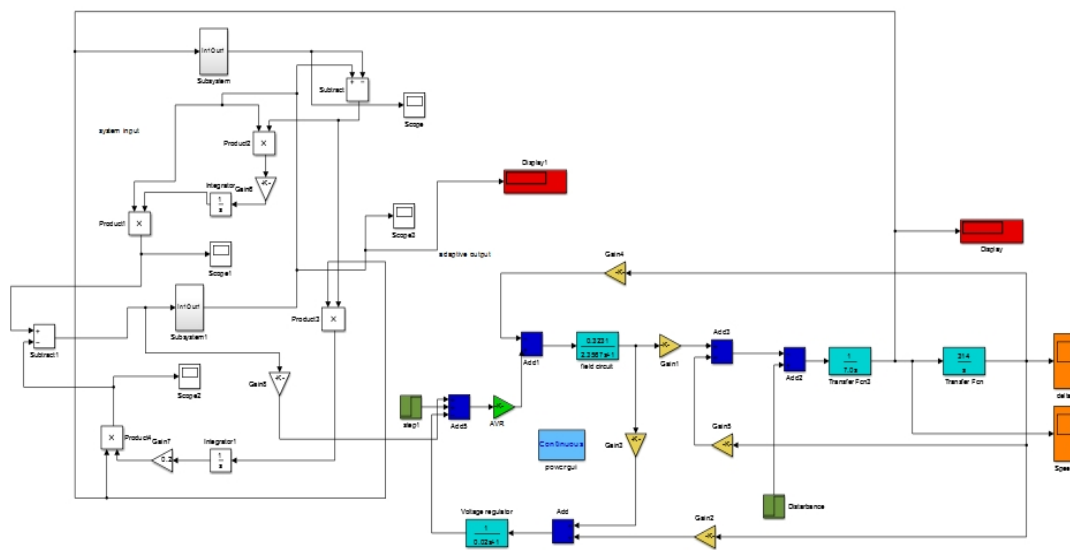


Figure (6.1) Simulink model of APSS in SMIB

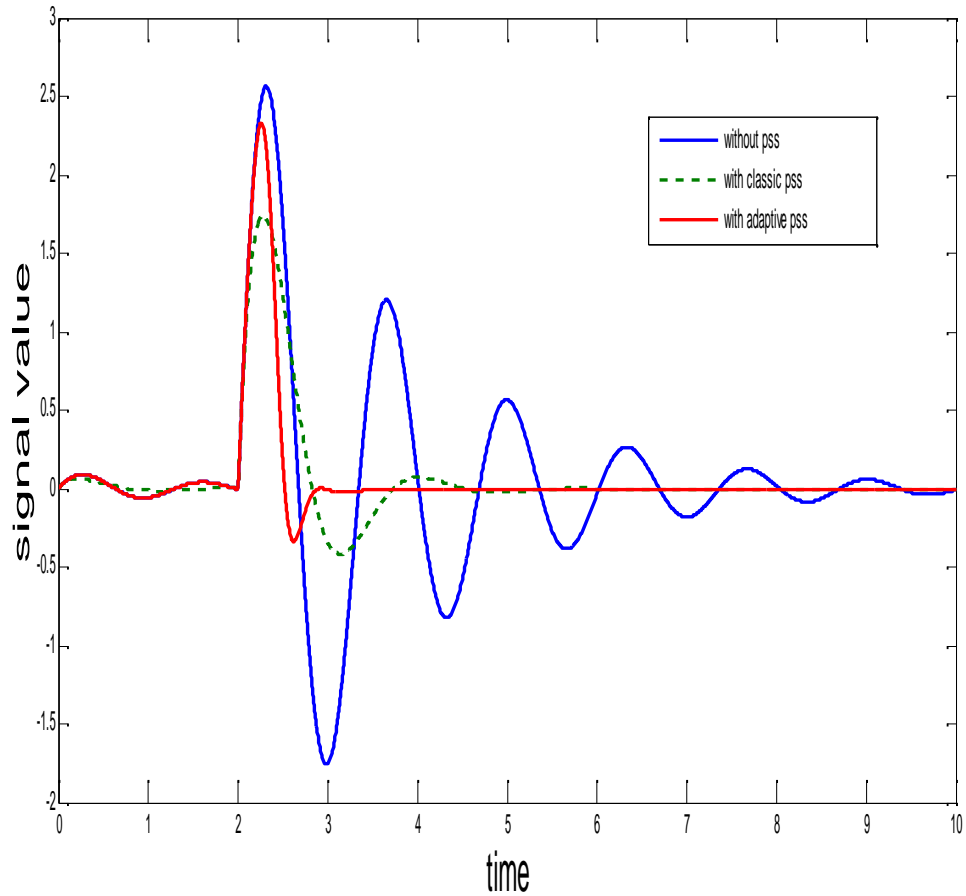


Figure (6.2) Rotor Speed deviation with APSS

### 6.3 Effect of Conventional PSS on Different Operation points

The figure (6.3) shows speed deviation response in different operation points, normal load , heavy load and light load. It's clear from the figure the classic power system stabilizer cannot damp out power system oscillation in different operation points.

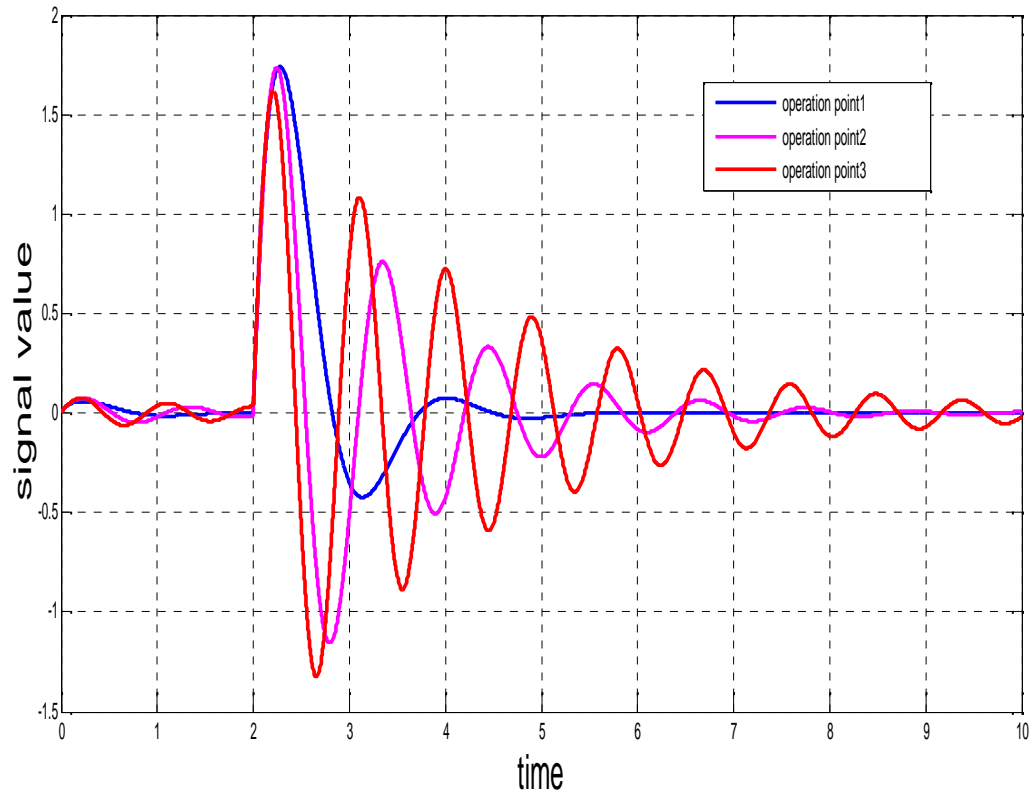


Figure (6.3) Speed deviation response in different operation points

### **6.4 Effect of adaptive PSS on different operation points**

The figure (6.4) shows speed deviation response in different operation point, normal load ,heavy load and light load. It's clear from the figure the adaptive power system stabilizer damp out most of oscillation in different operation points. It's better than conventional power system stabilizer.

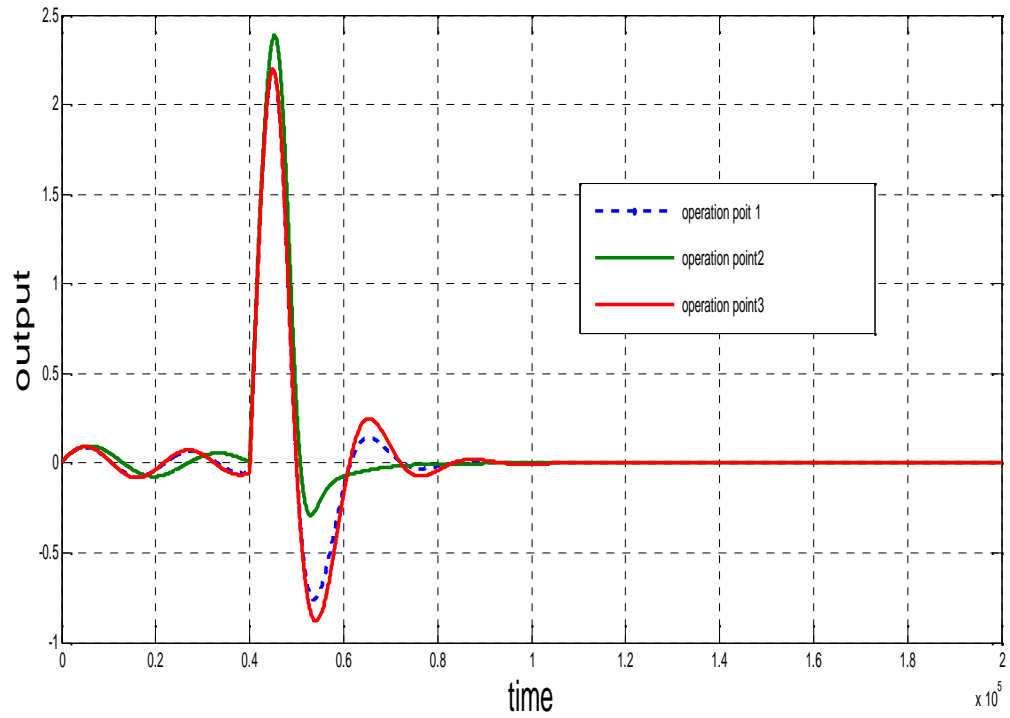


Figure (6.4) Speed deviation response in different operation in case of adaptive PSS

## 6.5 Model Reference Adaptive Control Design Based on Gradient Method

The Model reference Adaptive Control Scheme is applied to plan describe in equation ( 5.6) by using MIT. The models are simulated in Matlab which are shown in Figure (6.5) and Figure (6.6) shows simulation diagram.

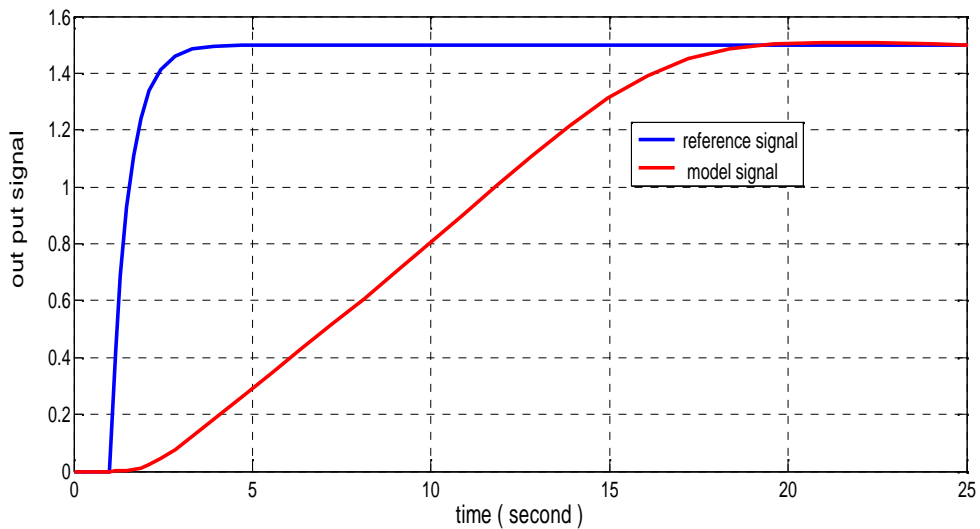


Figure (6.5) model reference tracking based on MIT rules

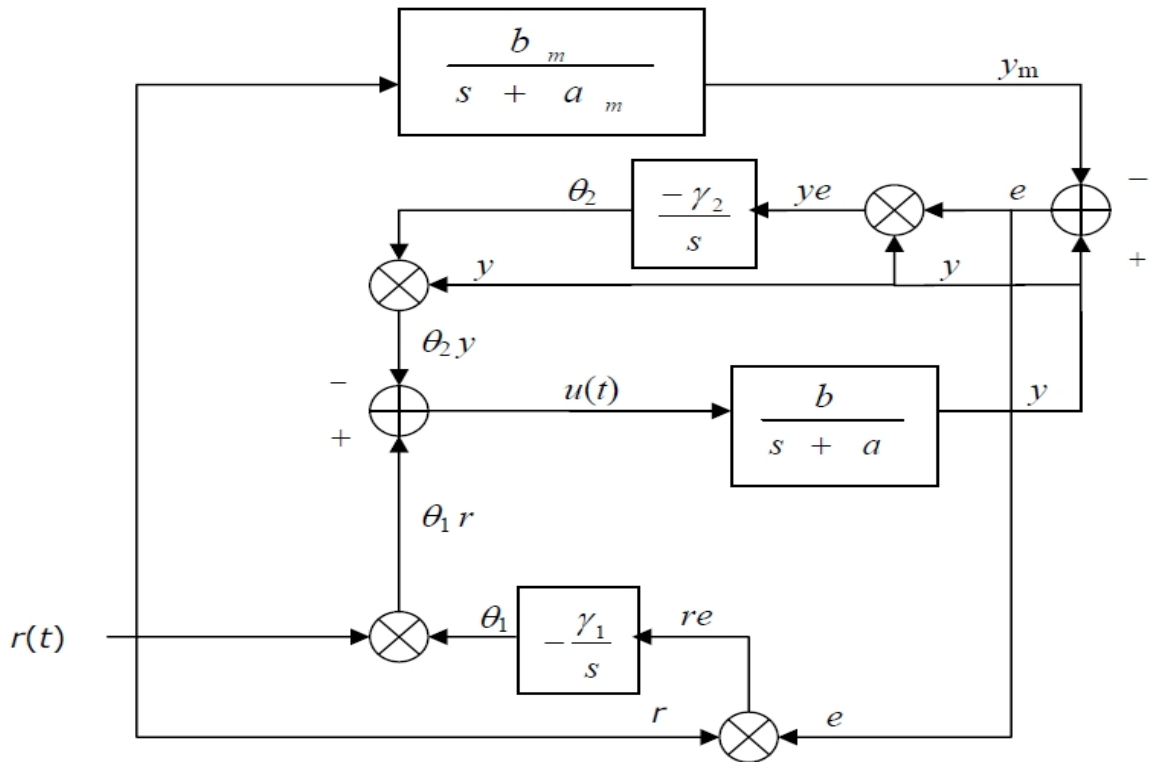


Figure (6.6) Simulink diagram based on MIT rules

## 6.6 Comparative of Convergence of Theta based on MIT and Lyapunov

Figures (6.8),(6.8),(6.9) and (6.10) compares the time responses of same plant controlled by MIT and Lyapunov rules for the same adaptation gain. The characteristics show that there is midrate difference in responses for both the models, though the complicity is reduced to large extent in Lyapunov rule. Figure (6.7) and (6.8) shows the variation of  $\theta_1$  and  $\theta_2$  with respect to time for MIT rule. It can be observed that controller parameter 1 ( $\theta_1$ ) converges to 1.5 and controller parameter 2 ( $\theta_2$ ) converges to -0.31. Similarly fig (6.9) and (6.10) shows the variation of  $\theta_1$  and  $\theta_2$  with respect to time for Lyapunov rule. Here  $\theta_1$  converges to 0.9 and  $\theta_2$  converges to -0.55. There is difference in convergence, though it is faster with Lyapunov rule.

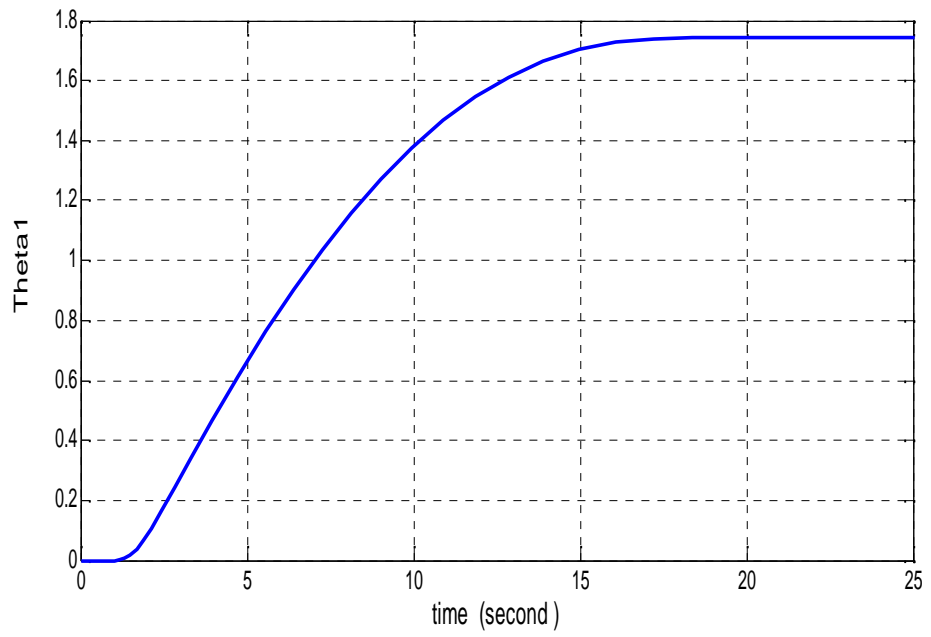


Figure (6.7) shows time response of theta 1 based on MIT rules

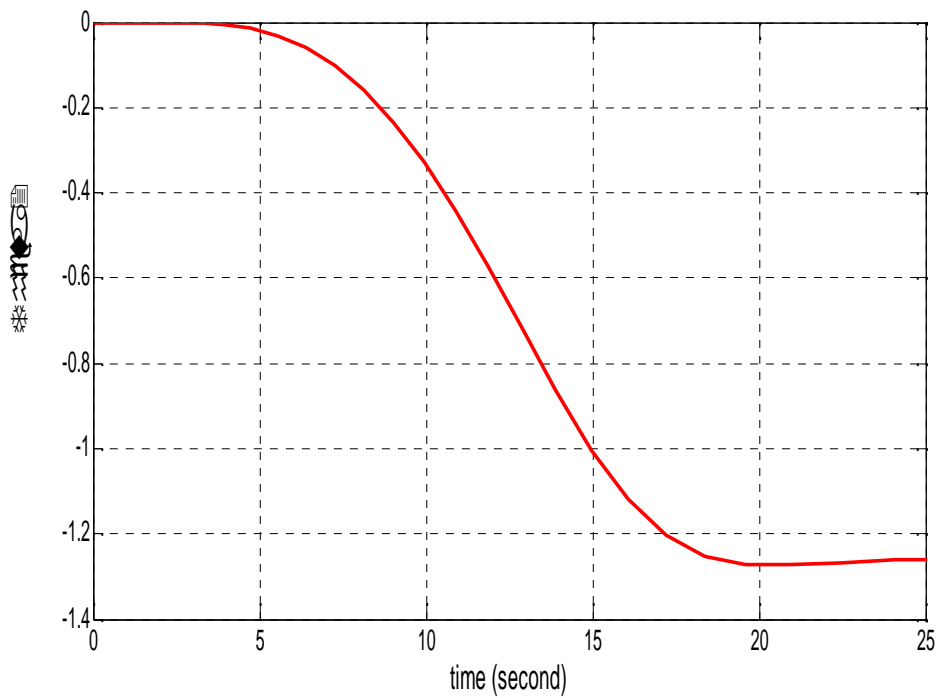
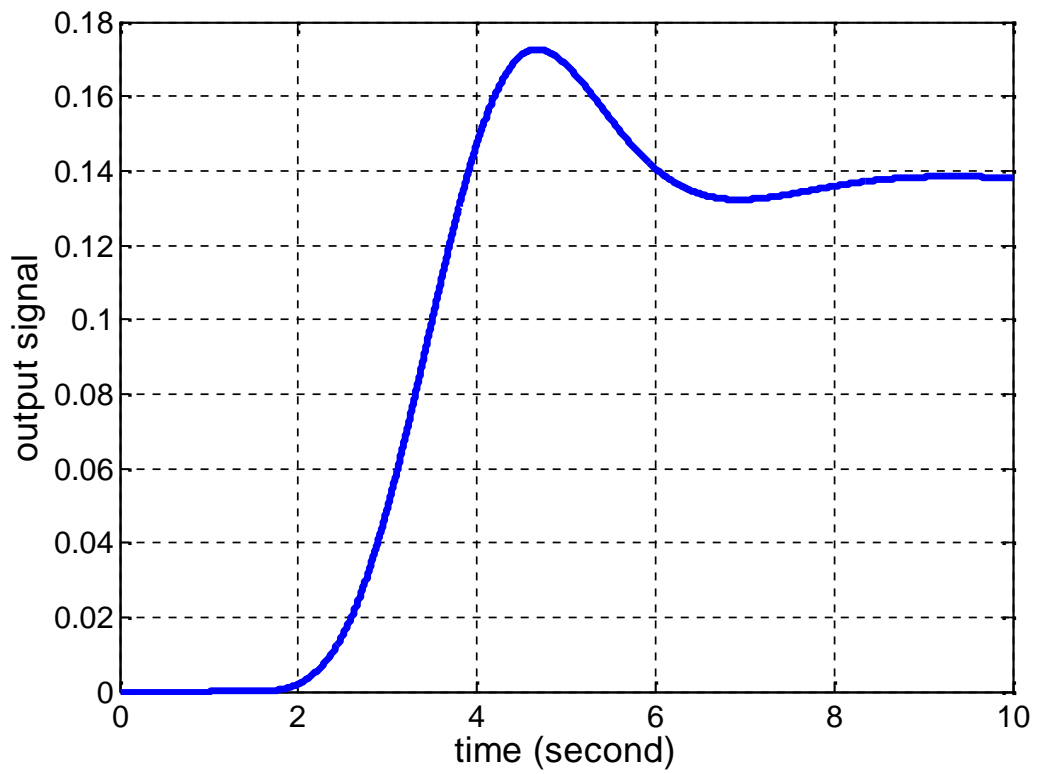
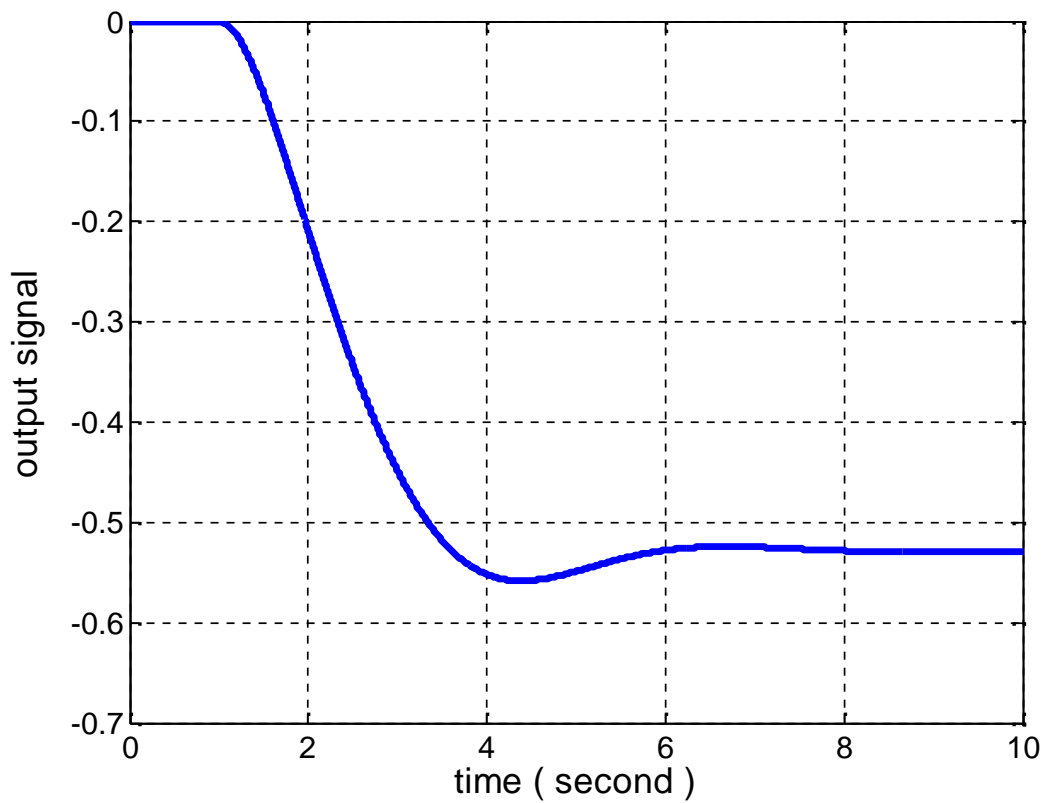


Figure (6.8) Time response of theta 2 based on MIT rule



Figure(6.9) Time response of theta1 based on lyapunovmethod



Figure(6.10)Time response of theta2 based on lyapunov rule

## 6.7 Model reference based on lyapunov method

The Model reference Adaptive Control Scheme is applied to plant describe in equation(5.24) by using lyapunov method. The models are simulated in Matlab which are shown in figure (6.11) and fig(6.12) show simulation diagram .

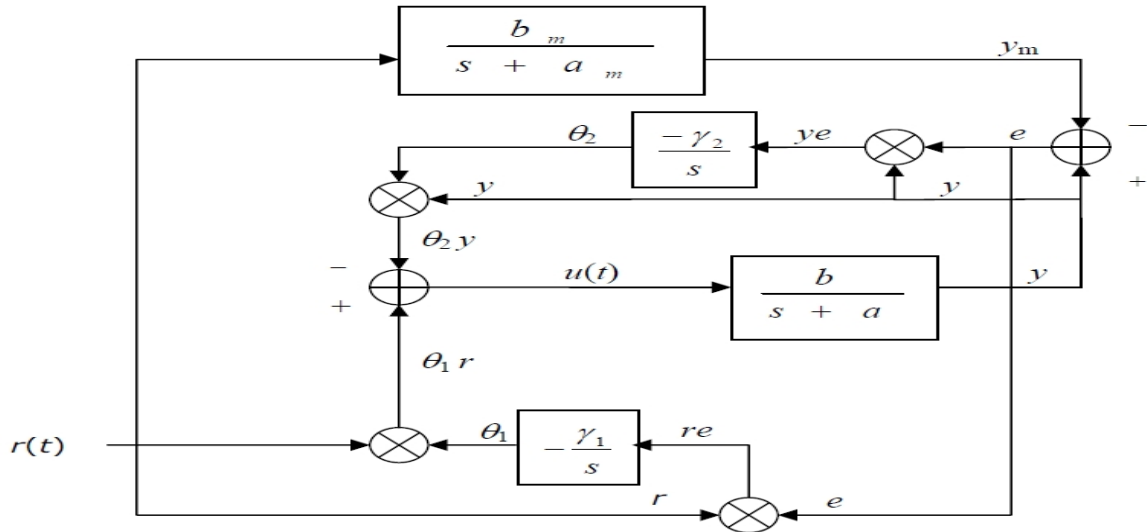


Figure (6.12) Shows Simulink diagram of system designed based on lyapunov method

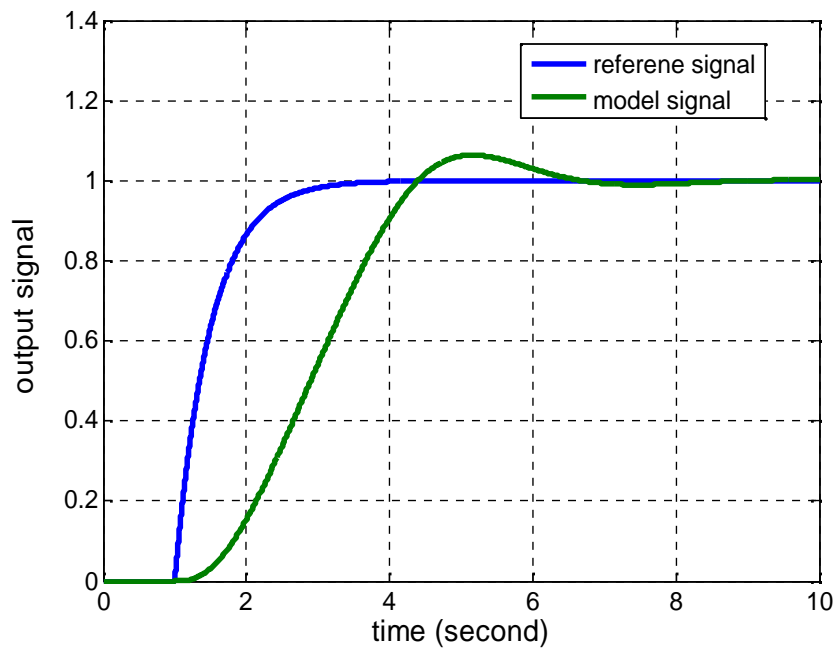


Figure (6.11) Model reference based on lyapunov method

## 6.8 Effect of adaptation Gain on Model Tracking In case of Gradient and Lyapunov Method

Figure (6.13) and figure (6.14) show the effect of adaptation gain on time response curves for MIT rule and Lyapunov rule respectively. There is improvement in the performance of the system with the increment in adaptation gain. Every system gives its best for the limited range of the adaptation gain. In this design the range of adaptation gain is chosen from 0.2 to 5 for the system under consideration. Beyond this range the system performance is going to high oscillatory. It has been seen that the response is very slow with the bigger value of adaptation gain.

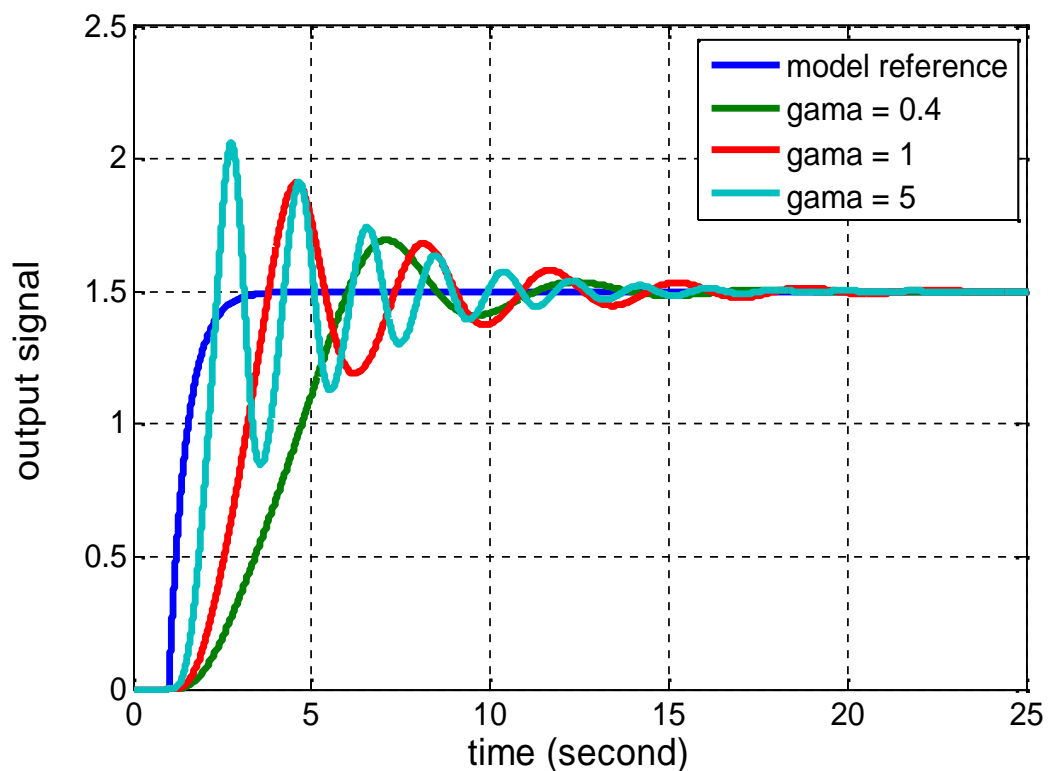


Figure (6.13) Effect of adaptation gain on model tracking In case of gradient

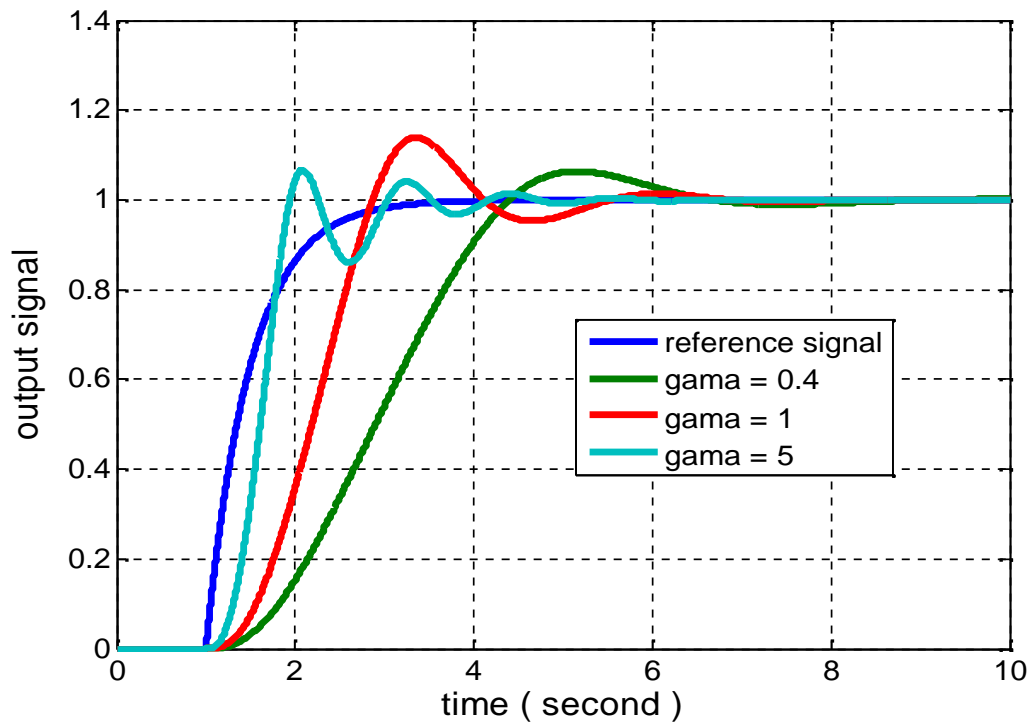


Figure (6.14) Effect of adaptation gain on model tracking In case of lyapunov

# CHAPTER SEVEN

## CONCLUSION AND FUTURE WORK

### 7.1 Conclusion

We discussed power system stability, oscillation modes, mechanisms and analysis methods to understand electromechanical oscillations phenomena.

We presented thesis motivations, and contribution of work. The design of Power System Stabilizer (PSS) involves a deep understanding of the dynamics model of the single machine infinite bus system and multi machine power system. Design conventional Power System Stabilizer using linear control principles and view the problem as a feedback control problem concerned in fixed gain.

Next introduced adaptive control to design power system stabilizer by MIT rule and lyapunov method, in two cases scalar and vectors. Finally evaluated performance of controller which designed by MIT rules and Lyapunov methods by time domain simulation in SMIB with different loading conditions, normal, heavy and light load.

### 7.2 Future Work

The results of this thesis open some interesting and challenging problems of great importance. In what follows, we point out of possible future research

- Use Model free Adaptive control (MFAC) for same work the model reference adaptive control has some disadvantage it takes some time to adapt desired performance of model reference.
- For more accuracy of model reference combine adaptive fuzzy or adaptive neural for same work.
- combine power system stabilizer with UPFC or FACT devises to more damp for same work
- Applied adaptive power stabilizer to multi machine power system.

## Reference

- [1] PrabhaKundur, Power System Stability and Control," The EPRI Power System Engineering Series,1994, McGraw-Hill, ISBN 0-07-063515-3.
- [2] J. Machowski and Others, Power System Dynamics: Stability and Control. United Kingdom: JohnWiley& Sons, Ltd, 2008.
- [3] G. Rogers, \Demystifying power system oscillations," Computer Applications in Power, IEEE, vol. 9, No. 3, pp. 30 {35, jul 1996}.
- [4] P. M. Anderson, A. A. Fouad, and H. H. Happ, \Power system control and stability," Systems, Man and Cybernetics, IEEE Transactions on, vol. 9, no. 2, p. 103, feb. 1979
- [5] K. R. Padiyar, \Power system dynamics: Stability and control," in printed in the Republic of Singapore, ISBN: 0-471-19002-0, 1996.
- [6] P. Kundur, N. J. Balu, and M. G. Lauby, Power system stability and control. NewYork: McGraw-Hill, 1994.
- [7] IEEE, "IEEE Guide for Identification, Testing, and Evaluation of the Dynamic Performance of Excitation Control Systems," in IEEE Std 421.2-1990, ed, 1990, p. 45.
- [8]. F.P.deMello, C.Concordia, "Concepts of synchronous machine stability asaffected by excitation control", IEEE Trans. on Power App. Syst., vol-88 pp.189-202, April 1969.
- [9]. E.V.Larsen, D.A.Swann, "Applying Power System Stabilizers", Part-1, Part-2, Part-3, IEEE Trans. on Power App. Syst, vol. PAS-100, pp. 3017-3046, June1981.
- [10] DebasishMondal, AbhijitChakrabarti, AparajitaSengupta-Power System Small Signal Stability Analysis and Control- Academic Press 2014.
- [11] Jsalins. And Jesus R Pacheco," modeling techniques and tuning in excitation system for dynamic representation,',6th WSEAS International
- [12] Graham Rogers, Power System Oscillations. Boston: Kluwer Academic, 1999.

- [13] G. Rogers, "Demystifying power system oscillations," *IEEE Computer Applications in Power*, vol. 9, no. 3, pp. 30 - 35, 1996.
- [14] AntalSoos, "An Optimal Adaptive Power System Stabilizer," Department of Electrical and Computer Engineering, University of Calgary, Calgary, Thesis 1997.
- [15] P. Kundur, M. Klein, G.J. Rogers, and M.S. Zywno, "Application of Power System Stabilizers for enhancement of overall system stability," *IEEE Transactions on Power Systems*, vol. 4, no. 2, pp. 614-626, May 1989.
- [16] K.R. Padiyar, "Power System Dynamics Stability and Control," Bangalore: Wiley, 1996.
- [17] E.V. Larsen and D.A. Swann, "Applying Power System Stabilizers, Part I; General concepts, Part II; Performance objectives and Tuning concepts, Part III; Practical considerations," *IEEE Trans. on Power Apparatus and Systems*, vol. PAS-100, pp.3017-3046, 1981.
- [18] AntalSoós and O.P Malik, "An H2 Optimal Adaptive Power System Stabilizer," *IEEE transaction on energy conversion*, vol. 17, no. 1, pp. 143-149, Conference on circuits, systems, electronic, control&signal processing, Cairo, Egypt, Dec 29-31, 2007
- [19] A. Ghosh, G. Ledwich, O. P. Malik, and G. S. Hope, "Power System Stabilizer Based on Adaptive Control Techniques," *IEEE Transaction on Power Apparatus and Systems*, , vol. Vol. PAS-103, no. 8, pp. 1983-1989, August 1984.
- [20] Shark Zhang and Fang Lin Luo, "An Improved Simple Adaptive Control Applied to Power System Stabilizer," *IEEE transaction onpowerelectronics*, vol. 24, no. 2, February 2000.
- [21] A. Hariri and O.P. Malik, "Adaptive-Network-Based Fuzzy Logic Power System Stabilizer," in *IEEE we scanexproceedings*, 1995, pp. 111-116.
- [22] Zhang S and Fang Lin Luo, "An Improved Simple Adaptive Control Applied to Power System Stabilizer," *IEEE transaction on power electronics*, vol. 24, no. 2, pp. 369-375, FEBRUARY 2009.

- [23] Graham Rogers ,power system oscillations ,by Kluwer Academic Publishers , 2000.
- [24] P. Kundur, M. Klein, G. J. Rogers, and M. S. Zywno, "Application of Power System Stabilizers for Enhancement of Overall System Stability", IEEE Transactions on Power Systems, Vol. 4, 1989, pp. 614-626.
- [25]. J. H. Chow, J. J. Sanchez-Gasca, "Pole-placement Designs of Power System Stabilizers", IEEE Transactions on Power Systems, Vol. 4, No. 1, pp271-277
- [26]. M. A. Abido, "Hybridizing Rule-Based Power System Stabilizers with Genetic Algorithms", IEEE Transactions on Power Systems, Vol. 14, 1999, pp. 600-607
- [27]Y.L. Abdel-Magid, M.A. Abido, S. Al-BaiyatanA.H.Mantawy,"Simultaneous Stabilization of Multi-machine Power Systems via Genetic Algorithms", IEEE transactions on Power Systems, Vol. 14, 1999, 1428-1438.
- [28] Y.L. Abdel-Magid, M.A. Abido and A.H. Mantawy, "Robust Tuning of Power System Stabilizers in Multimachine Power Systems", IEEE transactions on Power Systems, Vol. 15, 2000, pp 735-740.
- [29] J. Lu, M.H. Nehrir and D.A. Pierre, "A Fuzzy Logic-based Adaptive Power System Stabilizer for Multi-machine Systems", Electric Power Systems Research, Vol. 60, 2001, pp115-pp121
- [30] Anta1 Soos et al,"An Optimal Adaptive Power System Stabiliz"..0-7803-5569-5/99/\$10.00 0 1999 IEEE Proc. 2007 42nd Int. Univ. Power Eng. Conf., Brighton, U.K., Sep.2
- [31] P. He Y.B.WeiC.X.Yang et al "adaptive powerstabilizer designfor multi-machine power systems", School of Electrical Engineering, Zhengzhou University.
- [32] Chun Liu, PSS design for damping of inter-area power oscillation by coherency-based equivalent model, Tokyo Metropolitan University, 1-1 Minamiosawa, Hachioji, Tokyo 192-0397, Japan

- [33] Recommended Practice for Excitation System Models for Power System *Stability Studies*, IEEE Standard 421.52005, April 2006.
- [34] P.L. Dandeno, A.N. Karas, K.R. McClymont, and W. Watson, "Effect of High-Speed Rectifier Excitation System on Generator Stability Limits," *IEEE Trans.*, Vol. PAS-87, pp. 190-201, January 1968.
- [35] W. Watson and G. Manchur, "Experience with Supplementary Damping Signals for Generator Static Excitation Systems," *IEEE Trans.*, Vol. PAS-92, pp. 199-203, January/February 1973.
- [36] W. Watson and M.E. Coultres, "Static Exciter Stabilizing Signals on Large Generators – Mechanical Problems," *IEEE Trans.*, PAS-92, pp. 204-211, January/ February 1973
- [37] E.V Larsen and D .A swaan ,’’ applying power system stabilizer ,part I,II, and III ,*IEEE trans*,vol.pas-100 ,June 1981 pp.3017-3046.
- [38] Fariborz Parandin, Ali Mohammadi, Hosain Sariri. Power System Stabilizer Design based on Model Reference Adaptive System. *J Am Sci* 2012;8(7):751-755]. (ISSN: 1545-1003).
- [39] Fariborz Parandin, Ali Mohammadi, Hosain Sariri, ’ Adaptive Multi Machine PSS Design for Low Frequency Oscillations Damping, Vol:5 Issue:12 December 2012 ISSN:0974-6846 *Indian Journal of Science and Technology*.
- [40] D. Nazarpour, S. H. Hosseini, G. B. Gharehpetian. ’ Damping of Generator Oscillations Using an Adaptive UPFC-based Controller , *American Journal of Applied Sciences* 3 (1): 1662-1668, 2006 ISSN 1546-9239
- [41] Kothari, M L Bhattacharya, K Nanda Adaptive power system stabilizer based on pole-shifting technique, *generation, Transmission and*
- [ 42] Yuan-Yih Hsu et al (1996) discussed the identification and tuning of exciter constants for a generating unit at the Second Nuclear Power Plant of Taiwan Power Company , *IEEE transaction on power system* , volume 18, issues 4

- [43] A. J. A. *Simoes Costa* ; F. D. Freitas ; A. S. e Silva a method for the design of power system controllers aimed at damping out electromechanical oscillations. *IEEE transaction on power system* ,volume 18,issues 4
- [44] S.S. Choi, inherent dynamical relationship between the under-excitation limiter (UEL) and the PSS control loops in synchronous generators using the frequency response technique, Sep 2000; Date of Current Version : Tue Aug 06 .., 2000, Page(s):1154 - 1160
- [45] H. M. Soliman, A simple robust PSS, *IEEE transaction on power system* ,volume 18,issues 4 Sep 2000; Date of Current Version : Tue Aug
- [46] J. V. Milanovic, Dynamic interactions among various controllers used for stabilizing a synchronous generator , *IEEE transaction on power system* ,volume 147,issues 6
- [47] R. Ajabi-Farshbaf and el al Design of A Self-Tuning Adaptive Power System Stabilizer *Journal of Artificial Intelligence in Electrical Engineering*, Vol. 2, No. 5, May 2013
- [48] Shaoru Zhang and Fang Lin Luo, Power System Stabilizer Based on Improved Simple Adaptive Control, *IEEE Nanyang Technological University*, Nanyang Avenue, Singapore 639798, 978-1-4244-1718-6/08/\$25.00 ©2008 IEEE
- [49] V. Bobtail, J. Bhm, J. Fessl, and J. Macháček, *Digital Self tuning Controllers Algorithms implementation and Applications*, Springer-Verlag London Limited 2005)
- [50] K. J. Astrom and B. Wittenmark, *Adaptive Control*, Addison-Wesley, Reading, Massachusetts, 1989.
- [51] Chen, C.T., *Introduction to Linear System Theory*, Holt, Rinehart and Winston Inc., New York, 1970.
- [52] Anderson, B.D.O., "Adaptive Systems, Lack of Persistency of Excitation and Bursting Phenomena," *Automatica*, Vol. 21, pp. 247-258, 1985.
- [53] Petros\_Aoannou \_Jing\_Sun\_Robust\_Adaptive\_Control

[54] Chen et al,'Design of an Adaptive PSS Based on Recurrent Adaptive Control Theory',IEEE Transactions on Energy Conversion ( Volume: 8, Issue: 4, Dec 1993 )

[55] J.H. Chow" practical experience in assigning PSS IEEE Transactions on Power Systems ( Volume: 19, Issue: 1, Feb. 2004 )

[56] Hui Ni et al (2002) Power System Stability Agents Using Robust Wide Area Control IEEE transaction on power systems, vol. 17, NO. 4,november 2002

[57] Elices et al ,' Physical Interpretation of State Feedback Controllers to Damp Power System Oscillationsin IEEE Transactions on Power Systems 19(1):436 - 443 · March 2004

[58] Hassan Ghasemi (2006). On-line Monitoring and Oscillatory Stability Margin Prediction in Power Systems Based on System Identification. UW Space

[59] Gupta et al ,'designed PSS for a SMIB using periodic output feedback'2006 IEEE GCC Conference (GCC)

[60 ] M.A. Abido,"A novel approach to conventional power system stabilizer design using tabu search, Science Direct,Volume 21, Issue 6, August 1999, Pages 443–454.

## APPENDIX (A)

The appendix (A) obtain the eigenvalues, damping ratio and frequency oscillations when applied PSS to single machine connected in finite bus and multi machine example three machine nine bus system at different scenarios'

Table (A.1) Eigenvalues of System In case of Normal load

The eigenvalues of System Without any controller in case of Normal load		
Eigen values	Fn(Hz)	Zeta
-0.2522 + 6.3580i	1.0127	1.0000
-0.2522 - 6.3580i	0.5937	0.0396
-0.1783	0.0284	1.0000
-3.7305	1.0127	0.0396
The eigenvalues of System With included AVR		
Eig	Fn(Hz)	Zeta
-18.8952	3.0073	1.0000
-0.1640 + 6.3555i	1.0118	0.0258
-0.1640 - 6.3555i	1.0118	0.0258
-1.3292	0.2115	1.0000
-3.8607	0.6145	1.0000
The Eigen values of System With included AVR+PSS		
eig	Fn(Hz)	Zeta
-27.8615	4.4343	1.0000
-6.4694 + 8.7779i	1.7355	0.5933
-6.4694 - 8.7779i	1.7355	0.5933
-2.8930 + 6.0794i	1.0715	0.4297
-2.8930 - 6.0794i	1.0715	0.4297

-3.8707	0.6160	1.0000
-1.2401	0.1974	1.0000
-0.1012	0.0161	1.0000

Table (A.2) Eigenvalues of System In case of heavy load

The eigenvalues of System Without any Controller in case heavy load		
Eig	Fn(Hz)	Zeta
-0.1781 + 8.4194i	1.3403	0.0211
-0.1781 - 8.4194i	1.3403	0.0211
-0.2263	0.0360	1.0000
-3.8307	0.6097	1.0000
The eigenvalues of System With included AVR		
Eig	Fn(Hz)	Zeta
-18.8258	2.9962	1.0000
-0.1213 + 8.4051i	1.3379	0.0144
-0.1213 - 8.4051i	1.3379	0.0144
-1.4690	0.2338	1.0000
-3.8757	0.6168	1.0000
The eigenvalues of System With included AVR+PSS		
Eig	Fn(Hz)	Zeta
-27.5475	4.3843	1.0000
-2.6503 + 9.8039i	1.6163	0.2610
-2.6503 - 9.8039i	1.6163	0.2610
-6.7727 + 6.5933i	1.5043	0.7165
-6.7727 - 6.5933i	1.5043	0.7165
-3.8821	0.6179	1.0000
-1.4221	0.2263	1.0000
-0.1006	0.0160	1.0000

Table (A.3) Eigenvalues of System case of light load

The eigenvalues of System Without any Controller in case of light load		
Eig	Fn(Hz)	Zeta
-0.5480 + 6.2334i	0.9959	0.0876
-0.5480 - 6.2334i	0.9959	0.0876
-0.2238	0.0356	1.0000
-3.0934	0.4923	1.0000
The eigenvalues of System With included AVR		
Eig	Fn(Hz)	Zeta
-18.8667	3.0027	1.0000
-0.5181 + 6.2403i	0.9966	0.0827
-0.5181 - 6.2403i	0.9966	0.0827
-1.2711	0.2023	1.0000
-3.2391	0.5155	1.0000
The eigenvalues of System With included AVR+PSS		
Eig	Fn(Hz)	Zeta
-26.2055	4.1707	1.0000
-8.3084 + 7.0857i	1.7379	0.7609
-8.3084 - 7.0857i	1.7379	0.7609
-2.2215 + 6.4503i	1.0858	0.3256
-2.2215 - 6.4503i	1.0858	0.3256
-3.2413	0.5159	1.0000
-1.1906	0.1895	1.0000
-0.1010	0.0161	1.0000

Table (A.4) Eigenvalues of System in case of leading power factor load.

The eigenvalues of System Without any ControllerLeading power factor		
Eig	Fn(Hz)	Zeta
0.0649	0.0103	-1.0000
-0.1733 + 3.8571i	0.6145	0.0449
-0.1733 - 3.8571i	0.6145	0.0449
-4.1313	0.6575	1.0000
The eigenvalues of System With included AVR		
EigFn(Hz)	Zeta	
-18.9791	3.0206	1.0000
0.2827 + 3.8814i	0.6194	-0.0726
0.2827 - 3.8814i	0.6194	-0.0726
-1.9032	0.3029	1.0000
-4.0962	0.6519	1.0000
The eigenvalues of System With included AVR+PSS		
EigFn(Hz)	Zeta	
-28.7768	4.5800	1.0000
-7.0721 +10.1977i	1.9751	0.5699
-7.0721 -10.1977i	1.9751	0.5699
-1.4662 + 3.2730i	0.5708	0.4088
-1.4662 - 3.2730i	0.5708	0.4088
-4.1011	0.6527	1.0000
-1.7411	0.2771	1.0000
-0.1025	0.0163	1.0000

Table (A.5) Power flow and voltages in case of in normal load

Bus	V	phase	P gen	Q gen	P load	Q load
	[p.u.]	[rad]	[p.u.]	[p.u.]	[p.u.]	[p.u.]
Bus 1	1.04	0	0.36725	0.11017	0	0
Bus 2	1.025	0.20499	1.63	-0.0427	0	0
Bus 3	1.025	0.11956	0.85	-0.19705	0	0
Bus 4	1.0341	-0.01967	0	0	0	0
Bus 5	1.0142	-0.0285	0	0	1	0.35
Bus 6	1.0256	-0.03889	0	0	0.9	0.2
Bus 7	1.0324	0.10857	0	0	0	0
Bus 8	1.0247	0.05844	0	0	0.9	0.3
Bus 9	1.0374	0.0727	0	0	0	0

Table (A.6) Eigen value and frequency oscillation in case of normal load

Eigevalue	Most Associated States	Real part	Imag. Part	Pseudo-Freq.	Frequency
Eig As # 1	vm_Exc_1	-1000	0	0	0
Eig As # 2	vm_Exc_1	-1000	0	0	0
Eig As # 3	vm_Exc_3	-1000	0	0	0
Eig As # 4	omega_Syn_3, delta_Syn_3	-0.62989	11.6791	1.8588	1.8615
Eig As # 5	omega_Syn_3, delta_Syn_3	-0.62989	-11.6791	1.8588	1.8615
Eig As # 6	omega_Syn_2, delta_Syn_2	-0.14679	7.5514	1.2018	1.2021
Eig As # 7	omega_Syn_2, delta_Syn_2	-0.14679	-7.5514	1.2018	1.2021
Eig As # 8	vr1_Exc_2, vf_Exc_2	-5.4663	7.9496	1.2652	1.5355
Eig As # 9	vr1_Exc_2, vf_Exc_2	-5.4663	-7.9496	1.2652	1.5355
Eig As #10	vr1_Exc_1, vf_Exc_1	-5.2251	7.8402	1.2478	1.4995
Eig As #11	vr1_Exc_1, vf_Exc_1	-5.2251	-7.8402	1.2478	1.4995
Eig As #12	vr1_Exc_3, vf_Exc_3	-5.319	7.9288	1.2619	1.5196
Eig As #13	vr1_Exc_3, vf_Exc_3	-5.319	-7.9288	1.2619	1.5196
Eig As #14	e1d_Syn_3	-5.3256	0	0	0
Eig As #15	e1d_Syn_2	-3.5386	0	0	0
Eig As #16	e1q_Syn_1, vr2_Exc_1	-0.46492	1.1069	0.17617	0.19108
Eig As #17	e1q_Syn_1, vr2_Exc_1	-0.46492	-1.1069	0.17617	0.19108
Eig As #18	e1q_Syn_2, e1q_Syn_1	-0.43485	0.72504	0.11539	0.13456
Eig As #19	e1q_Syn_2, e1q_Syn_1	-0.43485	-0.72504	0.11539	0.13456
Eig As #20	e1q_Syn_3, vr2_Exc_3	-0.40349	0.47317	0.07531	0.09897
Eig As #21	e1q_Syn_3, vr2_Exc_3	-0.40349	-0.47317	0.07531	0.09897
Eig As #22	delta_Syn_1	0	0	0	0
Eig As #23	omega_Syn_1	0	0	0	0
Eig As #24	e1d_Syn_1	-3.2258	0	0	0

Table (A.7) Participation factor of all state in case of normal load

	delta_Syn_1	omega_Syn_1	e1q_Syn_1	e1d_Syn_1	delta_Syn_2
Eig As # 1	0	0	0	0	0
Eig As # 2	0	0	0	0	0
Eig As # 3	0	0	0	0	0
Eig As # 4	0.00417	0.00417	0	0	0.08722
Eig As # 5	0.00417	0.00417	0	0	0.08722
Eig As # 6	0.14087	0.14087	0.00023	0	0.29858
Eig As # 7	0.14087	0.14087	0.00023	0	0.29858
Eig As # 8	0.00017	0.00017	0.00012	0	0.00104
Eig As # 9	0.00017	0.00017	0.00012	0	0.00104
Eig As #10	0.00017	0.00017	0.01732	0	0.00026
Eig As #11	0.00017	0.00017	0.01732	0	0.00026
Eig As #12	0.00017	0.00017	0.00056	0	7e-005
Eig As #13	0.00017	0.00017	0.00056	0	7e-005
Eig As #14	5e-005	5e-005	0	0	0.00581
Eig As #15	0.01902	0.01902	0.00058	0	0.00925
Eig As #16	0.01103	0.01103	0.25718	0	0.00743
Eig As #17	0.01103	0.01103	0.25718	0	0.00743
Eig As #18	0.00536	0.00536	0.21137	0	0.00371
Eig As #19	0.00536	0.00536	0.21137	0	0.00371
Eig As #20	0.00011	0.00011	0.00248	0	0.00227
Eig As #21	0.00011	0.00011	0.00248	0	0.00227
Eig As #22	0.34796	0.34796	0	0	0.1036
Eig As #23	0.34796	0.34796	0	0	0.1036
Eig As #24	0	0	0	1	0

	e1q_Syn_3	e1d_Syn_3	vm_Exc_1	vr1_Exc_1	vr2_Exc_1
Eig As # 1	0	0	0.50254	0	0
Eig As # 2	0	0	0.49223	0	0
Eig As # 3	0	0	0.00523	0	0
Eig As # 4	0.01513	0.02405	0	0	0
Eig As # 5	0.01513	0.02405	0	0	0
Eig As # 6	0.00272	0.00134	0	0.00017	5e-005
Eig As # 7	0.00272	0.00134	0	0.00017	5e-005
Eig As # 8	0.00054	0.00041	0	0.00425	0.00121
Eig As # 9	0.00054	0.00041	0	0.00425	0.00121
Eig As #10	0.00201	0.00044	0.00016	0.38354	0.11619
Eig As #11	0.00201	0.00044	0.00016	0.38354	0.11619
Eig As #12	0.01008	0.00288	1e-005	0.0364	0.01059
Eig As #13	0.01008	0.00288	1e-005	0.0364	0.01059
Eig As #14	0.01297	0.47689	0	0	0
Eig As #15	0.00429	0.4446	1e-005	0	0.00863
Eig As #16	0.07278	0.00416	0.0003	0.02554	0.19461
Eig As #17	0.07278	0.00416	0.0003	0.02554	0.19461
Eig As #18	0.05488	0.00471	0.00016	0.01926	0.16401
Eig As #19	0.05488	0.00471	0.00016	0.01926	0.16401
Eig As #20	0.33438	0.03586	0	0.00022	0.00192
Eig As #21	0.33438	0.03586	0	0.00022	0.00192
Eig As #22	0	0	0	0	0
Eig As #23	0	0	0	0	0
Eig As #24	0	0	0	0	0

continue

	omega_S yn_2	e1q_Syn_ 2	e1d_Syn_2	delta_Sy n_3	omega_Syn_3
Eig As # 1	0	0	0	0	0
Eig As # 2	0	0	0	0	0
Eig As # 3	0	0	0	0	0
Eig As # 4	0.08722	0.00519	0.00616	0.38232	0.38232
Eig As # 5	0.08722	0.00519	0.00616	0.38232	0.38232
Eig As # 6	0.29858	0.01675	0.00041	0.04766	0.04766
Eig As # 7	0.29858	0.01675	0.00041	0.04766	0.04766
Eig As # 8	0.00104	0.01263	0.00152	0.00031	0.00031
Eig As # 9	0.00104	0.01263	0.00152	0.00031	0.00031
Eig As #10	0.00026	0.0011	0.00084	0.00036	0.00036
Eig As #11	0.00026	0.0011	0.00084	0.00036	0.00036
Eig As #12	7e-005	0.00132	0.00055	0.00146	0.00146
Eig As #13	7e-005	0.00132	0.00055	0.00146	0.00146
Eig As #14	0.00581	0.00661	0.46114	0.01079	0.01079
Eig As #15	0.00925	0.00206	0.44857	0.0107	0.0107
Eig As #16	0.00743	0.14162	0.00799	0.00413	0.00413
Eig As #17	0.00743	0.14162	0.00799	0.00413	0.00413
Eig As #18	0.00371	0.2122	0.00987	0.00123	0.00123
Eig As #19	0.00371	0.2122	0.00987	0.00123	0.00123
Eig As #20	0.00227	0.12401	0.00789	0.00194	0.00194
Eig As #21	0.00227	0.12401	0.00789	0.00194	0.00194
Eig As #22	0.1036	0	0	0.04844	0.04844
Eig As #23	0.1036	0	0	0.04844	0.04844
Eig As #24	0	0	0	0	0

## Increasing load at buses 8,6,5

Table (A.8) power flow and voltages in case of increasing load

Bus	V [p.u.]	Phase [rad]	P [p.u.] gen	Q [p.u.] gen	P [p.u.] load	[p.u.] Q load
Bus 1	1.04	0	1.2305	0.78725	0	0
Bus 2	1.025	0.10746	1.63	0.32838	0	0
Bus 3	1.025	0.01651	0.85	0.22516	0	0
Bus 4	0.99873	-0.06829	0	0	0	0
Bus 5	0.95986	-0.11003	0	0	1.25	0.7
Bus 6	0.94835	-0.1297	0	0	1.3	0.8
Bus 7	1.0099	0.00888	0	0	0	0
Bus 8	0.99085	-0.05249	0	0	1.1	0.5
Bus 9	1.0133	-0.03147	0	0	0	0

Table (A.9) Eigenvalue of state matrix and the frequency of oscillation

Eigenvalue	Most Associated States Freq.	Real part	Imag. Part	Pseudo-	Frequency
Eig As # 1	vm_Exc_1	-1000	0	0	0
Eig As # 2	vm_Exc_1	-1000	0	0	0
Eig As # 3	vm_Exc_3	-1000	0	0	0
Eig As # 4	omega_Syn_3, delta_Syn_3	-0.87026	11.4437	1.8213	1.8266
Eig As # 5	omega_Syn_3, delta_Syn_3	-0.87026	-11.4437	1.8213	1.8266
Eig As # 6	delta_Syn_2, omega_Syn_2	-0.21599	7.5571	1.2028	1.2032
Eig As # 7	delta_Syn_2, omega_Syn_2	-0.21599	-7.5571	1.2028	1.2032
Eig As # 8	vr1_Exc_2, vf_Exc_2	-5.5904	7.9572	1.2664	1.5477
Eig As # 9	vr1_Exc_2, vf_Exc_2	-5.5904	-7.9572	1.2664	1.5477
Eig As #10	vr1_Exc_1, vf_Exc_1	-5.2391	7.8091	1.2429	1.4967
Eig As #11	vr1_Exc_1, vf_Exc_1	-5.2391	-7.8091	1.2429	1.4967
Eig As #12	vr1_Exc_3, vf_Exc_3	-5.429	7.9033	1.2579	1.526
Eig As #13	vr1_Exc_3, vf_Exc_3	-5.429	-7.9033	1.2579	1.526
Eig As #14	e1d_Syn_2	-4.8535	0	0	0
Eig As #15	e1d_Syn_3	3.3167	0	0	0
Eig As #16	e1q_Syn_1, e1q_Syn_2	-0.45827	1.2809	0.20386	0.21652
Eig As #17	e1q_Syn_1, e1q_Syn_2	-0.45827	-1.2809	0.20386	0.21652
Eig As #18	e1q_Syn_1, vr2_Exc_1	-0.46288	0.76046	0.12103	0.14169
Eig As #19	e1q_Syn_1, vr2_Exc_1	-0.46288	-0.76046	0.12103	0.14169

Eig As #20	<b>e1q_Syn_3, vr2_Exc_3</b>	<b>-0.50137</b>	<b>0.56304</b>	<b>0.08961</b>	0.11999
Eig As #21	<b>e1q_Syn_3, vr2_Exc_3</b>	<b>-0.50137</b>	<b>-0.56304</b>	<b>0.08961</b>	0.11999
Eig As #22	<b>delta_Syn_1</b>	<b>0</b>	<b>0</b>	<b>0</b>	0
Eig As #23	<b>omega_Syn_1</b>	<b>0</b>	<b>0</b>	<b>0</b>	0
Eig As #24	<b>e1d_Syn_1</b>	<b>-3.2258</b>	<b>0</b>	<b>0</b>	<b>0</b>

Table (A.10) Participation factor of all states

	delta_Syn_1	omega_Syn_1	e1q_Syn_1	e1d_Syn_1	delta_Syn_2
Eig As # 1	0	0	0	0	0
Eig As # 2	0	0	0	0	0
Eig As # 3	0	0	0	0	0
Eig As # 4	0.00451	0.00451	4e-005	0	0.08469
Eig As # 5	0.00451	0.00451	4e-005	0	0.08469
Eig As # 6	0.12995	.12995	0.00011	0	0.30595
Eig As # 7	0.12995	0.12995	0.00011	0	0.30595
Eig As # 8	0.00014	0.00014	0.00023	0	0.00085
Eig As # 9	0.00014	0.00014	0.00023	0	0.00085
Eig As #10	6e-005	6e-005	0.01964	0	6e-005
Eig As #11	6e-005	6e-005	0.01964	0	6e-005
Eig As #12	0.00021	0.00021	0.00112	0	6e-005
Eig As #13	0.00021	0.00021	0.00112	0	6e-005
Eig As #14	6e-005	6e-005	4 e-005	0	0.01081
Eig As #15	0.00208	0.00208	0.00173	0	0.00146
Eig As #16	0.00037	0.00037	0.21349	0	0.00085
Eig As #17	0.00037	0.00037	0.21349	0	0.00085
Eig As #18	0.00032	0.00032	0.26906	0	0.00059
Eig As #19	0.00032	0.00032	0.26906	0	0.00059
Eig As #20	1e-005	1e-005	0.00153	0	0.0009
Eig As #21	1e-005	1e-005	0.00153	0	0.0009
Eig As #22	0.36137	0.3613	0	0	0.09391
Eig As #23	0.36137	0.36137	0	0	0.09391
Eig As #24	0	0	0	1	0

## Continue

	delta_Syn_1	omega_Syn_1	e1q_Syn_1	e1d_Syn_1	delta_Syn_2
Eig As # 1	0	0	0	0	0
Eig As # 2	0	0	0	0	0
Eig As # 3	0	0	0	0	0
Eig As # 4	0.00451	0.00451	4e-005	0	0.08469
Eig As # 5	0.00451	0.00451	4e-005	0	0.08469
Eig As # 6	0.12995	0.12995	0.00011	0	0.30595
Eig As # 7	0.12995	0.12995	0.00011	0	0.30595
Eig As # 8	0.00014	0.00014	0.00023	0	0.00085
Eig As # 9	0.00014	0.00014	0.00023	0	0.00085
Eig As #10	6e-005	6e-005	0.01964	0	6e-005
Eig As #11	6e-005	6e-005	0.01964	0	6e-005
Eig As #12	0.00021	0.00021	0.00112	0	6e-005
Eig As #13	0.00021	0.00021	0.00112	0	6e-005
Eig As #14	6e-005	6e-005	4e-005	0	0.01081
Eig As #15	0.00208	0.00208	0.00173	0	0.00146
Eig As #16	0.00037	0.00037	0.21349	0	0.00085
Eig As #17	0.00037	0.00037	0.21349	0	0.00085
Eig As #18	0.00032	0.00032	0.26906	0	0.00059
Eig As #19	0.00032	0.00032	0.26906	0	0.00059
Eig As #20	1e-005	1e-005	0.00153	0	0.0009
Eig As #21	1e-005	1e-005	0.00153	0	0.0009
Eig As #22	0.36137	0.36137	0	0	0.09391
Eig As #23	0.36137	0.36137			0.09391
Eig As #24	0	0		1	0

## Continue

	omega_Syn_2	e1q_Syn_2	e1d_Syn_2	delta_Syn_3	omega_Syn_3
Eig As # 1	0	0	0	0	0
Eig As # 2	0	0	0	0	0
Eig As # 3	0	0	0	0	0
Eig As # 4	0.08469	0.00505	0.007	0.3747	0.3747
Eig As # 5	0.08469	0.00505	0.007	0.3747	0.3747
Eig As # 6	0.30595	0.01194	0.01135	0.04947	0.04947
Eig As # 7	0.30595	0.01194	0.01135	.04947	0.04947
Eig As # 8	0.00085	0.01395	0.0015	0.00053	0.00053
Eig As # 9	0.00085	0.01395	0.0015	0.00053	0.00053
Eig As #10	6e-005	0.00217	0.00102	0.00012	0.00012
Eig As #11	6e-005	0.00217	0.00102	0.00012	0.00012
Eig As #12	6e-005	0.0036	0.00082	0.00109	0.00109
Eig As #13	6e-005	0.0036	0.00082	0.00109	0.00109
Eig As #14	0.01081	0.00821	0.54972	0.01497	0.01497
Eig As #15	0.00146	0.00032	0.35454	0.01146	0.01146
Eig As #16	0.00085	0.15846	0.01148	0.00057	0.00057
Eig As #17	0.00085	0.15846	0.01148	0.00057	0.00057
Eig As #18	0.00059	0.15037	0.00779	0.0002	0.0002
Eig As #19	0.00059	0.15037	0.00779	0.0002	0.0002
Eig As #20	0.0009	0.17657	0.01241	0.00133	0.00133
Eig As #21	0.0009	0.17657	0.01241	0.00133	0.00133
Eig As #22	0.09391	0	0	0.04472	0.04472
Eig As #23	0.09391	0	0	0.04472	0.04472
Eig As #24	0	0	0	0	0

## Continue

	e1q_Syn_3	e1d_Syn_3	vm_Exc_1	vr1_Exc_1	vr2_Exc_1
Eig As # 1	0	0	0.33795	0	0
Eig As # 2	0	0	0.65728	0	0
Eig As # 3	0	0	0.00477	0	0
Eig As # 4	0.00835	0.04948	0	3e-005	0
Eig As # 5	0.00835	0.04948	0	3e-005	0
Eig As # 6	0.00124	0.00194	0	5e-005	2e-005
Eig As # 7	0.00124	0.00194	0	5e-005	2e-005
Eig As # 8	0.00109	0.00055	0	0.0045	0.00126
Eig As # 9	0.00109	0.00055	0	0.0045	0.00126
Eig As #10	0.00338	0.00035	0.00018	0.37393	0.11451
Eig As #11	0.00338	0.00035	0.00018	0.37393	0.11451
Eig As #12	0.01422	0.00214	1e-005	0.04438	0.0129
Eig As #13	0.01422	0.00214	1e-005	0.04438	0.0129
Eig As #14	0.01673	0.36374	0	0	0.00013
Eig As #15	0.00334	0.57784	1e-005	0	0.01227
Eig As #16	0.1185	0.00511	0.00029	0.0228	0.1575
Eig As #17	0.1185	0.00511	0.00029	0.0228	0.1575
Eig As #18	0.06743	0.00595	0.00022	0.02476	0.21204
Eig As #19	0.06743	0.00595	0.00022	0.02476	0.21204
Eig As #20	0.28437	0.03073	0	0.00014	0.0013
Eig As #21	0.28437	0.03073	0	0.00014	0.0013
Eig As #22	0	0	0	0	0
Eig As #23	0	0	0		0
Eig As #24	0	0	0	0	0

## Three short circuit in bus5 but without power system stabilizer

Table (A.11) Power flow and voltages in case of short circuit

Bus	V [p.u.]	phase [rad]	P gen [ p.u.]	Q gen [p.u.]	P load p.u.]	Q load [p.u.]
Bus 1	1.04	0	0.71548	0.17938	0	0
Bus 2	1.025	0.16152	1.63	0.0116	0	0
Bus 3	1.025	0.0818	0.85	0.13519	0	0
Bus 4	1.0308	0.03845	0	0	0	0
Bus 5	1.009	-0.06963	0	0	1.25	0.35
Bus 6	1.0166	0.06377	0	0	0.9	0.3
Bus 7	1.0291	0.06479	0	0	0	0
Bus 8	1.0185	0.01302	0	0	1	0.35
Bus 9	1.0339	0.03478	0	0	0	0

Table (A.12) Eigenvalue of state matrix and the frequency oscillations

Eigenvalue	Most Associated States	Real part	Imag. Part	Pseudo-Freq.	Frequency
Eig As # 1	vm_Exc_1	-1000	0	0	0
Eig As # 2	vm_Exc_1	-1000	0	0	0
Eig As # 3	vm_Exc_3	-1000	0	0	0
Eig As # 4	delta_Syn_3, omega_Syn_3	-0.66944	11.6428	1.853	1.8561
Eig As # 5	delta_Syn_3, omega_Syn_3	-0.66944	-11.6428	1.853	1.8561
Eig As # 6	delta_Syn_2, omega_Syn_2	-0.14765	7.5803	1.2064	1.2067
Eig As # 7	delta_Syn_2, omega_Syn_2	-0.14765	-7.5803	1.2064	1.2067
Eig As # 8	vr1_Exc_2, vf_Exc_2	-5.4817	7.9494	1.2652	1.5368
Eig As # 9	vr1_Exc_2, vf_Exc_2	-5.4817	-7.9494	1.2652	1.5368
Eig As #10	vr1_Exc_1, vf_Exc_1	-5.2297	7.8416	1.248	1.5001
Eig As #11	vr1_Exc_1, vf_Exc_1	-5.2297	-7.8416	1.248	1.5001
Eig As #12	vr1_Exc_3, vf_Exc_3	-5.3286	7.927	1.2616	1.5202
Eig As #13	vr1_Exc_3, vf_Exc_3	-5.3286	-7.927	1.261 6	1.5202
Eig As #14	e1d_Syn_2	5.2439	0	0	0
Eig As #15	e1d_Syn_3	-3.5526	0	0	0
Eig As #16	e1q_Syn_1, vr2_Exc_1	-0.47219	1.0899	0.17347	0.18905
Eig As #17	e1q_Syn_1, vr2_Exc_1	-0.47219	-1.0899	0.17347	0.18905
Eig As #18	e1q_Syn_1, e1q_Syn_2	-0.44056	0.72956	0.11611	0.13564
Eig As #19	e1q_Syn_1, e1q_Syn_2	-0.44056	-0.72956	0.11611	0.13564
Eig As #20	e1q_Syn_3, vr2_Exc_3	-0.4174	0.48718	0.07754	0.1021
Eig As #21	e1q_Syn_3, vr2_Exc_3	-0.4174	-0.48718	0.07754	0.1021
Eig As #22	omega_Syn_1	0	0	0	0
Eig As #23	delta_Syn_1		0	0	0
Eig As #24	e1d_Syn_1		3.2258	0	0

Table (A.13) Participation factor of all states

	delta_Syn_1	omega_Syn_1	e1q_Syn_1	e1d_Syn_1	delta_Syn_2
Eig As # 1	0	0	0	0	0
Eig As # 2	0	0	0	0	0
Eig As # 3	0	0	0	0	0
Eig As # 4	0.00418	0.00418	0	0	0.08623
Eig As # 5	0.00418	0.00418	0	0	0.08623
Eig As # 6	0.13939	0.13939	0.0001	0	0.30087
Eig As # 7	0.13939	0.13939	0.0001	0	0.30087
Eig As # 8	0.00016	0.00016	0.00013	0	0.00098
Eig As # 9	0.00016	0.00016	0.00013	0	0.00098
Eig As #10	0.00013	0.00013	0.01723	0	0.00016
Eig As #11	0.00013	0.00013	0.01723	0	0.00016
Eig As #12	0.00016	0.00016	0.00053	0	6e-005
Eig As #13	0.00016	0.00016	0.00053	0	6e-005
Eig As #14	0.00012	0.00012	0	0	0.00573
Eig As #15	0.02326	0.02326	0.00036	0	0.01107
Eig As #16	0.01382	0.01382	0.25305	0	0.00849
Eig As #17	0.01382	0.01382	0.25305	0	0.00849
Eig As #18	0.006	0.006	0.21306	0	0.00417
Eig As #19	0.006	0.006	0.21306	0	0.00417
Eig As #20	0.00014	0.00014	0.00223	0	0.00218
Eig As #21	0.00014	0.00014	0.00223	0	0.00218
Eig As #22	0.34693	0.34693	0	0	0.10454
Eig As #23	0.34693	0.34693	0	0	0.10454
Eig As #24	0	0	0	1	0

## Continue

	Omega_Syn_2	delta_Syn_3	omega_Syn_3	e1q_Syn_2	e1d_Syn_2
Eig As # 1	0	0	0	0	0
Eig As # 2	0	0	0	0	0
Eig As # 3	0	0	0	0	0
Eig As # 4	0.08623	0.00499	0.00661	0.38169	0.38169
Eig As # 5	0.08623	0.00499	0.00661	0.38169	0.38169
Eig As # 6	0.30087	0.01615	0.00099	0.04757	0.04757
Eig As # 7	0.30087	0.01615	0.00099	0.04757	0.04757
Eig As # 8	0.00098	0.01292	0.00152	0.00033	0.00033
Eig As # 9	0.00098	0.01292	0.00152	0.00033	0.00033
Eig As #10	0.00016	0.00106	0.00075	0.00029	0.00029
Eig As #11	0.00016	0.00106	0.00075	0.00029	0.00029
Eig As #12	6e-005	0.00136	0.00056	0.00147	0.00147
Eig As #13	6e-005	0.00136	0.00056	0.00147	0.00147
Eig As #14	0.00573	0.00708	0.47607	0.0126	0.0126
Eig As #15	0.01107	0.00194	0.42317	0.01234	0.01234
Eig As #16	0.00849	0.13996	0.00666	0.00553	0.00553
Eig As #17	0.00849	0.13996	0.00666	0.00553	0.00553
Eig As #18	0.00417	0.20613	0.00985	0.00145	0.00145
Eig As #19	0.00417	0.20613	0.00985	0.00145	0.00145
Eig As #20	0.00218	0.1292	0.00845	0.00194	0.00194
Eig As #21	0.00218	0.1292	0.00845	0.00194	0.00194
Eig As #22	0.10454	0	0	0.04853	0.04853
Eig As #23	0.10454	0	0	0.04853	0.04853
Eig As #24	0	0	0	0	0

## Continue

	e1q_Syn_3	e1d_Syn_3	vm_Exc_1	vr1_Exc_1	vr2_Exc_1
Eig As # 1	0	0	0.46326	0	0
Eig As # 2	0	0	0.53211	0	0
Eig As # 3	0	0	0.00463	0	0
Eig As # 4	0.01422	0.02788	0	0	0
Eig As # 5	0.01422	0.02788	0	0	0
Eig As # 6	0.00243	0.00145	0	7e-005	2e-005
Eig As # 7	0.00243	0.00145	0	7e-005	2e-005
Eig As # 8	0.00055	0.0004	0	0.00407	0.00116
Eig As # 9	0.00055	0.0004	0	0.00407	0.00116
Eig As #10	0.00197	0.00037	0.00016	0.38638	0.11696
Eig As #11	0.00197	0.00037	0.00016	0.38638	0.11696
Eig As #12	0.01066	0.00291	1e-005	0.03452	0.01004
Eig As #13	0.01066	0.00291	1e-005	0.0345 2	0.01004
Eig As #14	0.01386	0.4567	0	0	0
Eig As #15	0.00543	0.45484	1e-005	0	0.0074
Eig As #16	0.07449	0.00269	0.00029	0.02494	0.19252
Eig As #17	0.07449	0.00269	0.00029	0.02 494	0.19252
Eig As #18	0.05771	0.00521	0.00016	0.0194 3	0.16605
Eig As #19	0.05771	0.00521	0.00016	0.01943	0.16605
Eig As #20	0.32846	0.03658	0	0.0002	0.00176
Eig As #21	0.32846	0.03658	0	0.0002	0.00176
Eig As #22	0	0	0	0	0
Eig As #23	0	0	0	0	0
Eig As #24	0	0	0	0	0

## Case four short circuit in bus5 but with PSS

Table (A.14) Power flow and voltages in case of short circuit

	V	phase	P gen	Q gen	P load	Q load
Bus	[p.u.]	[rad]	[p.u.]	[p.u.]	[p.u.]	[p.u.]
Bus 1	1.04	0	0	71548	0.17938	0
Bus 2	1.025	0.16152	1.63	0.0116	0	0
Bus 3	1.025	0.0818	0.85	<b>-0.13519</b>	<b>0</b>	<b>0</b>
Bus 4	1.0308	-0.03845	0	<b>0</b>	0	0
Bus 5	1.009	-0.06963	0	0	1.25	0.35
Bus 6	1.0166	-0.06377	0	0	0.9	0.3
Bus 7	1.0291	0.06479	0	0	0	0
Bus 8	1.0185	0.01302	0	0	1	0.35
Bus 9	1.0339	0.03478	0	0	0	0

Table (A.15) Eigenvalues in case of short circuit with PSS

Eigenvalue	Most Associated States	Real part	Imag. Part	Pseudo-Freq.	Frequency
Eig As # 1	vm_Exc_1	-1000	0	0	0
Eig As # 2	vm_Exc_1	-1000	0	0	0
Eig As # 3	vm_Exc_3	-1000	0	0	0
Eig As # 4	v3_Pss_2, v2_Pss_2	-50.1701	2.9273	0.46589	7.9984
Eig As # 5	v2_Pss_2, v3_Pss_2	-50.1701	-2.9273	0.46589	7.9984
Eig As # 6	v2_Pss_1, v3_Pss_1	-50.3121	4.0392	0.64286	8.0332
Eig As # 7	v3_Pss_1, v2_Pss_1	-50.3121	-4.0392	0.64286	8.0332
Eig As # 8	omega_Syn_3, delta_Syn_3	-0.69099	12.4453	1.9807	1.9838
Eig As # 9	omega_Syn_3, delta_Syn_3	-0.69099	-12.4453	1.9807	1.9838
Eig As #10	omega_Syn_2, delta_Syn_2	-0.42352	7.8534	1.2499	1.2517
Eig As #11	omega_Syn_2, delta_Syn_2	-0.42352	-7.8534	1.2499	1.2517
Eig As #12	vr1_Exc_1, vf_Exc_1	-5.2376	7.8688	1.2524	1.5044
Eig As #13	vr1_Exc_1, vf_Exc_1	-5.2376	-7.8688	1.2524	1.5044
Eig As #14	vr1_Exc_2, vf_Exc_2	-4.9566	7.8197	1.2445	1.4735
Eig As #15	vr1_Exc_2, vf_Exc_2	-4.9566	-7.8197	1.2445	1.4735
Eig As #16	vr1_Exc_3, vf_Exc_3	-5.0217	7.4718	1.1892	1.4328
Eig As #17	vr1_Exc_3, vf_Exc_3	-5.0217	-7.4718	1.1892	1.4328
Eig As #18	e1d_Syn_2	-5.2486	0	0	0
Eig As #19	e1d_Syn_3	-3.5526	0	0	0
Eig As #20	e1q_Syn_1, e1q_Syn_2	-0.42261	1.1567	0.18409	0.19599
Eig As #21	e1q_Syn_1, e1q_Syn_2	-0.42261	-1.1567	0.18409	0.19599
Eig As #22	e1q_Syn_1, vr2_Exc_1	-0.41399	0.74434	0.11847	0.13556
Eig As #23	e1q_Syn_1, vr2_Exc_1	-0.41399	-0.74434	0.11847	0.13556
Eig As #24	e1q_Syn_3, vr2_Exc_3	-0.41842	0.47462	0.07554	0.1007
Eig As #25	e1q_Syn_3, vr2_Exc_3	-0.41842	-0.47462	0.07554	0.1007

Eig As #26	omega_Syn_1	-0.33527	0	0	0
Eig As #27	v1_Pss_1	-0.10078	0	0	0
Eig As #28	delta_Syn_2	0	0	0	0
Eig As #29	delta_Syn_2	0	0	0	0
Eig As #30	e1d_Syn_1	-3.2258	0	0	0

Table (A.16) Participation factor of all states

	delta_Syn_1	omega_Syn_1	e1q_Syn_1	e1d_Syn_1	delta_Syn_2
Eig As # 1	0	0	0	0	0
Eig As # 2	0	0	0	0	0
Eig As # 3	0	0	0	0	0
Eig As # 4	7e-005	7e-005	0	0	0.00043
Eig As # 5	7e-005	7e-005	0	0	0.00043
Eig As # 6	1e-005	1e-005	0	0	0.00025
Eig As # 7	1e-005	1e-005	0	0	0.00025
Eig As # 8	0.00287	0.00287	1e-005	0	0.06025
Eig As # 9	0.00287	0.00287	1e-005	0	0.06025
Eig As #10	0.10476	0.10476	4e-005	0	0.23953
Eig As #11	0.10476	0.10476	4e-005	0	0.23953
Eig As #12	0.00051	0.00051	0.01562	0	0.00078
Eig As #13	0.00051	0.00051	0.01562	0	0.00078
Eig As #14	0.00361	0.00361	0.00171	0	0.02167
Eig As #15	0.00361	0.00361	0.00171	0	0.02167
Eig As #16	0.00027	0.00027	0.0002	0	0.01667
Eig As #17	0.00027	0.00027	0.0002	0	0.01667
Eig As #18	0.00011	0.00011	0	0	0.00585
Eig As #19	0.02326	0.02326	0.00036	0	0.01104
Eig As #20	0.04413	0.04413	0.17503	0	0.02206
Eig As #21	0.04413	0.04413	0.17503	0	0.02206
Eig As #22	0.02062	0.02062	0.24727	0	0.0119
Eig As #23	0.02062	0.02062	0.24727	0	0.0119
Eig As #24	0.00241	0.00241	0.00199	0	0.01932
Eig As #25	0.00241	0.00241	0.00199	0	0.01932
Eig As #26	0.20741	0.20741	0.00361	0	0.0964
Eig As #27	0	0	0	0	0.003
Eig As #28	0.09454	0.09454	0	0	0.22883
Eig As #29	0.09454	0.09454	0	0	0.22883
Eig As #30	0	0	0	1	0

continue

	omega_Syn_2	e1q_Syn_2	omega_Syn_3	e1d_Syn_2	delta_Syn_3
Eig As # 1	0	0		0	0
Eig As # 2	0	0	0	0	0
Eig As # 3	0	0	0	0	0
Eig As # 4	0.02256	0.02319	0	1e-005	0.00317
Eig As # 5	0.02256	0.02319	0	1e-005	0.00317
Eig As # 6	0.00395	0.00429	7e-005	0.00159	0.02894
Eig As # 7	0.00395	0.00429	7e-005	0.00159	0.02894
Eig As # 8	0.06791	0.00886	0.00434	0.274	0.31325
Eig As # 9	0.06791	0.00886	0.00434	0.274	0.31325
Eig As #10	0.26324	0.04426	0.00065	0.03661	0.04217
Eig As #11	0.26324	0.04426	0.00065	0.03661	0.04217
Eig As #12	0.00138	0.00173	0.00013	9e-005	0.00019
Eig As #13	0.00138	0.00173	0.00013	9e-005	0.00019
Eig As #14	0.03645	0.04372	0.00181	0.00225	0.0022
Eig As #15	0.03645	0.04372	0.00181	0.00225	0.0022
Eig As #16	0.01318	0.01453	0.00185	0.0375	0.01882
Eig As #17	0.01318	0.01453	0.00185	0.0375	0.01882
Eig As #18	0.00567	0.00718	0.47311	0.01295	0.01231
Eig As #19	0.01106	0.00192	0.42316	0.01235	0.01232
Eig As #20	0.01336	0.14875	0.00442	0.01776	0.00433
Eig As #21	0.01336	0.14875	0.00442	0.01776	0.00433
Eig As #22	0.00681	0.15577	0.0077	0.00556	0.00257
Eig As #23	0.00681	0.15577	0.0077	0.00556	0.00257
Eig As #24	0.00236	0.13483	0.0088	0.0114	0.0012
Eig As #25	0.00236	0.13483	0.0088	0.0114	0.0012
Eig As #26	0.06119	0.01651	8e-005	0.11489	0.02917
Eig As #27	0	0.00042	3e-005	0.00419	0
Eig As #28	0.02849	0	0	0.17664	0.01323
Eig As #29	0.02849	0	0	0.17663	0.01323
Eig As #30	0	0	0	0	0

**continue**

	e1q_Syn_3	e1d_Syn_3	vm_Exc_1	vr1_Exc_1	vr2_Exc_1
Eig As # 1	0	0	0.46326	0	0
Eig As # 2	0	0	0.53211	0	0
Eig As # 3	0	0	0.00463	0	0
Eig As # 4	0.00318	4e-005	0	0	0
Eig As # 5	0.00318	4e-005	0	0	0
Eig As # 6	0.03091	9e-005	0	0	0
Eig As # 7	0.03091	9e-005	0	0	0
Eig As # 8	0.04173	0.01947	0	0	0
Eig As # 9	0.04173	0.01947	0	0	0
Eig As #10	0.00941	0.00142	0	4e-005	1e-005
Eig As #11	0.00941	0.00142	0	4e-005	1e-005
Eig As #12	0.0002	0.0001	0.00015	0.40681	0.12186
Eig As #13	0.0002	0.0001	0.00015	0.40681	0.12186
Eig As #14	0.00774	9e-005	2e-005	0.01672	0.00524
Eig As #15	0.00774	9e-005	2e-005	0.01672	0.00524
Eig As #16	0.04294	0.00357	0	0.00129	0.00046
Eig As #17	0.04294	0.00357	0	0.00129	0.00046
Eig As #18	0.01436	0.4545	0	0	0
Eig As #19	0.00539	0.4548	1e-005	0	0.00739
Eig As #20	0.08083	0.00166	0.00021	0.01799	0.12853
Eig As #21	0.08083	0.00166	0.00021	0.01799	0.12853
Eig As #22	0.04795	0.0047	0.00019	0.02277	0.1882
Eig As #23	0.04795	0.0047	0.00019	0.02277	0.1882
Eig As #24	0.29664	0.03455	0	0.00018	0.00157
Eig As #25	0.29664	0.03455	0	0.00018	0.00157
Eig As #26	0.01714	0.00064	0	0.00013	0.00113
Eig As #27	0.0006	0.00011	0	0	0
Eig As #28	0	0	0	0	0
Eig As #29	0	0	0	0	0
<b>Eig As #30</b>	<b>0</b>	<b>0</b>	<b>0</b>	<b>0</b>	<b>0</b>

## Appendix (B)

The appendix (B) obtains data of single machine connected in finite bus and data of three machine nine bus system.

Table (B1) Single machine data

<b>Machine Parameters:</b>			
$X_d = 1.757$ p.u	$X_q = 0.6$ p.u	$X_d' = 0.424$ p.u	$M = 2 * H = 6.0$ s
$F = 60.0$ Hz	$X_q' = 0.6$ p.u $T_{d0} = 6.66$ s $T_{q0} = 0.44$ s	$X_d'' = 0.4$ p.u $E_b = 1.0$ p.u	$H = 3$
<b>Transmission Line:</b>			
$X_{TL} = 0.835$ p.u		$R_e = 0$ p.u	
<b>Transformer:</b>			
$X_{tr} = 0.0364$ p.u			
<b>Load parameters:</b>			
Nominal Load	Heavy Load	Light Load	Leading P.F
$P_b = 0.6$ p.u $Q_b = 0.016$ p.u	$H_b = 1.2$ p.u $Q_b = 0.5$ p.u	$L_b = 0.25$ p.u $Q_b = 0.016$ p.u	$L_b = 0.8$ p.u $Q_b = -0.4$ p.u
<b>Constants</b>			
$T_A = 0.05$ s	$K_A = 10$	$T_w = 10$ s	$K_{ps} = 40$
$T_1 = 0.3373$ s	$T_3 = 0.3373$ s	$T_2 = 0.0733$ s	$T_4 = 0.0733$ s

Table (B2) Data of three Generators

Generator	H	$X'_d$
1	23.64	0.0608
2	6.4	0.1198
3	3.01	0.1813

Table (B3) Line data

Bus No.		Half line charging	Reactance (p.u.)	Resistance (p.u.)
From Bus	To Bus	Admittance(p.u.)		
1	4	0.0	0.0576	0.0
4	6	0.079	0.092	0.017
3	9	0.0	0.0586	0.0
6	9	0.179	0.17	0.039
5	7	0.153	0.161	0.032
7	8	0.0745	0.072	0.0085
2	7	0.0	0.0625	0.0
8	9	0.1045	0.1008	0.0119

Table (B4) Load data

Bus No.	P <sub>G</sub>	Q <sub>G</sub>	P <sub>L</sub>	Q <sub>L</sub>	V <sub>spc</sub>
1	0.0	-	0.0	0.0	1.04
2	1.63	0.0	0.0	0.0	1.025
3	0.85	0.0	0.0	0.0	1.025
4	0.0	0.0	0.0	0.0	--
5	0.0	0.0	1.25	0.5	--
6	0.0	0.0	0.9	0.3	--
7	0.0	0.0	0.0	0.0	--
8	0.0	0.0	1.0	0.35	--
9	0.0	0.0	0.0	0.0	--

# Appendix C

( **IOSR Journal of Electrical and Electronics Engineering (IOSR-JEEE)** e-ISSN: 2278-1676,p-ISSN: 2320-3331, Volume 12, Issue 1 Ver. I (Jan. – Feb. 2017), PP 12-17 [www.iosrjournals.org](http://www.iosrjournals.org) ).

(**American Journal of Engineering Research (AJER)** e-ISSN: 2320-0847 p-ISSN : 2320-0936 Volume-6, Issue-1, pp-194-199 [www.ajer.org](http://www.ajer.org) ).